THE EFFECT OF LIPIDS ON GLUCOREGULATORY HORMONE ACTIONS

By

Carrie Alicia Everett Grueter

Dissertation
Submitted to the Faculty of the
Graduate School of Vanderbilt University
in partial fulfillment of the requirements
for the degree of

DOCTOR OF PHILOSOPHY

in

Molecular Physiology and Biophysics
December, 2006
Nashville, Tennessee

Approved:
Professor Owen McGuinness

Professor Masakazu Shiota

Professor Larry L. Swift

Professor Alyssa Hasty

Professor Raymond F. Burk

To my parents, Pete and Rahonda, my brother Josh, and my husband, Brad

ETERNAL THANKS

RESPECT

LOVE

ACKNOWLEDGMENTS

First and formost, I would like to thank my mentor, Dr. Alan Cherrington. I am proud to have received training from someone who has such love and enthusiasm for physiology. I am very grateful for the guidance, support and knowledge I have received over the years and I feel that he has provided me with a strong scientific foundation that will serve me well in the years to come. I am also very appreciative that he gave me the freedom to choose a project that was close to my heart, even though it was outside his area of expertise. Despite the challenges, we have both advanced our knowledge and understanding of lipid metabolism tremendously. I look forward to taking what I have learned from this experience to better my future endeavors in both science and in life.

Secondly, I would like to thank the members of my dissertation committee, Drs. Raymond Burke, Alyssa Hasty, Owen McGuinness, Masakazu Shiota, and Larry Swift for willingly contributing their time, effort, and insightful comments to this research. I am especially grateful for their encouragement and support in moving forward with such a challenging project.

There are a number of people that I would like to thank from whom I received help in my research throughout my graduate career. First, the Cherrington laboratory has become my family providing me with tremendous support technically, intellectually, and most importantly personally. Without the technical expertise of Doss Neal, Ben Farmer, and Tiffany Rodewald my numerous experiments would have never been so successful. I especially want to thank Tiffany for going above and beyond her call of duty and making my life in the lab much easier. I am forever indebted to her and will cherish our

friendship always. Margaret Lautz, Melanie Scott, Jon Hastings, and Marta Smith have all been true supporters during my time here. Past and present graduate students have included Jamie Grubert, Stephanie Gustavson, Kathryn Stettler, and Zhibo An who have all contributed to my experimental work. To ALL members of the Cherrington Lab, especially Tiffany, Mel and Marta, a HUGE thank you for all of the numerous hours spent doing the repeated lipid/saline infusions!!!! Without their help, the hepatic steatosis project would have taken me twice as long to complete.

Excellent assistance was provided by the individuals from the Animal Resources Core with special thanks to Phil Williams, Brooks Lacy, Amy Nunnally and Jamie Adcock. I am particularly appreciative to Phil for his genuine interest and helpful advice in my research. In addition, numerous individuals from the Hormone Core Laboratory were instrumental in my graduate career including Eric Allen, Angela Sater, Angelina Penaloza, Suzan Vaughan, Wanda Snead and especially E. Patrick Donahue who together with Dr. Masakazu Shiota developed the cAMP assay. To Wanda: a special thank you for just being you, a truly loving and thoughtful individual. Excellent assistance was also provided by Dr. Larry Swift and Carla Harris from the Lipid Core.

There are several individuals whom I have met in the Cherrington lab that have played particularly important roles in my time here at Vanderbilt. First, a very special thank you to the lab Mom, Patsy Raymer, who was truly my Mom away from home. Not only did she take care of me but she spoiled me and we developed a special bond that I will cherish always. I will deeply miss her.

Secondly, I would like to thank both Dale Edgerton and Noelia Rivera who were the greatest lab partners that I could have ever asked for. Dale guided me through my

first few years of studies and then I had the privilege to guide Noelia through hers. Having them both as a lab partner, not only made me a better scientist but more importantly made me a better person. Their positive outlook on life and strong faith is contagious and I hope that I touch the lives of others as they have touched mine.

I would also like to thank Genie Moore for always having an open door where I could ask her questions, cry on her shoulder, or just have a venting session. She has become a very special friend to me and I truly admire her as a scientist, a mother, and a wife.

Of the Cherrington laboratory, I most of all would like to thank Catherine DiCostanzo. When Catherine and I first joined the lab, we would have never guessed that she would one day be the maid of honor in my wedding and I the matron of honor in hers. However, the true honor is mine, having shared many of life's experiences with her. We have shed many tears together but thankfully we have had more laughs. I look forward to the numerous *positive* memories we will share together in the future because God knows things can only get better from here.

Lastly, I would like to thank my family whom has been my greatest support. I am who I am today because of them. My mother, Rahonda, is probably the most enthusiastic person I know. By example, she has taught me the joy of learning. My father, Pete, also by example, has shown me the benefits of being patient, paying close attention to detail, and having a great sense of humor. Josh, who has the biggest heart of any man I know, also has the strongest sense of purpose and I am so blessed to have him as my brother. Above all, I am grateful for the unconditional love and support my family has provided throughout my life.

My greatest accomplishment during my graduate career was my marriage to Brad Grueter. Several times throughout this process, I had misgivings as to whether I should complete this dissertation. However, had I not stayed in the program, I may not have met Brad, as he was a fellow graduate student in the department. Knowing that it was God's plan for our paths to cross, I have no doubt that He also intended for me to obtain this Ph.D. I am truly blessed to share the rest of my life with such an amazing individual and I look forward to many memories we will share as husband and wife and as scientists.

Financially, this research was supported by a supplement (S1) to a National Institute of Diabetes and Digestive and Kidney Diseases (NIDDK) Grant, R37 DK-18243 and by a NIDDK grant for the Diabetes Research and Training Center at Vanderbilt University, SP60 AM-20593.

TABLE OF CONTENTS

LIST OF TABLES

LIST OF FIGURES

CHAPTER I

INTRODUCTION

Although diabetes mellitus was long considered a disease of minor significance to world health, it is now the most common disease in the world. The past two decades have seen an explosive increase in the number of people diagnosed with diabetes worldwide. The epidemic is chiefly of type 2 diabetes and is largely due to the escalating rates of obesity. Analyses by the International Obesity Task force indicate that approximately 58% of diabetes mellitus globally can be attributed to weight gain. More specifically, in western countries, around 90% of type 2 diabetes cases are attributable to weight gain.

Obesity and type 2 diabetes are thus causally linked. Weight gain leads to insulin resistance and consequently hyperglycemia due to increase hepatic glucose production and decreased peripheral glucose uptake. Insulin resistance places a greater demand on the pancreatic capacity to produce insulin, which also declines with age, leading to the development of clinical diabetes. Although the primary cause of the disease is unknown, the major causative link between type 2 diabetes and obesity is an elevation of circulating FFA and intracellular lipids. To optimize therapy with insulin sensitizing agents, it would be useful to understand how increased lipids contribute to insulin resistance. Therefore, the goal of this dissertation is to gain a better understanding of how changes in lipid metabolism alter glucose homeostasis. This chapter will first provide an introduction to the following: the role of FFA in hormonal regulation of hepatic glucose

production and mechanisms by which elevated lipids alter insulin regulation of glucose homeostasis.

Basic Glucose Metabolism

A schematic of basic glucose metabolism in the hepatocyte is shown in Fig.1.1. Glucose entry into the cell occurs via facilitated diffusion using glucose transporters (GLUT-1 to -5). While GLUT-1 is distributed ubiquitously, GLUT-2 is found in liver, pancreas, intestine and kidney, and GLUT-4 in muscle and adipose tissue, GLUT-3 and -5 are found in brain and testis, and intestinal epithelial cells, respectively. Although GLUT-1 is also expressed in the liver, GLUT-2 is considered to be the most significant hepatic glucose transporter because of its kinetics. GLUT-2 is a membrane bound glucose transporter with a high K_m relative to physiological blood glucose levels. As GLUT-2 is a high capacity transporter, rapid equilibration occurs between the plasma and intracellular compartments, and therefore cellular glucose transport is virtually a linear function of the circulating glucose level (66). Thus, GLUT-2-mediated glucose transport is not thought to be a regulatory site for glucose uptake but rather a glucose sensor, consequently allowing β-cells and hepatocytes to respond accordingly (172). In contrast, insulin stimulates translocation of GLUT-4 from intracellular vesicles to the plasma membrane: therefore it is an important determinant in glucose uptake in muscle and adipose tissue.

Once glucose enters the cell it is phosphorylated by either glucokinase (GK) in the liver and pancreatic β-cells or hexokinase (HK) in muscle and adipose tissue, producing glucose-6-phosphate (G6P). After phosphorylation glucose enters into either

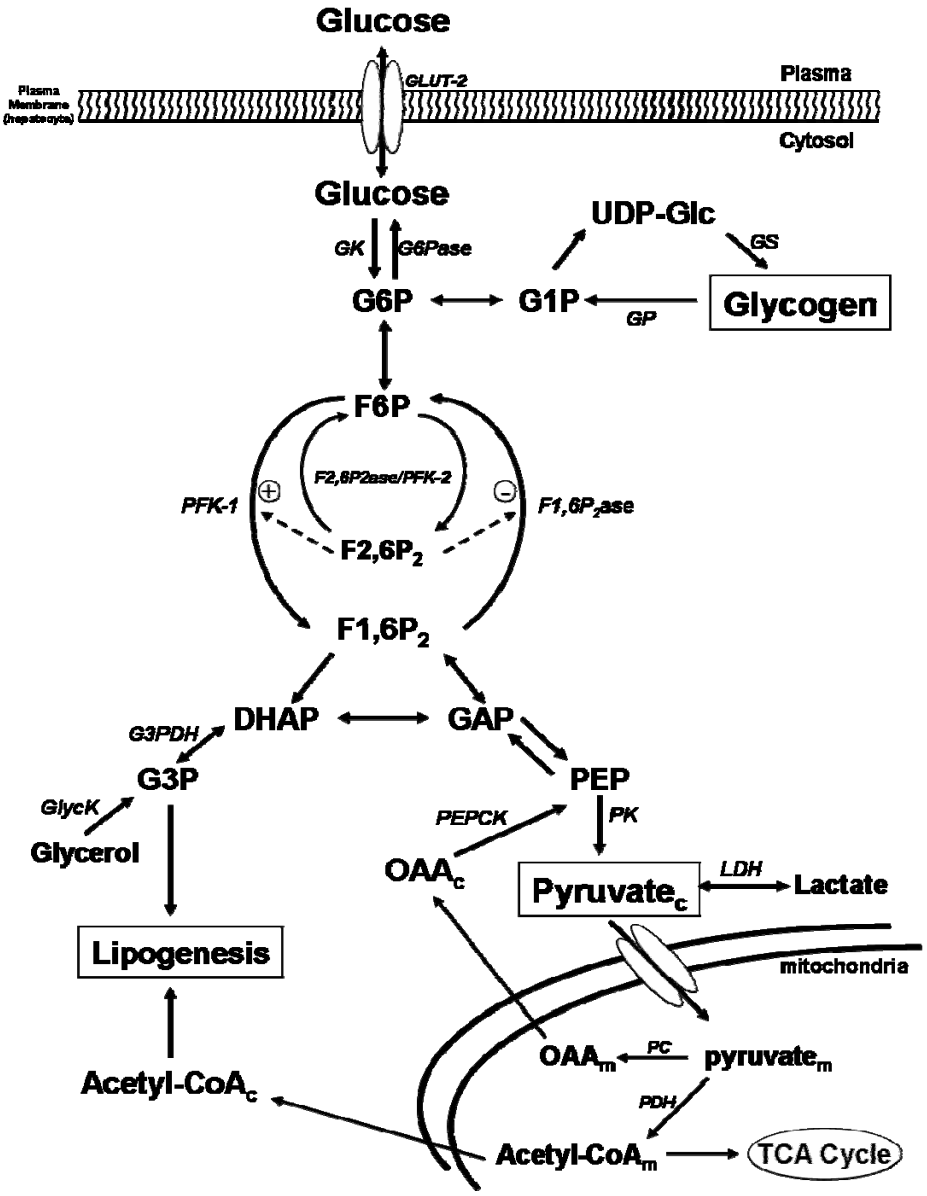

Figure 1.1: Basic glucose metabolism in the hepatocyte. Transporter: glucose transporter -2 (GLUT-2). Substrates: glucose-6-phosphate (G6P); glucose-1-phosphate (G1P); uridine diphosphate-glucose (UDP-Glc); fructose-6-phosphate (F6P); fructose-2,6-bisphosphate ($F2,6P_2$); fructose-1,6-bisphosphate ($F1,6P_2$); dihydroxyacetone phosphate (DHAP); glyceraldehyde-3-phosphate (GAP); phosphoenylpyruvate (PEP); oxaloacetate (OAA); glycerol-3-phosphate (G3P). Enzymes: glucokinase (GK); Glucose-6-phosphatase (G6Pase); glycogen synthase (GS); glycogen phosphorylase (GP); 6-phosphofructo-1-kinase (PFK-1); fructose-1,6-bishposphatase ($F1,6P_2$); phosphofructo-2-kinase/fructose-2,6-bisphosphatase (PFK-2/$F2,6P_2$ase); L-type pyruvate kinase (PK); pyruvate carboxylase (PC); lactate dehydrogenase (LDH); pyruvate dehydrogenase (PDH); phosphoenolpyruvate carboxykinase (PEPCK); glycerol kinase (GlycK); glyceraldehyde-3-phosphate dehydrogenase (G3PDH). cytosolic, (c); mitochondrial, (m).

glycogen synthesis or glycolysis (6, 56). In the liver and kidney the carbon in G6P may also be released into the plasma after removal of phosphate by glucose-6-phosphatase (G6Pase).

Glucose channeled into glycogen, provides a carbohydrate reserve. Glycogen is a branched polymer of glucose which consists of two types of glycosidic linkages, chains of α1→4-linkages with α1→6-branches spaced about 4 to 6 residues along the α1→4 chain. Glycogen synthesis is initiated by the conversion of G6P to glucose-1-phosphate (G1P) by phosphoglucomutase. G1P is then activated to uridine diphosphate (UDP)-glucose by UDP-glucose pyrophosphatase. Glycogen synthase, the regulatory enzyme of glycogen synthesis, then transfers the glucosyl residue of UDP-glucose to the nonreducing end of a glycogen branch. As glycogen synthase is unable to form α1→6 bonds these branches are formed by either glycogen-branching enzyme amylo-(1→4 to 1→6)-transferase or glycosyl-(4→6)-transferase.

When levels of G6P are in excess, (i.e. beyond that needed to replenish carbohydrates reserves) G6P is then channeled into glycolysis for energy production and conversion into triglycerides. In glycolysis, a six-carbon molecule of glucose is degraded by a series of enzyme catalyzed reactions to produce 2 three-carbon molecules of pyruvate. First G6P is converted to fructose-6-phosphate (F6P) which in turn is phosphorylated by phosphofructokinase (PFK-1) to yield fructose-1,6-bisphosphate ($F1,6P_2$). F1,6 P_2 is next split into two three carbon molecules, dihydroxyacetone phosphate (DHAP) and glyceraldehyde-3-phosphate (GAP). Only GAP continues through glycolysis, however DHAP is isomerized into GAP so that both three-carbon molecules can be metabolized to pyruvate. Of note, although DHAP does not continue

through glycolysis, it can enter another metabolic pathway, *de novo* lipogenesis, and thus contributes to the intracellular lipid content. Through a series of reactions, GAP is then converted to phosphoenylpyruvate (PEP) which in turn is phosphorylated by pyruvate kinase to produce pyruvate. Under anaerobic conditions, pyruvate is converted to lactate by lactate dehydrogenase whereas under aerobic conditions, pyruvate is oxidized to acetyl-CoA via pyruvate dehydrogenase and utilized for lipid synthesis (cytosol) or for energy production entering the tricarboxylic acid (TCA) cycle (mitochondria).

Under fasting conditions, glucose is produced by the liver and kidney via two mechanisms: gluconeogenesis and glycogenolysis. Gluconeogenesis is the *de novo* synthesis of glucose from three-carbon molecules such as amino acids (alanine, glutamine) from muscle proteolysis, lactate from glycolysis, and glycerol from lipid catabolism. FFA also provide energy for gluconeogenesis (will be discussed later in this chapter). Gluconeogenesis is conceptually the opposite of anaerobic glycolysis. Alanine and lactate are converted into pyruvate by alanine aminotransferase and lactate dehyrdrogenase, respectively. Pyruvate then enters the mitochondria and is carboxylated by pyruvate carboxlase to produce oxaloacetate, which in turn is decarboxylated by phosphoenolypyruvate carboxykinase (PEPCK) yielding PEP. Through a series of reactions, PEP is converted to $F1,6P_2$. Glycerol enters the gluconeogenic pathway after being phosphorylated by glycerol kinase as DHAP which is then converted to $F1,6P_2$. Fructose-1,6-bisphosphatase ($F1,6P_2$ase) then converts $F1,6P_2$ to F6P which is in equilibrium with G6P. Gluconeogenesis is primarily regulated by fructose-2,6-bisphosphate ($F2,6P_2$), which, in the liver, allosterically activates PFK-1 and inhibits $P1,6P_2$ase. $F2,6P_2$ levels are regulated by the bifunctional enzyme 6-phosphofructo-2-

kinase/fructose-2,6-bisphosphatase (PFK-2/F2,6P_2ase). F2,6P_2 is produced via phosphorylation of F6P by PFK-2 and this reaction is reversed by F2,6 P_2ase. Phosphorylation of the bifunctional enzyme activates F2,6P_2ase while at the same time inhibiting FPK-2, and thus reduces F2,6P_2 levels. This therefore relieves inhibition of P1,6P_2ase and decreases PFK-1 activity, thereby simultaneously stimulating gluconeogenesis and hindering glycolysis.

The second mechanism of glucose production is the degradation of glycogen into glucose, or glycogenolysis. External $\alpha 1 \rightarrow 4$-linked residues of glycogen are removed by glycogen phosphorylase forming G1P, which in turn is converted to G6P by phosphoglucomutase. The rate-limiting regulatory step in glycogenolysis is glycogen phosphorylase as G1P and G6P are in equilibrium.

The final reaction in glucose production, by either gluconeogenesis or glycogenolysis is the conversion of G6P to free glucose by glucose-6-phosphatase (G6Pase). The liver and kidney are the only two sites which are known to express G6Pase (228) but it has been suggested that the gluconeogenic pathway exists in the gut (179). Free glucose is then released into the plasma via GLUT-2.

The Role of FFA in Hormone Regulation of Hepatic Glucose Production (HGP)

Regulation of Hepatic Glucose Production

The liver plays a central role in maintaining glucose homeostasis. This is due to both its anatomical location (it receives portal supply of absorbed nutrients) as well as its ability to consume and produce glucose (183). Following an overnight fast (in the post

absorptive state), the liver is the major contributor of endogenous glucose production with the only other contributing organ being the kidneys. Contribution of the kidneys to endogenous glucose production has been estimated to be 5-23% in the overnight fasted human (41, 88, 269), and 10% (176) or less (118) in the overnight fasted dog leaving the remaining 90% to be produced by the liver. Therefore it is the liver that is primarily responsible for delivering glucose to both the non-insulin-sensitive (nervous, red blood cells, skin, smooth muscle) and the insulin sensitive (muscle and fat) tissues. Thus, the factors which regulate hepatic glucose production (HGP) are particularly important to glucose homeostasis.

HGP is tightly controlled on a minute-to-minute basis by systemic levels of hormones and substrates. When plasma glucose levels rise, the rate of glucose produced by the liver decreases, and vice versa. The simplest regulator of HGP is the plasma glucose level itself, which has direct effects on the liver. However, the endocrine pancreas plays the most significant role in controlling rates of HGP. Pancreatic β- and α-cells respond to circulating glucose levels by modifying their secretion of insulin and glucagon, respectively. Glucagon stimulates glucose production, while insulin inhibits it. The brain also regulates HGP by modulation of liver and pancreatic function via sympathetic and parasympathetic signals, as well as release of epinephrine from the adrenal medulla. Hormones which chronically regulate HGP are cortisol, growth hormone, and thyroid hormone. Recently, the role of the adipocyte in maintaining glucose homeostasis has become evident not only through its effect on the plasma FFA levels but also via the release of adipocyte secreted proteins, such as leptin, resistin,

tumor necrosis factor-α, and adiponectin, to name a few. However, the function(s) of these hormones are not completely understood and will not be discussed in detail here.

Each hormone mentioned above directly and/or indirectly regulates HGP in a specific manner. The first goal of this dissertation is to describe the direct and indirect mechanisms by which insulin, epinephrine, and glucagon acutely regulate HGP (gluconeogenesis and glycogenolysis) and how FFA play a role in regulating their physiological actions at the liver *in vivo*.

Inhibition of HGP by Insulin

Insulin Signaling

Insulin signaling regulates cell growth and differentiation, and promotes energy storage of substrates in fat, liver, and skeletal muscle by stimulating lipogenesis, glycogen and protein synthesis, and inhibiting lipolysis, glycogen and protein breakdown. The effects of insulin are rapid occurring within seconds to minutes after it binds to the insulin receptor and are mediated through a complex network of signaling pathways. The insulin receptor is present in almost all cell types, although the numbers vary from only a few in the erythrocyte to a very significant quantity in insulin-sensitive cells found in liver, skeletal muscle, and adipose tissue.

The insulin receptor is a tetrameric protein that consists of two extracellular α-subunits and two intracellular β-subunits (236, 275). It belongs to a subfamily of receptor tyrosine kinases, which also includes the insulin-like growth factor I receptor and the insulin receptor-related receptor (203). Each of these receptor tyrosine kinases are the

products of separate genes, in which the two subunits are derived from a single chain precursor or proreceptor that is processed by a furin-like enzyme to produce a single α-β-subunit complex. Two of the α–β dimers are linked with disulfide bonds to form the tetramer. Likewise, an additional receptor isoform can be created by the linkage of α–β dimers of the insulin receptor and insulin-like growth factor which form a hybrid complex. Functionally, the insulin receptor acts like an allosteric enzyme in which the α-subunit inhibits the tyrosine-kinase activity of the β-subunit. Upon binding of insulin to the α-subunits, the kinase of the β-subunits is activated. Immediately following activation, the β-subunits undergo transphosphorylation which in turn leads to a conformational change and a further increase in kinase activity.

Upon activation of the insulin receptor, the β-subunits phosphorylate insulin recepotor substrates (IRS) that are linked to two main signaling pathways: the phosphatidylinositol 3-kinase (PI3-K) - AKT/protein kinase B (PKB) pathway and the Ras-mitogen-activated protein kinase (MAPK) pathway. The PI3K/PKB pathway is responsible for most of the metabolic actions of insulin whereas the MAPK pathway regulates cell growth and differentiation. As the focus of this dissertation is the hormone regulation of lipid and glucose metabolism, only the PI3K/PKB pathway will be discussed here (Fig.1.2).

In general, after phosphorylation of tyrosine residues by the insulin receptor, activated IRS proteins bind to intracellular proteins containing *Src* homology-2 (SH2) domains, such as the regulatory subunit(s) of PI3K. Binding of PI3K to phosphotyrosines on IRS proteins leads to the production of the lipid second messenger phosphatidylinositol-3,4,5-triphosphate (PIP_3) from PIP_2 at the plasma membrane. PIP_3

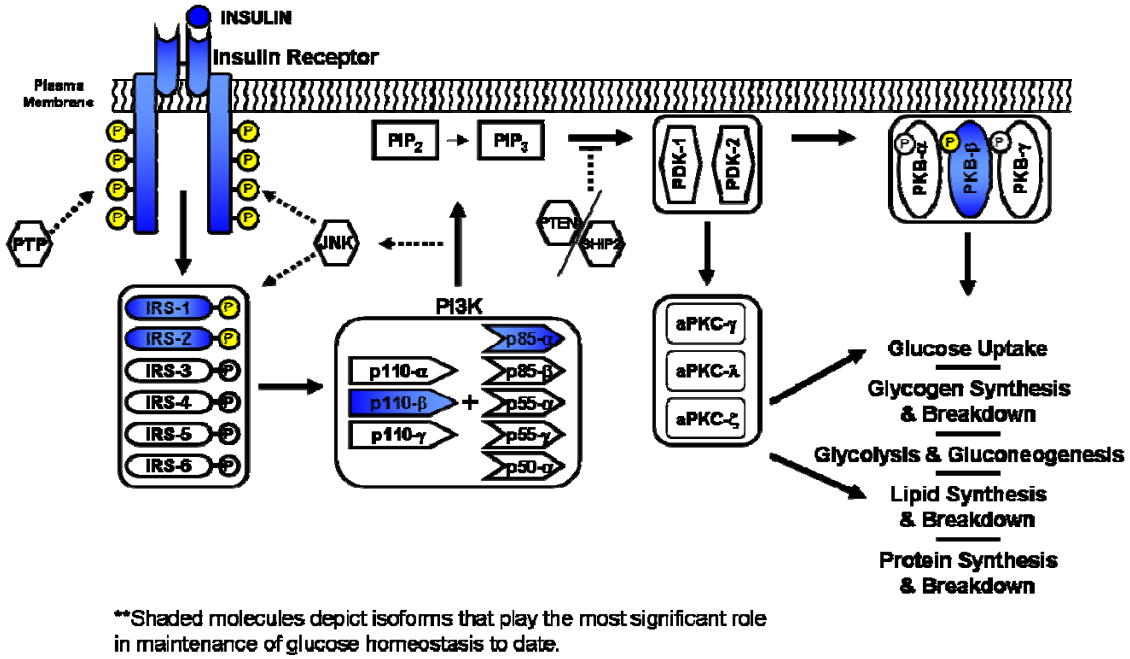

Figure 1.2: Insulin receptor-signaling pathway. Important steps in the insulin pathway are the insulin receptor, the insulin receptor substrates (IRS) 1-6, and the phosphatidylinositol 3-kinase (PI3K) with its multiple isoforms of its regulatory and catalytic subunits, phosphoinositide-dependent kinase (PDK) and protein kinase B (PKB). Negative regulators include c-Jun-N-terminal kinase (JNK), protein tyrosine phosphatase (PTP), phosphotase and tensin homoloque (PTEN), and Src-homology-2 domain-containing inositol phosphatase-2 (SHIP-2). Downstream or intermediate effectors, as well as modulators of these steps atypical protein kinase C (aPKC) and phosphatidylinositol 4,5-biphosphate (PIP2), and phosphatidylinositol 3,4, 5 triphosphate (PIP3). From reference (276).

Then recruits phosphoinositide dependent kinase (PDK) and PKB at the membrane where PKB is phosphorylated by PDK. Activated (phosphorylated) PKB is released into the cytosol where it then mediates many metabolic actions of insulin. The specific metabolic actions of the PI3K/PKB signaling pathway result from differences in the tissue distribution, subcellular localization, and downstream targets of the many isoforms of IRS proteins, PI3K, and PKB (276).

There are six members of the IRS family which have been shown to be activated by the insulin receptor and insulin growth factor-1 receptor kinases (35, 93, 157, 273, 274). IRS-1 and -2 are widely distributed, IRS-3 is largely restricted to adipocytes and brain, IRS-4 is expressed primarily in embryonic tissues, and IRS-5 and -6 have limited tissue expression. Although the IRS proteins are highly homologous, studies in knockout mice and cell lines indicate that the isoforms are not redundant but have harmonizing roles in insulin signaling. IRS-1 knockout mice have impaired insulin action largely in muscle (9). IRS-2 knockout mice have greater defects in insulin signaling in the liver, and show altered growth in neurons and pancreatic β-cells (155). More specifically, tissue specific knockdown of hepatic IRS-1 and IRS-2 using adenovirus short hairpin RNAs *in vivo* has demonstrated that IRS-1 mediates expression of genes involved in gluconeogenesis whereas IRS-2 mediates the expression of genes involved in lipogenesis (277). The functional roles of IRS proteins 3-6 have not been investigated extensively, however it has been shown that IRS-3 and -4 cannot activate MAPK or PI3K to the same degree as IRS-1 and IRS-2 (282). Isoforms of IRS proteins also differ in their cellular compartmentalization (136) and activation kinetics (199).

Studies have demonstrated a pivotal role of PI3K in mediating the metabolic actions of insulin. Inhibitors or dominant negative constructs of PI3K block almost all of insulin's metabolic actions including stimulation of glucose transport, glycogen synthesis, and lipid synthesis. Additionally, PI3K has been shown to play an important role in other insulin-regulated processes such as protein synthesis and attenuation of PEPCK (3) and G6Pase (73) gene expression. The PI3K enzyme consists of a SH2-containing regulatory subunit of ~85 kDa and a catalytic subunit of ~110 kDa, each of which occurs in several isoforms. Several isoforms of the regulatory subunit of PI3K have been identified. These isoforms are derived from three separate genes, *Pik3r-1*, *-2*, and *-3* (8). Pik3r-1 encodes 65-75% of the regulatory subunits, mostly in the form of p85-α, but is also responsible for producing the splice variants, p55-α and p50-α. Tissue distributions of these specific isoforms vary where p85-α is expressed ubiquitously, p55α is limited to skeletal muscle, and p50α is restricted to the liver. *Pik3r-2* produces p85-β and accounts for ~20% of the regulatory subunits in the cell. *Pik3r-3* encodes p55PIK and is expressed at low levels in most tissues. Under normal circumstances, the levels of regulatory subunits are in excess of the catalytic subunits and phosphorylated IRS proteins and therefore free monomeric regulatory subunits compete with the p85-p110 heterodimer for binding to the phosphotyrosines on IRS proteins. Additionally, it has been shown that free p85-α sequester IRS-1 and compartmentalize PI3K activity (167).

The three catalytic isoforms, p110-α, -β, and -δ are derived from three different genes and show different tissue distribution (245). p110-α and -β are expressed in most tissues whereas -δ are limited to leukocytes. Studies over-expressing p110-α and –β suggest p110-β is more important in mediating insulin-stimulated glucose uptake than

p110-α (10). Dimerization of the catalytic subunits to regulatory subunits stabilizes p110 because free p110 is unstable and quickly degraded (301). Binding of p110 to the regulatory subunits also allosterically inhibits enzymatic function until the heterodimer binds to phosphorylated IRS proteins, which relieves its inhibition (301).

PKB has three isoforms, each encoded by a different gene, PKB-α, -β, and –γ (also known as AKT 1-3). PKB-α and –β are widely distributed with PKB-β highly expressed in insulin-sensitive tissues whereas PKB-γ is predominantly expressed in the nervous system. Although PKB-α and –γ do not seem to play a significant role in glucose homeostasis (51, 281), PKB-β deficient mice display insulin resistance and develop diabetes due to the ability of insulin to decrease hepatic glucose output and induce glucose untilization (50). Additionally, PKB-β has been found to be co-localized with GLUT-4-containing vesicles, a characteristic not observed by PKB-α and –γ (37).

Another downstream effecter in the PI3K pathway in mediating the metabolic effects of insulin is the activation of aPKC. In contrast to conventional or novel PKCs, aPKCs are not senstitive to the second messengers, calcium and diacylglycerol (DAG). The mechanisms of aPKCs are similar to PKB, in that they require PIP3 and phosphorylation by PDK-1 (262). aPKCs have been shown to play a role in insulin-stimulated glucose uptake and GLUT-4 translocation in adipocytes and muscle (94). aPKCs are also involved in the regulation of lipid synthesis in the liver by increasing sterol-regulatory-element binding protein 1-c expression (95). The PKC isoenzymes -ζ and -λ are encoded by two different genes, and their levels of expression vary, PKC-λ is the main aPKC in skeletal muscle and adipose tissue of mouse whereas PKC-ζ is more prominent in humans (94).

There is negative regulation of the PI3K pathway at the levels of the insulin receptor, IRS proteins, PI3K, and PKB. One class of regulatory proteins involved is the protein tyrosine phosphatases (PTPs), the most studied of which is PTP-1B. PTB-1B interacts directly with the insulin receptor and dephosphorylates important tyrosine residues, thereby reducing activity (89). IRS proteins are also negatively regulated by PTPs, serine phosphorylation, and ligand-induced downregulation. Many kinases that can phosphorylate IRS proteins on serine residues, such as c-Jun-N-terminal kinase (JNK)(178), extracellular signal-regulated kinase (ERK) (31), and S6 kinase (122) are activated by insulin, which suggests that serine phosphorylation of IRS proteins might represent a negative-feedback mechanism for the insulin-signaling pathway. PI3K can be negatively regulated by phosphatase and tensin homologue (PTEN) (292) and SH2-containing inositol 5'-phosphatase-2 (SHIP-2) (258), which dephosphorylates and inactivates PIP_3. PKB activity is regulated by several inhibitory molecules including protein phosphatase-2A and the PH-domain leucine-rich repeat protein phosphatase (PHLPP) (102), which directly dephosphorylates and deactivates PKB. Another regulator, tribbles-3 (TRB-3), binds to unphosphorylated PKB and inhibits its phosphorylation and therefore activation (81). Cross-talk from other pathways have also been shown to negatively regulate insulin signaling, however this will be discussed later in this chapter.

Insulin Action In Vivo

Acute inhibition of HGP primarily involves suppression of glycogenolysis (GLY) with only a modest effect on gluconeogenesis (GNG). It was previously thought that insulin completely suppressed GNG, however, this concept was based on *in vitro* studies

where insulin suppresses expression and activity of key GNG enzymes (138, 166). More recently, *in vivo* studies in humans (25, 106) and dogs (83) indicate that insulin only moderately reduces GNG. During a 4-h hyperinsulinemic-euglycemic clamp in over-night-fasted normal subjects, Boden et al. (25) showed GNG to fall from 1.5 to 0.67 mg/kg/min after 4-h of hyperinsulinemia ($P < 0.05$). Under similar conditions, Gastaldelli et al. (106) reported that GNG decreased from 1.2 to 0.8 mg/kg/min during a 2½-h hyperinsulinemic-euglycemic clamp ($P < 0.05$). Although significant decreases were observed, both of these studies utilized the ^2H_2O method to approximate rates of GNG, which overestimates the effects of insulin on GNG (by underestimating GNG because of glycogen cycling), indicating that insulin only has a modest impact on GNG. Using three techniques to assess GNG, one of which being the ^2H_2O method, Edgerton et al. (83) reported no significant drop in GNG flux during a 3-h intraportal infusion of insulin (twofold basal) in over-night-fasted dogs. However, peripheral insulin levels were significantly lower compared to the human studies mentioned above. In a subsequent study, Edgerton et al. (85) showed that insulin at levels fourfold above basal, did not significantly inhibit of GNG, even in the absence of appreciable glycogen breakdown. In these same studies, rates of GLY (mg/kg/min) fell from 1.3 to -0.3 in the Boden study (25), from 0.8 to -0.2 in the Gastaldelli study (106), and from 1.0 to 0.4 in the Edgerton study (83) (values of ^2H_2O method). Taken together, insulin inhibits HGP primarily by suppressing GLY, since only a small fraction of GNG accounted for the fall in HGP.

The traditional view has been that insulin, being secreted directly into the liver via the portal vein, was responsible for the hormone's inhibitory effect on the liver. Work

from our lab has shown that the liver sinusoidal insulin level does indeed potently regulate HGP. Studies were carried out in overnight-fasted, pancreatic clamped conscious dogs in which the insulin level was either increased (253) or decreased (256) in the portal vein (thus resulting in a rise or fall in hepatic sinusoidal insulin levels, respectively) in the absence of any change in the arterial plasma insulin level. Glucose was infused peripherally in order to maintain euglycemia and glucagon was successfully clamped at basal values in both studies. Net hepatic glucose output (NHGO) fell 40% by 30 minutes in response to a rise in hepatic sinusoidal insulin whereas NHGO increased fourfold by 15 minutes in response to a decline in hepatic sinusoidal insulin. Our lab has also shown that this effect is independent of the route (hepatic artery vs. portal vein) by which insulin enters the liver (254). Taken together, these studies clearly show that HGP is rapidly and sensitively regulated by the direct action of insulin at the liver. Additionally, as net hepatic lactate output did not increase or decrease in response to a selective rise or fall of hepatic sinusoidal insulin respectively, and there was no significant change in GNG in either study, these studies provide further evidence that insulin suppresses HGP primarily by inhibiting GLY.

In 1987, Prager et al. (215) was the first to suggest that peripheral insulin could suppress HGP in the absence of any change in the portal insulin level, and thus implicated an indirect mechanism of inhibition. This concept has been supported by many investigators (1, 16, 109, 162) but the indirect mechanisms by which insulin suppresses HGP is probably best demonstrated in an elegant study performed by Sindelar et al. (253). This study suggested that HGP is inhibited by selective increases in the portal vein or arterial insulin level. A greater than 50% reduction in NHGO was

observed in response to either a 14 μU/ml rise in the portal insulin level (no change in arterial insulin) or a 14 μU/ml rise in the arterial insulin level (no change in portal insulin). Although the extent by which insulin inhibited HGP was similar in both groups, the time required to detect a marked suppression was significantly different. The rise in portal insulin quickly (~30 min) suppressed NHGO whereas 1-h was necessary to detect significant suppression following a rise in the arterial insulin. Most interestingly, the above studies also showed that the direct effect of insulin on HGP resulted from a rapid decrease in GLY, whereas the indirect effect of insulin resulted primarily from a reduction of GNG flux. This decrease in GNG resulted from a fall in net hepatic uptake of gluconeogenic precursors due a reduction in gluconeogenic amino acids from muscle, glycerol from adipose tissue, and the diversion of carbon derived from glycolysis to lactate within the hepatocyte. Furthermore, Sindelar et al. (254) went on to show that equimolar increments in arterial and portal insulin levels resulted in an additive effect on the liver.

Insulin can also indirectly affect HGP by acting on the pancreatic α cell to inhibit the secretion of glucagon, a known potent stimulating hormone of glucose production. In fact, the suppression of glucagon secretion is dose dependently regulated by insulin starting as low as 10 μU/ml (189). It is thought that the architecture of the murine pancreatic islet where α-cells reside in the periphery of the β-cell core, is unique in that blood flows from the β-cells to the α-cells, allowing insulin to inhibit glucagon secretion. However, the pattern of cell distribution in the pancreatic islet architecture of humans, non-human primates, and dogs is such that the α-cell is dispersed throughout the islet (33). Nevertheless, it has been shown in both humans (161) and dogs (108) that insulin-

inhibited glucagon secretion can explain a fraction of the indirect effects of insulin on the liver. Additionally, it has been thought that insulin has an indirect effect on the liver via its action on the brain. Our lab has previously shown that under hypoglycemic conditions, insulin acts on the brain to rapidly stimulate sympathetic outflow, increasing circulating levels of epinephrine, glucagon, and cortisol, and ultimately enhancing HGP (70). Furthermore, studies from the Rossetti group, showed that a chronic decrease in hypothalamic insulin receptors and hepatic vagotomy both resulted in a 50% decrease of insulin-suppressed glucose production (196, 213). Subsequent work by this group suggests that insulin acts in the medial hypothalamus via adenosine triphosphate (ATP)-sensitive potassium channels to inhibit hepatic gluconeogenesis (197, 213). However, in the overnight-fasted conscious dog, in the presence of arterial hyperinsulinemia and hepatic insulin deficiency, an acute fourfold rise in the head insulin level did not bring about any inhibition of HGP (86). Compared to chronic manipulation of the "brain-liver' circuit, it is possible that an acute rise in insulin is not sufficient to cause a change in the hypothalamic signal to the liver, and thus does not play a role in the acute regulation of HGP. Additionally, it is likely that the significance of insulin's indirect action on the liver via the brain varies among species. Differences in rates of basal HGP in rats (~6 mg/kg/min), mice (15-20 mg/kg/min), and dogs and humans (~2-3 mg/kg/min) may be due to dissimilarities in neural drive to the liver. Therefore, insulin action in the brain may be essential to regulate HGP in rodents but not species with lower rates of basal HGP.

In summary, it is clear that insulin regulates HGP by both direct action on the liver, inhibiting GLY and indirect actions on skeletal muscle, adipose tissue, and perhaps

the brain, reducing GNG. As insulin is secreted from pancreatic β-cells directly into the portal vein, and 50% of the insulin that survives first pass degradation by the liver subsequently acts on peripheral tissues, it seems logical for insulin to quickly inhibit GLY (predominant contributor to HGP except under extreme fasting conditions), whereas GNG is reduced at a much slower rate.

Role of FFA in Mediating Insulin Inhibition of HGP

In the study by Sindelar et al. (253) in which the direct and indirect mechanisms of insulin on HGP were addressed, they found that the only ~20% of the suppression of HGP could be explained by the change in hepatic gluconeogenic precursor uptake. Additionally, a correlation between the time course of peripheral insulin's suppressive effect on HGP and the suppression of lipolysis was observed. One hour following a selective rise in peripheral insulin (no change portal insulin), levels of plasma FFA were maximally suppressed and NHGO was significantly reduced. Bergman and colleagues also noted a strong correlation between the effects of a rise in systemic insulin on the liver and its effects on the adipocyte (2, 14). To determine the extent of contribution of FFA suppression to insulin's overall action on the liver, Sindelar et al. (255), again brought about a selective rise in the arterial plasma insulin concentration in the overnight-fasted conscious dog. In one group, the fall in FFA and glycerol was prevented by an Intralipid (triglyceride emulsion) and heparin infusion, while in the other group, FFA and glycerol were allowed to fall. When plasma FFA levels were prevented from falling, 50% of insulin's indirect inhibition of HGP was eliminated. As expected, a small increase in net hepatic glycerol uptake occurred due to the mild elevation of glycerol that

occurred during the Intralipid/heparin infusion. However, this change in glycerol uptake in the liver could only account for small fraction of the reduction of the fall in NHGO. Therefore, the main substrate responsible for the reduction in insulin's indirect effect on HGP was FFA. In agreement with this, Bergman and colleagues also showed that the inhibitory effect of a rise in systemic insulin on HGP could be partially reduced by preventing the fall in plasma FFA (225).

In the original studies by Sindelar et al. (253), addressing the direct and indirect effects of insulin on HGP, they suggested that the indirect action resulted primarily from a reduction of GNG. Although net hepatic GLY and GNG were not assessed in their study in which falls of FFA and glycerol were prevented, the data suggest that a decrease in FFA relieves the inhibition of glycolysis and in turn reduces the net rate of GNG. The fall in plasma FFA levels and therefore hepatic FFA uptake correlated almost perfectly with an increase in net hepatic lactate production that was not evident when the FFA level was clamped.

In a normal overnight-fasted dog, basal HGP results primarily (~60%) from GLY. When glycogen is being degraded, some of the carbon derived appears to be routed down the glycolytic pathway to pyruvate and then exits the liver as lactate. Increased cellular FFA uptake and subsequent increases in fatty acid oxidation can alter enzymatic activity of glucose metabolic pathways. Active β-oxidation during fasting leads to increased intracellular NADH and acetyl-CoA in the mitochondria. An elevation of NADH would favor the activation of lactate dehydrogenases, converting the gluconeogenic precursors to pyruvate. Acetyl-CoA also supports activation of the gluconeogenic pathway as it is an essential activator of pyruvate carboxylase . Additionally, NADH and acetyl-CoA are

known allosteric inhibitors of pyruvate dehydrogenase. This inhibition blocks the utilization of pyruvate for energy metabolism and directs pyruvate, lactate, and alanine toward the synthesis of glucose. Furthermore, inhibition of PDH promotes formation of oxaloacetate (OAA) (107) and citrate (221). An increase in intracellular citrate levels leads to the inhibition of PFK, a rate limiting enzyme in the glycolytic pathway, thus impeding glycolysis and further promoting gluconeogenesis.

When FFA levels were allowed to fall in the study by Sindelar et al. (255), the ratio of β-hydroxybutyrate (β-OHB) to aceteoacetate (Acac) fell from 1 to 0.5 indicating that less fatty acids were being oxidized by the liver. In contrast, when the FFA level was clamped, the β-OHB/Acac ratio did not change. Therefore, it is possible that the fall in FFA, resulted in a decrease in hepatic β-oxidation, lowering intracellular NADH, acetyl-CoA, and citrate levels. This in turn decreased the promotion of gluconeogenesis and relieved the inhibition of glycolysis, redirecting glycogenolytically derived carbon within the hepatocyte. Indeed, the increase in hepatic lactate output corresponded to the decrease in NHGO.

Although the work shown here suggests that the indirect effects of insulin on the adipocyte mediate the hormone's ability to suppress GNG, it is possible that decreased FFA may also enhance insulin's ability to suppress GLY. In fact, it has been shown that elevated FFA produce hepatic insulin resistance by inhibiting insulin suppression of GLY (25). Additionally, it has been suggested that increases in plasma FFA impair insulin signaling in the liver. However, the mechanisms by which FFA alter hepatic insulin sensitivity will be discussed later in this chapter under *FFA-Induced Insulin Resistance*.

Stimulation of HGP by Epinephrine and Glucagon

Epinephrine and Glucagon Signaling

To stimulate HGP, epinephrine and glucagon bind to the adrenergic receptors and the glucagon receptor, respectively, all of which belong to the G-protein coupled superfamily of receptors. G-proteins are heterotetrameric, plasma-membrane, guanosine-nucleotide-binding proteins that are closely associated with hormone receptors bound to the inner surface of the plasma membrane and consist of three subunits, α, β, and γ. G-proteins are classified according to the different α-subunits. For example, $G_{\alpha s}$ stimulates adenylate cyclase which lead to in increase in intracellular cAMP, $G_{\alpha q}$ activates phospholipase C and ultimately releases stored intracellular Ca^{2+}, and $G_{\alpha i}$ decreases adenylate cyclase activity and therefore lowers intracellular cAMP levels. In the resting state, guanosine diphosphate (GDP) is bound to the GTPase on the α-subunit. Binding of a hormone results in a conformational change of the receptor and recruits G-proteins stimulating exchange of GDP for guanosine triphosphate (GTP) on the Gα-subunit. GTP binding leads to release of the β- and γ-subunits, allowing the subunits to either positively or negatively influence a variety of signaling pathways.

Adrenergic receptors are classified into two classes, α and β. The α class is subdivided into α_1 and α_2 adrenergic subclasses. According to the present classification, subclasses α_1 and α_2 have been further subdivided into α_{1A}, α_{1B}, and α_{1D} which belong to the $G_{\alpha q}$ coupled receptors and α_{2A}, α_{2B}, α_{2C}, and α_{2D} which belong to the $G_{\alpha i}$ coupled receptors, respectively (127). The β class are $G_{\alpha s}$ coupled receptors and consists of β_1, β_2, and β_3 (and perhaps β_4) subtypes (29). The distribution of adrenergic receptor

subtypes in dog and human liver are primarily α_1 and β_2 (144, 160, 164). It has been shown that epinephrine acts primarily on hepatic β_2-receptors in the dog (55) and human (18, 72, 227). Like the β_2-adrenergic receptor, the glucagon receptor is mainly coupled to $G_{\alpha s}$ proteins. Therefore, epinephrine- and glucagon-stimulated HGP is mediated by increases in intracellular levels of cAMP (91, 271). Since epinephrine and glucagon act on the same pathway, although through different receptors, the rise in cAMP presumably results in similar changes in cellular mechanisms following hormone binding. Evidence has been provided that concomitant administration of the hormones at doses giving maximal activity results in an increase in glycogenolysis that was no larger than with either individual hormone, implying that both hormones act via the same pathway (182).

Following hormone binding, active $G_{\alpha s}$ stimulates adenylate cyclase, increases cAMP levels, and activates protein kinase A (PKA) which in turn initiates a series of protein phosphorylation reactions (Fig. 1.3). As a single receptor can activate many α-subunits, the hormone response is amplified and results in a substantial increase in the strength of the signal. Within seconds of recognition of the hormone, this chain of reactions leads to subsequent changes in glycogenolysis, glycogen synthesis, gluconeogenesis and glycolysis.

Epinephrine and glucagon signaling promote hepatic GLY, while at the same time, opposing hepatic glycogen synthesis. Activated PKA phosphorylates and activates glycogen phosphorylase kinase (GPK) which subsequently phosphorylates glycogen phosphorylase (GP), leading to its activation. Activation of GP then phosphorylates

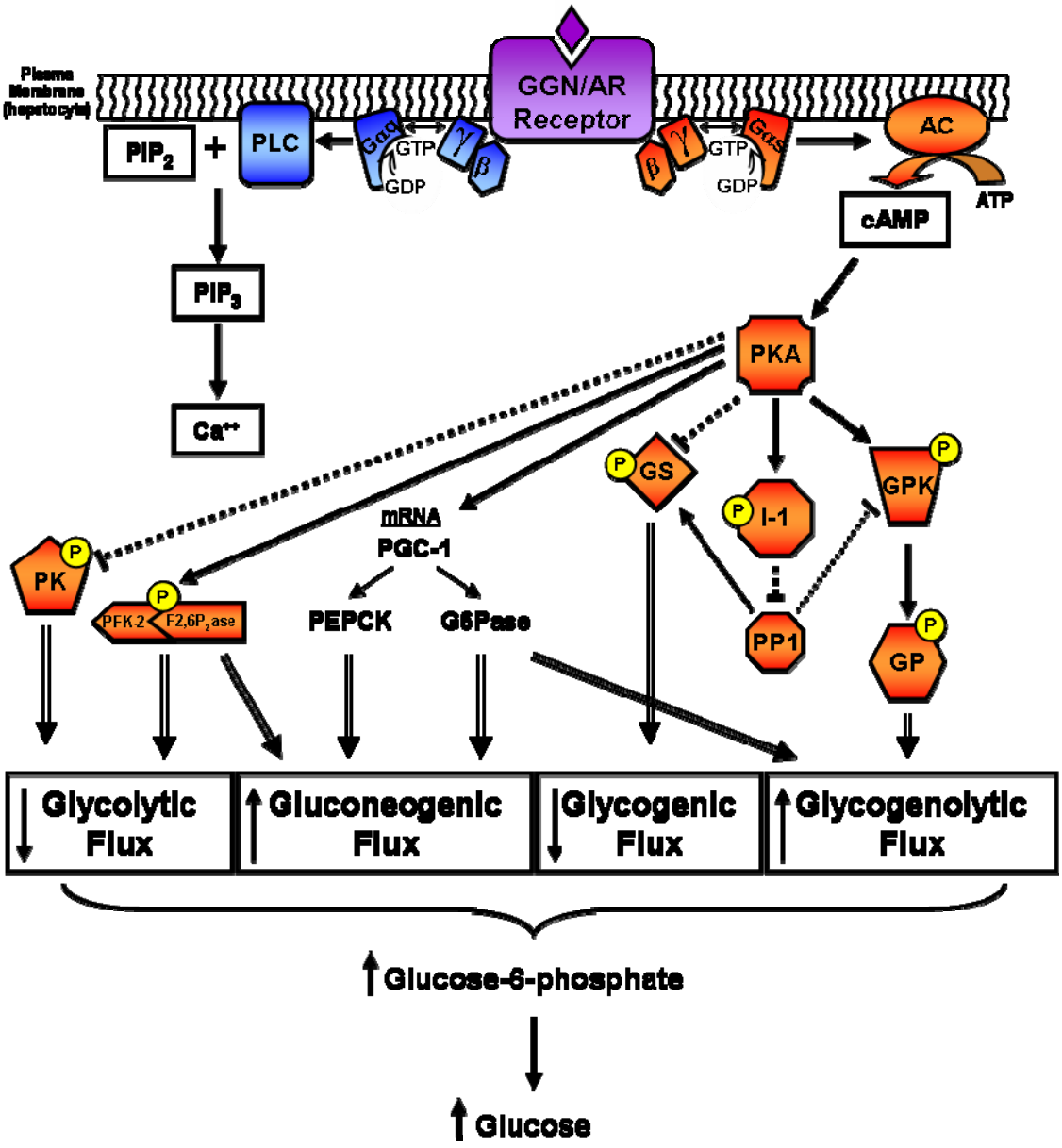

Figure 1.3: Glucagon /adrenergic receptor–signaling pathway. Glucagon (GGN); Adrenergic receptor (AR); adenylate cyclase (AC); adenosine 3', 5' –cyclic monophosphate (cAMP); protein kinase A (PKA); glycogen synthase (GS); glycogen phosphorylase kinase (GPK); glycogen phosphorylase (GP); inhibitor 1 (I-1); protein phosphatase 1 (PP1); peroxisome proliferators-activated receptor-γ coactivator-1 (PGC-1); phospoenolpyruvate carboxykinase (PEPCK); glucose-6-phosphatase (G6Pase); 6-phosphofructo-2-kinase/fructose-2,6-bisphosphatase (PFK-2/F2,6P_2ase); L-type pyruvate kinase (PK);.phospholipase C (PLC); phosphatidylinositol 4,5-biphosphate (PIP_2); phosphatidylinositol 3,4, 5 triphosphate (PIP_3). From reference .(140)

glycogen, which results in hepatic glycogenolysis and the production of G6P. PKA also directly phosphorylates and inactivates glycogen synthase (GS) in the liver (134, 135). Another target of PKA is Inhibitor-1, which is activated upon phosphorylation. Activation of this protein inhibits protein phosphatase-1 (PP1), which is turn reduces inhibition of GP and activation of GS. Taken together, activated PKA alters the activity of many enzymes involved in glycogen metabolism, simultaneously stimulating glycogenolytic flux and inhibiting glycogenic flux.

In addition to their effects on glycogen metabolism, epinephrine and glucagon stimulate HGP by increasing gluconeogenesis and inhibiting glycolysis. Phosphorylation of the bifunctional enzyme, PFK-2/F2,6P_2ase, by PKA results in inhibition of the kinase and activation of the bisphosphatase, causing a decrease in the intracellular levels of F2,6P_2. Likewise, isolated hepatocytes treated with either β-adrenergic agonists or glucagon results in a rapid decrease in F2,6P_2 levels . Reduction of intracellular levels of F2,6P_2 decreases PFK-1 activity and relieves inhibition of P1,6P_2ase, and therefore simultaneously inhibits glycolytic flux and promotes gluconeogenic flux . Additionally, glucagon has been shown to increase hepatic gene expression of PEPCK, a rate-limiting enzyme of GNG (114). PKA activation by cAMP leads to phosphorylation of a cAMP response element-binding (CREB) protein which in turn binds to a cAMP response element (CRE) in the promoter region of the transcriptional coactivator, peroxisome proliferator-activated receptor-γ coactivator-1 (PGC-1), and up-regulates its transcription. Together with another transcription factor, hepatocyte nuclear factor-4, PGC-1 increases PEPCK transcription (298). An increase in cAMP also results in phosphorylation and inactivation of pyruvate kinase. In fact, it has been shown that glucagon strongly inhibits

carbon flux through pyruvate kinase, whereas epinephrine was only marginally effective (45, 97, 231). Inactivation of pyruvate kinase would lead to an inhibition of glycolytic flux and an increase in gluconeogenic flux. These findings suggest that as both glucagon and epinephrine increase levels of cAMP and therefore activate PKA, these changes in phosphorylation and/or expression of the enzymes mentioned here may be possible mechanisms by which they stimulate hepatic GNG.

Concurrent stimulation of GLY/GNG fluxes and inhibition of glycogenic /glycolytic fluxes raises the amount of G6P available for dephosphorylation by G6Pase, thereby increasing the pool of glucose for HGP. It has been shown that both glucagon and cAMP induce stimulate gene expression of the catalytic subunit of G6Pase in the dog (129). Furthermore, recent studies suggest that the up-regulation of G6Pase by glucagon is at least partially due to increased transcription of the G6Pase gene in a PKA-dependent manner involving PGC-1 (298). It has also been shown that cAMP signals via a CRE located in the promoter region of G6Pase (129). Therefore it could be suggested that epinephrine and glucagon activation of PKA increases G6Pase activity, and thereby promote GLY as well as GNG.

Furthermore, both epinephrine and glucagon are known to activate and stimulate signal transduction of the $G_{\alpha q}$ class of G-proteins. The activation of $G_{\alpha q}$ leads to the activation of phospholipase C, production of PIP3, and subsequent release of intracellular calcium (Fig. 1.3) (271). As mentioned above, α_1-receptor, a $G_{\alpha q}$ coupled receptor, is also expressed in dog and human liver. Thus, epinephrine can technically increase intracellular calcium levels. However, activation of α-adrenergic receptors are not thought to be the primary site through which the catecholamine exerts its effects in the

dog (55, 91) and human (18, 72, 227). Although glucagon has been shown to affect glucose production by increasing intracellular calcium (153) the relevance of this observation is currently unclear. For instance, some investigators found that calcium increases only in the presence of supra-physiological glucagon levels (268), while others found that calcium can increase with physiological glucagon concentrations (153).

Epinephrine and Glucagon Action In Vivo

Although epinephrine and glucagon presumably stimulate liver glucose production via the same signaling pathway, their actions at liver *in vivo* are considerably different. Both hormones increase HGP in a rapid, time-dependent manner, however, sensitivities of each hormone at the liver differs on the molar basis. Additionally, the mechanism (GLY vs. GNG) by which the hormones stimulate HGP are dissimilar as a result of their differential direct and indirect actions on the liver.

Earlier studies in human and dog showed that the effect of epinephrine on HGP is, on a molar basis, much less potent than that of glucagon (265, 266). To establish an equal effect on HGP requires a fifty-fold rise in epinephrine but only a four-fold rise in glucagon. However, despite its low potency, epinephrine plays a critical role in glucoregulation during stress, as circulating levels of the hormone can increase by 100- to 200-fold.

The stimulatory effect of epinephrine on HGP has been shown to arise from both indirect actions on muscle and adipose tissue and direct action on the liver. Release of epinephrine from the adrenal medulla results in the stimulation of adipose tissue lipolysis, muscle glycogenolysis, and HGP. Early studies in the human suggested that increases in

circulating epinephrine stimulate HGP by increasing GNG via mobilization of alanine and lactate from muscle and FFA and glycerol from adipose tissue (56, 61, 177, 234). Epinephrine is also known to cause a release of lactate from adipose tissue (74). Studies in the conscious dog have shown that increases in net hepatic uptake of alanine, lactate, and glycerol are secondary to the effects of the hormone on peripheral tissues; thus further suggest that the indirect effects of epinephrine stimulate HGP by increasing GNG (46, 234). Additionally, Chu et al. (57) showed that the direct effects of epinephrine on HGP are a result of increases in GLY alone. The concept that epinephrine increases HGP by indirect and direct stimulation of GNG and GLY respectively, was elegantly demonstrated in a study by Chu et al (56). The study was carried out in over-night fasted, pancreatic clamped conscious dogs in which epinephrine was infused either intraportally or peripherally. The hepatic sinusoidal epinephrine levels were indistinguishable (~565 pg/ml) whereas the arterial levels differed significantly (Δ~1000 pg/ml) between the two groups. Intraportal infusion of epinephrine resulted in an increase in GLY but not GNG, suggesting epinephrine had no direct effect on GNG. In contrast, peripheral infusion of the hormone resulted in increased gluconeogenic precursor supply to the liver, and thereby stimulated HGP primarily by increasing GNG. Interestingly, this rise in GNG was accompanied by a compensatory decrease in GLY, despite equal levels of hepatic sinusoidal epinephrine in the two groups, which implies a reciprocal relationship between the two processes. Subsequent studies by Chu et al. (55) showed that the direct stimulation of GLY by epinephrine was completely inhibited by adrenergic blockade and that this effect was specific to β_2-adrenergic receptors. Furthermore, in a different study, peripheral infusion of epinephrine showed that portal delivery of adrenergic blockers

inhibited the GLY effect of epinephrine, but not its GNG effect (58). Taken together these studies clearly demonstrate that epinephrine stimulates HGP indirectly by increasing hepatic GNG and directly increases hepatic GLY.

The stimulatory effect of glucagon on HGP has been shown to arise from its direct action on the liver, with a half-maximal activation occurring in ~4.5 minutes (77). Glucagon-stimulated HGP results primarily in an increase in GLY and to a lesser extent in a modest and slower rise in GNG (48). Studies have also shown, however, that glucagon can stimulate both the transcription and activation of enzymes involved in hepatic GNG *in vitro* (91, 154, 211, 212) and that it can increase hepatic gluconeogenic flux *in vivo* (175, 266), yet the contribution of the rise in GNG to the overall increase in glucose production is small. The hormone can only cause a transient, modest increase in hepatic gluconeogenesis presumably because it has no effect on gluconeogenic substrate release from muscle and little or no effect on lipolysis in adipose tissue. Thus, any enhancement of gluconeogenic flux would transiently increase GNG. However, eventually plasma gluconeogenic substrate concentrations would fall, and the gluconeogenic contribution to total HGP would return toward its basal rate.

Taken together, it is clear that the actions of epinephrine and glucagon on the liver differ considerably despite the fact that they both trigger a rise in intracellular cAMP within the hepatocyte. Although the hormones are not equally potent at the liver, the main difference in the actions of the two hormones is their ability to act on peripheral tissues. Both epinephrine and glucagon act directly on the liver to stimulate GLY. However, unlike glucagon, epinephrine acts on muscle and adipose tissues to mobilize gluconeogenic precursors to the liver. Given the fact that glucagon is secreted from

pancreatic α-cells directly into the portal vein, and only a small percentage of glucagon survives first pass degradation by the liver, it would be expected that the hormone acts solely on the liver to stimulate HGP. Therefore, it could be hypothesized that during stress (i.e. hypoglycemia) when secretion of both glucagon and epinephrine is increased, the peripheral release of epinephrine from the adrenal medulla, augments HGP largely by stimulating GNG. In fact, our lab has shown that when glucagon and epinephrine are raised concurrently, they have additive effects and amplify hepatic glucose production by increasing both GLY and GNG (116).

Role of FFA in Mediating Epinephrine and Glucagon Stimulation of HGP

It has been well established that epinephrine simultaneously increases HGP and lipolysis. Epinephrine released from the adrenal medulla results in a concomitant rise in epinephrine levels in the hepatic sinusoids and the arterial circulation, with the latter causing an elevation in the plasma FFA level. As mentioned above, portal administration of epinephrine increased GLY but had no effect on GNG, whereas peripheral administration resulted in a rise in GNG that was accompanied by a compensatory decrease in GLY. A substantial increase in arterial levels (78%) and net hepatic uptake (122%) and fractional extraction (50%) of FFA occurred during the peripheral infusion of epinephrine that was not observed when the hormone was infused into the portal vein. In a different study (54), the authors showed that increases in plasma FFA resulted in a stimulation of GNG and inhibition of GLY, similar to that observed by the indirect action of epinephrine. Therefore, epinephrine stimulation of lipolysis could explain a significant portion of the indirect action of the hormone on the liver.

To determine the effect of elevated FFA on the glycogenolytic and gluconeogenic effects of epinephrine, Chu et al. (53) carried out a study in the over-night fasted, pancreatic clamped conscious dog in which the hormone was infused intraportally in the presence or absence of a simulated rise in lipolysis brought about by a peripheral infusion of Intralipid and heparin. The necessary hyperglycemic/hyperlipidemic control data were also obtained. As expected, the effect of intraportal administration of epinephrine on HGP arose solely from an increase in GLY. Interestingly, a rise in FFA and glycerol significantly limited epinephrine's glycogenolytic effect while at the same time augmenting its gluconeogenic action at the liver. This increase in GNG flux (230%) was greater than that observed in the hyperglycemic/hyperlipidemic control, despite similar increases in net hepatic uptake of FFA. Therefore it was clear that the increase in FFA potentiated the gluconeogenic effect of epinephrine. Notably, the arterial blood level and net hepatic of glycerol increased during the infusion of Intralipid/heparin. However, if all of the glycerol taken up by the liver was converted to glucose, it could only account for 22-25% of the observed increase in the net gluconeogenic flux. Taken together, this study strongly suggests that the indirect actions of epinephrine alter the mechanisms by which glucose is produced by the liver and that this result from its ability to release FFA from adipose tissue.

It is likely that elevated FFA mediate the effects of epinephrine on the liver by their ability to hamper glycolytic flux and promote gluconeogenic flux, which in turn could possibly result in an inhibition of glycogenolytic flux. In response to epinephrine-stimulated GLY, an increase in net hepatic lactate output (NHLO) occurs presumably because some of the carbon produced by glycogen breakdown enters the glycolytic

pathway and exits the liver as lactate. Indeed, in the study by Chu et al. (53) mentioned above, the rise in plasma FFA completely blocked epinephrine's increase in NHLO and actually resulted in a substantial increase in the uptake of lactate by the liver. As discussed in *Role of FFA in Mediating the Effects of Insulin on HGP* earlier in this chapter, increased cellular FFA uptake and subsequent increases in β-oxidation can lead to elevated intracellular levels of NADH, acetyl-CoA, and citrate which in turn collectively result in the inhibition of glycolytic flux and the promotion of gluconeogenic flux. Therefore, the subsequent increases in G6P could possibly result in the inhibition of GLY.

Although glucagon receptors are located on adipocytes and glucagon has been shown to stimulate lipolysis *in vitro*, the hormone has little to no effect on adipose tissue *in vivo*. However, if glucagon was simultaneously elevated with FFA (as seen postprandially in type 2 diabetes), it might be hypothesized that FFA would alter glucagon action in a similar manner to that seen with epinephrine. Therefore the goal of ***Specific Aim I*** was to determine the effects of physiological incremental increases in glucagon and FFA on the contributions of GLY and GNG of HGO.

The Effects of Elevated Lipids on Insulin Regulation of Glucose Homeostasis

Glucose homeostasis reflects a delicate balance between glucose production and glucose uptake. This balance is best demonstrated during periods following food consumption and fasting when plasma glucose levels remain in a narrow range. As it was alluded to earlier in this chapter, insulin serves as the primary regulator of plasma glucose

levels. Insulin rapidly suppresses hepatic glucose production and 50% of secreted insulin that survives first pass degradation by the liver subsequently acts on peripheral tissues to stimulate glucose uptake. Insulin action in peripheral tissues also alters lipid and protein metabolism and secretion of other glucoregulatory hormones (i.e. glucagon) which then indirectly mediate its actions on glucose homeostasis. When insulin-sensitive tissues become less responsive to the hormone, because of insulin resistance and/or insulin deficiency, as seen with type 2 diabetes, profound dysregulation of substrate metabolism and hormone secretion produces elevations in fasting and postprandial glucose levels.

Increased adiposity is strongly associated with insulin resistance and type 2 diabetes. Interestingly, not all fat is created equal; increased visceral adiposity shows a stronger correlation with insulin resistance than an increase in subcutaneous adiposity (63, 105). Because visceral adipocytes have a higher rate of lipolysis, they are thought to be less sensitive to the anti-lipolytic effects of insulin and therefore may release more FFA than subcutaneous adipocytes. Furthermore, increased visceral adiposity is thought to lead to greater FFA delivery to the liver. It is also thought that an increased mass of stored triglyceride in adipose tissue leads to enlarged adipocytes further worsening resistance (especially in visceral adipose tissue) to the ability of insulin to suppress lipolysis. This results in increased release and circulating levels of FFA.

Although it is not yet entirely understood why obesity results in insulin resistance/type 2 diabetes, FFA have emerged as a major causative link. There is strong evidence for increased fasting and postprandial plasma FFA levels both in individuals with diabetes and in those at risk for the disease. It has been estimated that elevated plasma FFA account for the entire insulin resistance in non-diabetic obese patients and

~50% of the insulin resistance in obese patients with type 2 diabetes (19). Acute elevations of FFA have been shown to induce insulin resistance (20, 26, 229, 257) in a dose-dependent manner (24). Chronic increases of FFA, as seen in most obese patients, also induce insulin resistance (20, 237). Moreover, Santomauro et al. (237) normalized chronically elevated FFA overnight in obese subjects and improved insulin sensitivity. Additionally, acute elevations of FFA results in stimulation of insulin secretion (67, 96, 111, 204) whereas, chronically elevated FFA impair insulin secretion (235). Thus, it is plausible that FFA-induced insulin resistance precedes the development of type 2 diabetes. In fact, it has been shown in individuals with impaired glucose tolerance that plasma FFA are increased despite normal glucose levels (12, 207, 224).

A second causative link between obesity and type 2 diabetes it that of lipotoxicity, or the accumulation of triglyceride in non-adipose tissues, such as the liver, skeletal muscle, and pancreas. Interestingly, lipotoxicity in skeletal muscle shows a stronger correlation with insulin resistance than elevated levels of plasma FFA (152, 195, 202). Lipotoxicity in the liver, or hepatic steatosis, has a very robust association with hepatic insulin sensitivity; in fact, studies have indicated that insulin resistance is more closely related to changes in hepatocellular than intramyocellular triglyceride content (11, 173, 242). Additionally, lipotoxicity in the pancreas has been implicated in β-cell apoptosis (143, 152).

For many decades the importance of insulin sensitivity and insulin deficiency as pathogenic factors which lead to the development of type 2 diabetes has been debated. Deletion of the insulin receptor in skeletal muscle (34) does not cause diabetes, suggesting that insulin resistance alone is not sufficient to cause diabetes. In fact,

population studies have confirmed that both impaired insulin action and β-cell dysfunction are observed in groups at risk for the disease (163). The remainder of this chapter will focus on the mechanisms by which elevated lipids induce insulin resistance and alter β-cell function.

The Effects of Elevated Lipids on Insulin Sensitivity

FFA-Induced Insulin Resistance

Substrate Competition

In 1963, Randle et al. were the first to propose that FFA play a role in the development of insulin resistance in obesity and type 2 diabetes and demonstrated that FFA compete with glucose for substrate oxidation in rat heart muscle and diaphragm (221). They speculated that an increase in FFA levels result in an elevation of the intramitochondrial acetyl-CoA/CoA and NADH/NAD+ ratios, with subsequent inactivation of PDH. This in turn causes citrate levels to increase in the cytoplasm, leading to inhibition of PFK, a rate limiting enzyme in glycolysis. Inhibition of glycolysis, and subsequent increases in G6P levels would inhibit hexokinase II activity, which would result in an increase in the intracellular glucose pool and decrease muscle glucose uptake. Consistent with this, hyperinsulinemic-euglycemic and –hyperglycemic clamps in healthy humans have shown that increased plasma FFA levels inhibit whole-body glucose disposal (98, 146, 229, 278, 297). A similar mechanism could operate the liver, however, with the caveat that glucokinase, rather than hexokinase II, is the primary

hepatic enzyme involved in glucose phosphorylation. In fact, our laboratory has shown that FFA-inhibition of net hepatic glucose uptake was associated with a shift in net hepatic lactate balance from output to uptake, suggesting an inhibition of glycolysis (185).

Randle's hypothesis of substrate competition can also apply in terms of FFA ability to stimulate GNG. As proposed in the *Role of FFA in Mediating the Effects of Insulin on HGP* section of this chapter, a rise in hepatic β-oxidation could result in elevated intracellular NADH, acetyl-CoA, and citrate levels, which subsequently results in increased P1,6P_2ase and decreased PFK-1 activities, thereby simultaneously stimulating gluconeogenesis and hindering glycolysis. Early evidence supported FFA regulation of GNG (92). However, due to the reciprocal relationship between GNG and GLY, a concept known as autoregulation, stimulation of GNG might not result in the overproduction of glucose by the liver. Our laboratory has shown that an acute rise in FFA inhibited GLY and stimulated GNG without altering the overall production of glucose by the liver (54). It has also been reported that a rise in FFA did not alter HGP in healthy (230) or type 2 diabetic subjects (141). In agreement with this, Boden et al. (21) showed that increasing and decreasing plasma FFA stimulated and suppressed GNG, respectively, but did not change glucose production.

Hexosamine Pathway

As the entry of F6P in the glycolytic pathway could be limited by the inhibition of PFK by FFA, carbon flux could be increased via the hexosamine pathway (F6P → glucosamine-6-P), a route of glucose metabolism, although quantitatively small, which

has been implicated in the development of insulin resistance (233). Saturated fatty acids have been shown to increase the expression of glutamine-fructose-6-phosphosphate aminotransferase, the rate-limiting enzyme in this pathway (288). Additionally, Hawkins et al. (123) demonstrated that prolonged increases of plasma FFA led to elevated UDP-GlcNAc (end-product of hexosamine pathway) which preceded muscle insulin resistance. However, Choi et al. (52) later showed that elevations of FFA at more physiological levels induced insulin resistance with no increase of end products of the hexosamine pathway. Thus, the role of the hexosamine pathway in FFA-induce insulin resistance remains uncertain.

Insulin Signaling

Studies by Boden et al. suggest that the mechanism of substrate competition alone cannot account for the effects of FFA on glucose disposal. They reported a 3-h lag before FFA-induced inhibition of glucose uptake was manifest, which is more consistent with a translational or post-translational event than with allosteric regulation as suggested by Randle (221). Additionally, Roden (229) and Boden (26) have shown that impaired insulin-stimulation of glucose uptake by FFA results in a decrease (rather than a increase) in intracellular G6P and that this precedes reduced rates of glucose oxidation and glycogen synthesis. These studies showed that one-third of the acute FFA-inhibition of glucose uptake occurs from substrate competition where as the remainder results via non-oxidative mechanisms. Indeed, human studies from the Shulman group have shown that increased plasma FFA inhibit insulin-stimulated glucose transport as a consequence of decreased IRS-1-associated PI3K activity (80, 252). These findings led to an alternative

hypothesis that increased delivery of FFA to skeletal muscle and subsequent elevations of intracellular FFA and/or FA metabolites [diacylglycerol (DAG), fatty acyl CoA, and ceramides] suppress insulin signaling upstream of, or directly at the level of PI3K. The Shulman group went on to show in rats that lipid infusion resulted in a reduction of insulin-stimulated IRS-1 tyrosine phosphorylation and was associated with activation of protein kinase C (PKC)-θ (115), a well-known serine kinase that has been shown to be potently activated by DAG. Subsequent studies from this group showed that PKC- θ knockout mice are protected from lipid-induced insulin resistance in skeletal muscle (149). Additionally, the Boden group, has shown in humans that FFA increased the translocation of PKC isoforms βII and δ from the cytosol to the membrane fraction(137). PKC has been shown to cause insulin resistance by decreasing tyrosine phosphorylation of IRS-1 and of the insulin receptor (103, 222, 300). Additionally, rats on a high fat diet show increases in the content of long-chain fatty acyl CoA and alter the PKC isozymes θ and ε in muscle (241).

FFA produce hepatic insulin resistance by inhibiting insulin suppression of GLY (25). Currently very little is known about the biochemical mechanisms by which FFA inhibit insulin signaling in the liver. However, it has been shown that the development of hepatic insulin resistance occurs within a 2 to 4-h delay after elevation of plasma FFA (24-26) suggesting that impaired insulin action at the liver may be similar to that seen in muscle. The fact that liver-specific insulin receptor knockout mice demonstrate severe hepatic insulin resistance (99) suggests that an impairment of insulin signaling could result in increased HGP. Additionally, Lam et al. have reported that FFA-induced hepatic insulin resistance is associated with activation of PKC-δ in liver of rats (156).

Of note, specific metabolic actions of the PI3K-mediated insulin signaling pathway results from differences in tissue distribution, subcellular localization, and downstream targets of the many isoforms of IRS proteins, PI3K, and PKB. Therefore, it is possible that only some metabolic pathways are impaired by FFA while others remain unaltered or even hyper-stimulated.

Inflammation

Adipose tissue has received a great deal of recognition in the pathogenesis of obesity-induced insulin resistance not only because of increased release of FFA but also because of its dysregulated production of cytokines which reflects an inflammatory state of the organ. In obesity, accumulation of lipid in adipocytes, initiates the activation of two classic inflammatory signaling pathways, the c-Jun N-terminal kinase (JNK) pathway and the IkB/NFκB pathway. Both pathways are thought to play important roles in insulin resistance but do so via dissimilar mechanisms. JNK has been shown to promote insulin resistance through the serine phosphorylation of IRS-1 (4, 128). Under resting conditions, nuclear factor-κB (NFκB) is bound to its inhibitor IκB. Phosphorylation of IkB by its kinase (IKK) leads to the degradation of IκB, releasing NFκB for translocation to the nucleus. Unlike JNK, IKK does not phosphorylate IRS-1 but rather does so through the transcriptional activation of NFκB, which targets gene products with potential involvement in insulin resistance (251). Stimulation of JNK and IkB/NFκB pathways regulate protein phosphorylation and transcriptional events which subsequently lead to the release of pro-inflammatory cytokines such as tumor necrosis factor-a (TNF-a) and interleukon-6 (IL-6). By mechanisms not completely understood,

macrophages then infiltrate the adipose tissue which also produce pro-inflammatory cytokines, further promoting local and potentially systemic inflammation.

As enlarged adipocytes are also resistant to the anti-lipolytic effects of insulin, increased FFA could potentially activate these pathways and induce-inflammation. Indeed, Olefsky and colleagues have demonstrated in 3T3-L1 adipocytes that FFA-impaired insulin signal transduction and decreased insulin stimulated GLUT-4 translocation was associated with activated JNK and IKK-β and increased secretion of TNF-α (194). Lipid accumulation in adipocytes also activates the unfolded protein response to increase endoplasmic reticulum (ER) stress in adipose tissue (200) which has been shown associated with the activation of JNK (200) and NFκB (133).

The Boden group (137) has found acute FFA-induced insulin resistance to be associated with the activation the IkB/NFκB pathway. High doses of salicylate, which block IKK activity (296), can ameliorate insulin resistance in diabetes and obesity (150, 302). It has also been shown in rats, that pretreatment with salicylate prevented the deleterious effects of elevated FFA in skeletal muscle and that this was associated with decreased serine/threonine phosphorylation of IRS-1 and increased IRS-1-associated PI3K activity (150). More over, mice lacking IKK-β are protected from lipid induced insulin resistance (150). In humans, FFA-induced insulin resistance in skeletal muscle was associated with increased DAG, PKC, and decreased IκB-α (137). Additionally, saturated fatty acids may also promote the synthesis of ceramides in muscle which may correlate with the degree of insulin resistance (267). Ceramides can also activate inflammatory pathways including JNK and NFκB (272). Taken together, these studies suggest that increased FFA delivery and subsequent increases in intracellular FA

metabolites leads to the activation of JNK and/or IKK which in turn decreases PI3K activity and thus glucose uptake.

Although not much is known in terms of FFA-activation of inflammation in the liver, transcriptional targets of NFκB are activated in the liver with increasing adiposity. Transgenic mice with liver-specific constitutively active IKK-β have profound hepatic and moderate systemic insulin resistance (36). Interestingly, hepatic production of pro-inflammatory cytokines IL-6, IL-1β and TNF-α was increased and this was accompanied by activated Kupffer cells (resident liver macrophages). Systemic neutralization of IL-6 and treatment with salicylate both improve insulin sensitivity in these mice. These results suggest that sub-acute hepatic inflammation by low-level activation of NFκB leads to local and systemic insulin resistance.

Of note, high-fat diet-induced and obesity-induced insulin resistance does not lead to macrophage infiltration (289) or activation of IKK-β/NFκB (232) in skeletal muscle. Additionally, deletion of IKK-β or inhibition of NFκB specifically in muscle does not normalize insulin resistance in obese mice. Therefore, even though inflammation can be activated in skeletal muscle, it appears that in obesity-associated insulin resistance, skeletal muscle is a target of inflammation rather than a site of initiation.

Vascular Function

It has been demonstrated that endothelial-dependent vasodilation is reduced in states of insulin resistance, including type 2 diabetes (264). Baron and colleagues have provided extensive evidence that insulin increases blood flow in skeletal muscle and they have implicated that the effect is mediated via the nitric oxide (NO) system (13). This

same group has shown that an 8-h infusion of Intralipid and heparin reduced the effect of insulin on blood flow by ~50% (263). Additionally, elevation of FFA causes an impairment of endothelial-dependent and insulin-mediated vasodilation associated with a small increase in systolic arterial pressure (264). Furthermore, postischemic flow-mediated dilation of the brachial artery was impaired after 2-h of lipid infusion and associated with activation of NFκB in mononuclear cells (280). FFA have also been shown to directly activate NFκB in cultured endothelial cells. Taken together these findings suggest that increased FFA *in vivo* might reduce insulin action by lowering blood flow in insulin-sensitive tissues and thus decreasing insulin availability.

Insulin Clearance

Insulin clearance, the plasma volume cleared of insulin in a unit of time, is characterized by the binding of insulin to its receptor, its internalization and degradation by the insulin degrading enzyme (IDE) or insulinase, or lysomal enzymatic processes (284). Removal of insulin from the circulation may be involved in mediating some aspects of insulin action by decreasing its availability. The main site for insulin clearance is the liver, removing ~50% following first-pass extraction (82, 239). In obese subjects with hyperinsulinemia and high levels of FFA, hepatic insulin clearance is impaired. Yoshii et al. (299) have previously shown in conscious dogs that an intraportal (vs. peripherally) oleate infusion decreased hepatic insulin clearance. Additional studies from this group using rats (156) have implied that activation of PKC-δ mediates the FFA-induced decrease in hepatocyte insulin binding. In fact, activation of PKC can increase insulin receptor internalization (39). Additionally, others have suggested that FFA

directly bind to IDE, inhibiting its activation (120). As insulin clearance is characteristic of all insulin-sensitive tissues (38, 40, 261), elevated FFA may decrease insulin availability to skeletal muscle and adipose tissue as well.

Lipotoxicity

Mechanisms of Lipotoxicity

The net content of intracellular triglyceride depends on the relative activities of enzymes involved in lipid metabolism that influence fatty acid uptake and synthesis versus those that influence fatty acid oxidation and export. When input (uptake or synthesis) of fatty acids to a cell exceeds its output (degradation or export), triglycerides accumulate within the tissue. The conventional explanation is that an impairment of fat deposition in adipose tissue due to either excess energy intake or decreased storage capacity result in increased release of FFA from adipocytes. FFA must then be partitioned for storage in other tissues such as the liver, skeletal muscle, and pancreas. In fact, Boden et al. have shown that raising blood FFA levels increased intramyocellular triglyceride in a time- and dose-dependent manner (27).

Dietary substrates can also contribute to lipotoxicity. Dietary fatty acids can serve as a direct source of substrate for tissue triglyceride via two mechanisms: spillover into the plasma FFA pool and through the uptake of lipoproteins [intestinally derived chylomicrons and very low density lipoproteins (VLDL, in which triglycerides are derived from either plasma FFA pool or dietary fatty acids)] and/or their remnants. Carbohydrates can be driven towards lipid synthesis by a process known as *de novo*

lipogenesis. Carbohydrates provide two routes to formation of triglycerides: the glycerol backbone via triose phosphate and fatty acids via acetyl CoA (Fig. 1.1). In the liver, fructose can directly contribute to both of these routes by two mechanisms: increased hepatic glucose uptake (an effect likely to be mediated by increased translocation of glucokinase) (198, 250) and bypassing the regulated conversion of F6P to $F1,6P_2$ (119). It is thus a relatively unregulated source of substrate for triglyceride synthesis. Dietary substrates are particularly relevant given the increased consumption of energy-dense diets (214). Interestingly, it has been suggested that fructose consumption (essentially in soft drinks) may be a causal factor for the development of insulin resistance (32).

The specific origin of the lipids that accumulate within non-adipose tissues remains unknown. However, in one study, using a multiple-stable-isotope approach, Park and colleagues very elegantly demonstrated that plasma FFA (59%), *de novo* lipogenesis (26.1%), and dietary FFA (14.9 %) all contribute to hepatic triglyceride accumulation in obese patients with hepatic steatosis (79). Contributions of these sources to muscle lipotoxicity are unknown although it is thought that lipid accumulation is largely due to increased delivery of plasma and dietary FFA to the tissue.

Decreased oxidation of lipids due to a functional mitochondrial impairment could lead to an increased deposition of triglycerides. Obese and type 2 diabetic individuals have smaller mitochondria in skeletal muscle (139, 145) and exhibit impaired activity of the respiratory chain (124). Magnetic resonance studies have shown that insulin resistance in offspring of patients with type 2 diabetes is characterized by both elevated intramyocellular triglycerides and impaired mitochondrial ATP synthesis (210). Peterson et al. (209) found similar defects in muscle and liver in lean elderly subjects with severe

insulin resistance compared to young controls. Additionally, ultrastructural mitochondrial defects in patients with NAFLD may be indicative of defective oxidation as these patients also have reduced respiratory chain activity (205) and impaired ATP synthesis after a fructose challenge (64). Collectively these studies suggests that impaired mitochondrial lipid oxidation can lead to the accumulation of triglycerides in myocytes and hepatocytes.

In the liver, decreased lipid export via VLDL production could also contribute to elevated hepatocellular triglycerides. The liver's ability to mobilize triglycerides depends on adequate VLDL formation and export which requires normal production of apolipoprotein B (apoB)-100 and microsomal triglyceride transfer protein (MTP) activity. Abetalipoproteinemia which is caused by a variety of mutations in the gene for a subunit of MTP (191, 226, 244, 290), is a recessive human disease characterized by near complete absence of apolipoprotein-B (apoB)-containing lipoproteins (e.g. chylomicrons, VLDL, and LDL) in plasma. MTP plays a pivotal, if not an obligatory role, in the assembly and secretion of triglyceride rich apoB-containing lipoproteins. As expected, liver specific MTP knockout mice (218) exhibit hepatic steatosis and decreased hepatic triglyceride secretion while mice overexpressing hepatic MTP show an increase in *in vivo* hepatic triglyceride secretion (279). Therefore, an impairment of hepatic triglyceride export could contribute to triglyceride accumulation in the liver. In fact, it has been shown that apolipoprotein production is impaired in patients with NAFLD (43).

Although insulin resistance is strongly correlated with liver and muscle lipotoxicity, triglyceride accumulation could be a result of conserved insulin sensitivity of lipogenic pathways. One mechanism by which insulin stimulates lipogenesis is the

activation of a key transcription factor, sterol regulatory element-binding protein-1c (SREBP-1c), a well know stimulator of all lipogenic genes. In states of insulin resistance, it might be expected that activation of SREBP-1c would be decreased. Surprisely, however, in two mouse models of profound insulin resistance, insulin stimulates hepatic SREBP-1c transcription, resulting in increased rates of *de novo* lipogenesis (249). Although SREBP-1c expression has not been determined, hepatic *de novo* lipogenesis has also been shown to be increased in patients with NAFLD (76). Moreover, SREBP-1c can also activate acetyl-CoA carboxylase (130) and inhibit MTP expression which would in turn suppress fatty acid oxidation (174) and VLDL formation (240), respectively, further contributing to a positive triglyceride balance. Therefore, while insulin signaling pathways regulating glucose metabolism may be impaired in states of insulin resistance, other metabolic pathways may be over-stimulated as a result of hyperinsulinemia.

Lipotoxicity-Induced Insulin Resistance

Although there is a strong correlation with lipotoxicity and type 2 diabetes it unclear as to whether the accumulation of intracellular lipid is a cause or effect of a decreased insulin response. The mechanisms by which lipotoxicity could possibly bring about insulin resistance is not precisely understood. It is hypothesized that the triglycerides themselves do not affect insulin action directly but rather represent a reservoir of FFA and/or fatty acid metabolites in which arise during esterification or hydrolysis of intracellular triglycerides and inhibit insulin signaling. It is supposed that the general mechanism of FFA-induced insulin resistance as described above also occurs

with lipotoxicity. Additionally, inflammatory gene expression increases in liver with adiposity (36). Therefore as lipotoxicity is strongly associated with obesity, this suggests that triglyceride accumulation might activate resident macrophages and induce a sub-acute inflammatory response similar to adipose tissue inflammation. Additionally, hepatic lipid accumulation also activates the unfolded protein response to increase ER stress, which is well known to activate both JNK and NFκB.

The Effects of Elevated Lipids on β-cell Function

It has been well-established that acute elevations in plasma FFA stimulate insulin secretion (67, 96, 111, 204). The chronic effects, however, are controversial. *Ex vivo* studies in animal islets or the perfused pancreas suggest a biphasic influence of FFA on insulin secretion in which elevated FFA stimulate insulin release for the first 6-h whereas after 24- to 48-h secretion is inhibited (235, 303). In humans, however, a 48-h lipid infusion increased glucose-stimulated insulin secretion (23). This suggested that it may take longer for FFA to suppress insulin secretion in humans. When chronically elevated FFA were lowered in obese diabetic and non-diabetic subjects, the rates of insulin secretion decreased by 30-50%, supporting the concept that FFA serve as a insulin secretagogue (22, 237). However, interpretations of these results are challenging. Bergman has proposed a hyperbolic relationship between insulin secretion and insulin sensitivity, such that a reduction in sensitivity can be compensated by a similar increase in β-cell responsiveness (15). Indeed, when chronic elevations of FFA were lowered in the studies mentioned above, peripheral insulin sensitivity improved. Therefore, it is

possible that the decrease in insulin secretion was not due to a direct effect of FFA on the β-cell but reduced peripheral insulin resistance. Although prolonged elevations of FFA appear to have negative effects on the β-cell *in vitro* and in smaller animals, their effects on insulin secretion in humans is doubtful. According to Boden and Carnell, even though most obese subjects have elevated FFA only 15-20% of them develop overt type 2 diabetes, suggesting a genetic predisposition to β-cell failure.

The concept of lipotoxicity in the β-cell has been put forward. Increased esterification of triglycerides (including *de novo* lipogenesis) appears to be the major metabolic avenue as pancreatic β-cells do not have mechanisms to rid themselves of surplus triglyceride. *In vitro* studies, forcing triglyceride synthesis impaired glucose-stimulated insulin secretion (147). Schwartz et al. (143) placed dogs on a high-fat diet (80%) and reported reduced insulin secretion after seven weeks, and putative β-cell lipotoxicity. The severe impairment of insulin secretion in Zucker diabetic *fa/fa* rats is associated with lipotoxicity in β-cells, as triglyceride levels were elevated fifty-fold (246-248, 283, 287). It has been suggested that lipotoxicity in pancreatic islets might lead to β-cell apoptosis via *de novo* ceramide formation (168), activation of PKC (87), inhibition of PKB (294), excessive NO production (68, 247), or induction of NFκB (295). Kharroubi et al. (148) have shown that apoptosis is the main mode of lipid-induced cell death however, the results implicate that this process is activated by an ER stress response independent of NFκB and NO.

Specific Aims

As β-cell function is impaired in overt type 2 diabetes, lower plasma insulin levels during the postprandial period should result in a decreased insulin response at both the pancreatic α-cell and adipocyte and therefore cause glucagon and FFA levels to be elevated. Indeed, in subjects with type 2 diabetes, it has been shown that glucagon secretion from α-cells is not suppressed and has even been shown to be elevated (75, 243). Additionally, FFA normally fall during the postprandial period, but in individuals with type 2 diabetes FFA levels remain elevated (223, 224). As an insufficient decrease in HGP is involved in the postprandial hyperglycemia observed in type 2 diabetes, it is possible that elevated levels of glucagon and FFA could be responsible for the increase in hepatic glucose production by the liver in these patients. Although it is well established that both glucagon and FFA are essential regulators of glucose production by the liver, it is unclear how they interact to acutely regulate HGP.

Like glucagon, epinephrine directly stimulates HGP by increasing GLY. However, the indirect actions of epinephrine alter the mechanisms (stimulate GNG/inhibit GLY) by which glucose is produced by the liver and that this results from its ability to release FFA from adipose tissue. Since the direct actions of both epinephrine and glucagon on HGP are mediated by cAMP, it could be hypothesized that the elevated FFA, as seen postprandially in type 2 diabetes, would alter hepatic glucagon action in a similar manner to that seen with epinephrine. Therefore the goal of ***Specific Aim I*** was to determine the effects of physiological increments in glucagon and FFA on the contributions of GLY and GNG of HGO.

Although there is a strong correlation with lipotoxicity (152, 195, 202) and type 2 diabetes it unclear as to whether the accumulation of intracellular lipid is a cause or an effect of a decreased insulin response. The putative role of triglyceride accumulation in non-adipose tissues is based solely upon correlative results. Therefore, one remains unconvinced regarding the importance of triglyceride accumulation as a direct cause of insulin resistance and a contributor to the pathogenesis of diabetes. Since our laboratory uses the conscious dog as an experimental model due to its good reflection of glucose metabolism in humans and allowance for invasive experimental design, the goal of ***Specific Aim II*** was to create a canine model of hepatic steatosis.

The net content of triglyceride in the liver depends on the relative activities of enzymes involved in lipid metabolism that influence fatty acid uptake and synthesis versus those that influence fatty acid oxidation and export. When input (uptake or *de novo* lipogenesis) of fatty acids to hepatocytes exceeds their output (degradation or export), triglycerides accumulate within the liver. Therefore, in an attempt to induce fatty liver in the dog, lipid metabolism was altered by 3 different treatments: 1) a 10% fructose diet, 2) elevating hepatic FFA flux, or 3) elevating hepatic FFA flux while simultaneously inhibiting triglyceride export from the liver using the microsomal triglyceride transfer protein inhibitor, CP-346086.

The goal of ***Specific Aim III*** was to examine whole body insulin sensitivity following treatment regimens to induce hepatic steatosis. To assess whole body insulin sensitivity, a two-step hyperinsulinemic-euglycemic clamp was performed on the day immediately following completion of the treatment period used to induce hepatic steatosis in the dog.

CHAPTER II

MATERIALS AND METHODS

Animals and Surgical procedures

Animal Care

Experiments were conducted on fifty-two 18 h fasted conscious mongrel dogs (10-30 kg) of either gender that had been fed a standard diet of meat (Pedigree canned beef, Vernon, CA) and chow (Laboratory Canine Diet no. 5006, PMI Nutrition International, INC., Brentwood, MO) once daily. The diet totaled 33% protein, 12% fat, 49.5% carbohydrates, and 5% fiber, based on dry weight. Water was available *ad libitum.* Only dogs that had a good appetite, a leukocyte count < 18,000/mm^3, a hematocrit >35%, and normal stools were used for studies. The animal housing and surgical facilities met Association for Assessment and Accreditation of Laboratory Animal Care International standards. Protocols were approved by the Vanderbilt University Medical Center Animal Care Committee.

Surgical Procedures

Surgery was performed on each dog under general anesthesia (15 mg/kg pentothal sodium presurgery and 2.5% isofluorane during surgery) approximately 16 (Specific Aim I) or 25 (Specific Aim III) days prior to the metabolic study. The dog was placed in a supine position on a surgical table with an 8.5 mm inner diameter (ID) endotracheal tube (Concord/Portex, Kenee, NH), and ventilated with a tidal volume of 400 ml at a rate of

14 breaths per minute. A laparotomy was performed by making a midline incision 1.5 cm caudal to the xyphoid process through the skin, subcutaneous layers and linea alba, and extending caudally 15-20 cm.

Silastic catheters (0.03 inch internal diameter; Dow-Corning Midland, MI) were placed into splenic and jejunal veins for the intraportal infusions of glucagon, insulin, and Intralipid/heparin (Specific Aim III). A portion of the spleen was retracted and a distal branch of the splenic vein was selected for cannulation. By blunt dissection, a small section of the vessel was exposed and then ligated with 4-0 silk (Ethicon, Inc, Sommerville, NJ). A small incision was made in the vessel and a silastic infusion catheter (0.04 in ID; HelixMedical, Carpintera, CA) was inserted and advanced until the tip of the catheter lay 1 cm beyond the bifurcation of the main splenic vein. Another silastic catheter (0.04 in ID) was inserted a branch of a jejunal vein and passed anterograde until the tip of the catheter lay approximately 1 cm proximal to the coalescence of two jejunal veins. The catheters were secured in place with 4-0 silk, filled with saline (Baxter Healthcare Corp, Deerfield, IL) containing 200 U/ml heparin (Abbott Laboratories, North Chicago, IL), knotted and placed in a subcutaneous pocket prior to closure of the skin.

For Specific Aim III, an additional silastic catheter (0.04 inch ID) was placed into the splenic vein (as described above) for the daily 3 h infusion of Intralipid and heparin. Excess catheter was tunneled subcutaneously, and attached to a vascular-access-port (Access Technologies, Inc., Skokie, IL). The vascular-access-port was sutured to the muscular bed between the scapulae.

For blood sampling, silastic catheters (0.04 inch i.d.) were placed into the left hepatic vein, the hepatic portal vein, and left femoral artery. The central and left lateral

lobes of the liver were retracted cephalically and caudally, respectively. The left common hepatic vein and the left branch of the portal vein were exposed. In the left branch of the portal vein, a 14-gauge angiocath (Benton Dickinson Vascular Access, Sandy, UT) was inserted 2 cm from the central lobe of the liver. In the hole created by the angiocath, a silastic catheter (0.04 in ID) was inserted and passed retrograde about 4 cm into the portal vein so that the tip of the catheter lay 1 cm beyond the bifurcation of the main portal vein. Another angiocath was inserted into the left common hepatic vein 2 cm from its exit from the left lateral lobe. A silastic sampling catheter was inserted and advanced anterograde 2 cm. Both catheters were secured with three ties of 4-0 silk through the adventitia of the vessels and around the catheters. The sampling catheters were filled with heparinized saline, knotted and placed in a subcutaneous pocket, with excess catheter looped within the peritoneum.

A catheter was inserted into the left femoral artery for sampling of arterial blood. An incision (2 cm) was made parallel to the vessel and the femoral artery was isolated and ligated distally. A 0.04 in ID silastic catheter was inserted and advanced 16 cm in order to place the tip of the catheter in the abdominal aorta. The catheter was secured, filled with saline, knotted and placed in a subcutaneous pocket

All catheters were filled with saline solution that contained 200 U/ml of heparin (Abbott Laboratories, North Chicago, IL). Excess catheter was looped within the peritoneum for infusion and sampling (hepatic artery and portal vein) catheters. With an exception of the silastic catheter attached to the vascular-access-port, venous catheters were knotted, secured to the abdominal wall, and placed in a subcutaneous pocket prior to

closure of the skin. The arterial sampling catheter was also knotted and placed in a subcutaneous pocket prior to closure of the skin.

Transonic flow probes (Transonic Systems, Ithaca, NY) were positioned around the hepatic artery and portal vein to determine liver blood flow during experiments. The duodenum was laterally retracted to expose sections of the hepatic artery and portal vein. A small segment of the common hepatic artery was carefully exposed. Taking care not to disturb the nerve bundle located around the portal vein, a small portion of the vessel was exposed by blunt dissection. 3 and 6 (or 8) mm ID ultrasonic flow probes (Transonic Systems Inc, Ithaca, NY) were secured around the hepatic artery and portal vein respectively. To prevent blood from entering the portal vein beyond the site of the flow probe, the gastroduodenal vein was isolated and ligated. Blood that would normally flow through the gastroduodenal vein was shunted through the caudal pancreatoduodenal vein draining the distal pancreas. The ultrasonic flow probe leads were positioned in the abdominal cavity, secured to the abdominal wall, and placed in a subcutaneous pocket prior to closure of the abdominal skin.

A continuous suture of 2-0 chromic gut (Ethicon, Inc.) was used to close the subcutaneous layer. The skin was closed with horizontal mattress sutures of 3-0 Dermalon (Ethicon, Inc.). Immediately following surgery, the dogs received an intramuscular injection of penicillin G (Procaine; Anthony Products, Irwindale, CA, 10^6 U) to minimize the possibility of infection. Additionally, Flunixin (Meglumine 50 mg/ml; Phoenix Scientific, Inc., St. Joseph, MO) was also injected intramuscularly (1 mg/kg body weight) for acute pain relief. Animals awoke from surgery within 2 h, were active, and ate normally approximately 8 h after surgery. Post-operatively, each dog also

received 500 mg ampicillin (Principen; Bristol-Myers Squibb, Princeton, NJ) orally twice a day for 3-d.

On the morning of the metabolic study, the transonic leads and catheters were removed from the subcutaneous pocket under local anesthesia (2% lidocaine; Abbott Laboratories, North Chicago, IL). The contents of each catheter were aspirated, and they were then flushed with saline. Blunt needles (18 gauge; Monoject, St. Louis, MO) were inserted into the catheter ends and stopcocks (Medex, Inc, Hilliard, OH) were attached to prevent the backflow of blood between sampling times. Angiocaths (20 gauge; Beckton Dickson) were inserted percutaneously into the left and right cephalic veins and into a saphenous vein for the infusion of somatostatin, tracers, dye and glucose. A continuous infusion of heparinized saline was started via the femoral artery at a rate to prevent any clotting in the line. Each animal was allowed to rest quietly in a Pavlov harness for 30 min prior to the start of the metabolic study.

Collection and Processing of Samples

Blood Samples

Blood samples were drawn from the femoral artery and portal and hepatic veins at the predetermined sampling points indicated in the experimental protocols. Prior to each sample taken, the respective catheter was cleared of saline by withdrawing 5 ml of blood into a syringe. The blood sample was then drawn using a separate, pre-labeled syringe that had been flushed with heparinized saline (1 U/ml; Abbott Laboratories, North Chicago, IL). After sampling, the blood taken during the clearing process was re-infused

into the animal, and the catheter was then flushed with heparinized saline (1U/ml; Abbott Laboratories, North Chicago, IL). The total volume of blood withdrawn did not exceed 20% of the animal's blood volume. Additionally, two volumes of saline (0.9% sodium chloride; Baxter Healthcare Co., Deerfield, IL) were given for each volume of blood taken. There was no significant decrease in hematocrit using this procedure.

Before the experiment started, a blood sample was drawn and centrifuged (3000 rpm for 7 min). The plasma from this blood sample was used for the preparation of hormone infusates and the indocyanine green standard curve. When samples were taken from all three vessels, arterial and portal blood samples were taken simultaneously approximately 30 s before collection of the hepatic vein samples to compensate for the transit time through the liver, and thus allow the most accurate estimates of net hepatic substrate balance (113). Whenever the experimental design required a glucose clamp, small (~0.5 ml) arterial samples were drawn every 5 min in order to maintain the desired plasma glucose concentration.

Immediately following each sample collection, the blood was processed. A 20 μl aliquot of arterial whole blood was used for the immediate duplicate measurement of hematocrit using capillary tubes (0.4 mm ID; Drummond Scientific Co., Broomall, PA). The remaining blood was placed into tubes containing 1.6 mg/ml potassium EDTA (Sarsdedt, Numbrecht, Germany). After gentle mixing, a 1 ml aliquot of whole blood was lysed with 3 ml 4% perchloric acid, centrifuged, and the supernatant was stored for later determination of metabolites (alanine, β-hydroxybuturate, glycerol, lactate). 90 μl aliquots of the supernatant were placed in 1 ml of 0.2 mol/l sodium acetate buffer with or without glutaminase (Sigma, St. Louis, MO) for the later analysis of whole-blood

concentrations of glutamine and glutamate, respectively. A 1 ml aliquot was also used for the measurement of acetoacetate. An aliquot (1 ml) of whole blood was placed in a tube containing 20 μl of glutathione (Sigma, St. Louis, MO), centrifuged, and the supernatant was stored for the future analysis of catecholamines, epinephrine and norepinephrine. A forth aliquot (1 ml) of whole blood was lysed with 1 ml of 10% sulfosalicylic acid, centrifuged, and the supernatant was stored for the later determination of gluconeogenic amino acids (glycine, serine, threonine). The remainder of the blood was centrifuged to obtain plasma.

Four 10-μl aliquots of plasma were used for the immediate analysis of glucose using a Beckman glucose analyzer (Beckman Instruments, Fullerton, CA). A 1 ml aliquot of plasma received 50 ml of 100, 000 KIU/ml Trasylol (FBA Pharmaceuticals, New York, NY) and was stored for the determination of glucagon concentrations. 5 μl of tetrahydrolipstatin (THL, Xenical; Roche Pharmaceuticals, Nutley, NJ) were added to a 0.5 ml aliquot of plasma for FFA. THL is an inhibitor of lipoprotein lipase and therefore inhibits *in vitro* lipolysis (9). The remainder of the plasma was used for the analysis of cortisol, 3-[3H]-glucose, insulin, and triglycerides. Additionally, the plasma arterial and hepatic insulin samples were used for measurement of indocyanine green, as described below.

After each sample was processed, it remained on wet ice for the remainder of the experiment. Immediately following the completion of the experiment, the glutamine and glutamate samples were incubated at 37ºC for 45 min in a water bath, and then frozen at 70ºC until the assay was completed. Also at the end of the experiment, the 1 ml aliquots from the deproteinized metabolite samples were neutralized for assessment of whole-

blood acetoacetate concentrations. 50-µl of Fisher Universal Indicator Solution (Fisher) was added. In addition, 200-µl of 10% potassium hydroxide was added and the tubes were vortexed. Small aliquots 35 µl aliquots of diluted potassium hydroxide solution (5:1 with water) were added, followed by vortexing. The endpoint was reached when samples turned yellow-green. If the endpoint was passed, 3% PCA diluted 3:1 (with water) was added in drop size manner. After neutralization, the weight of the tubes was recorded and the pre-weight was subtracted. Analysis was then performed the same day as described below in *Sample Analysis*. Plasma samples for the assessment of 3-[3H]-glucose were deproteinized according to the method of Somogyi-Nelson (259) Immediately after each experiment 1 ml aliquots of plasma were mixed with 5 ml of 0.067 N $Ba(OH)_2$ and 5 ml of 0.067 N $ZnSO_2$ (Sigma Chemical). Samples were stored at 4°C for 1-3 days and then processed.

Tissue Samples

Within 2 min of the final sampling time point, each animal was anesthetized with pentobarbital (390 mg/ml Fatal-Plus; Vortech Pharmceutical Inc., Dearborn, MI) at 1ml/5kg. The animal was then removed from the Pavlov harness while the tracers, hormones, and or Intralipid/heparin continued to infuse. A midline laporotomy incision was made, the liver exposed, and clamps cooled in liquid nitrogen were used to simultaneously freeze sections of hepatic lobes *in situ*. The hepatic tissue was then immediately cut free, placed in liquid nitrogen, and stored at -70°C. Liver (~100 mg) collected for histological examination was placed in disposable vinyl specimen molds

(Sakura Finetek U.S.A., Inc., Torrance, CA) and frozen in embedding medium (O.C.T. Compound, Sakura Finetek U.S.A., Inc., Torrance, CA).

Sample Analysis

Whole Blood Metabolites

Alanine, β-hydroxybutyrate, Glycerol and Lactate

Whole blood concentrations of alanine, β-hydroxybutyrate, glycerol, and lactate were measured using methods developed by Llyod et al. (165) for the Technicon Autoanalyzer (Tarrytown, NY) and were modified to the Packard Multi Probe Robotic Liquid Handling System (Perkin Elmer; Shelton, CT). Enzymes and coenzymes for metabolic analyses were obtained from Boehringer-Mannheim Biochemicals (Germany) and Sigma Chemicals. The methods rely upon a reaction in which NAD is reduced to NADH. The reduced form (NADH) has a native fluorescence, which is not exhibited by the oxidized form. Excess amounts of NAD and enzyme/coenzyme are added to the metabolite samples. NAD becomes reduced to NADH upon oxidation of the metabolite. A fluorometer in the system detects changes in the florescence resulting from changes in NADH levels. Therefore the concentration of the metabolite present is proportional to the NADH produced.

Metabolites were measured in the PCA-treated blood samples as described in *Collection and Processing of Samples*. A standard curve was created for each metabolite using known concentrations prepared in 3% PCA. The Packard Multi Probe Robotic Liquid Handling System pipettes the sample into one well of a 96 well plate. After an

initial absorbance is read, the Packard Multi Probe Robotic Liquid Handling System pipettes enzyme solution into each well and shakes the plate to mix the sample and enzyme. The reaction proceeds and after an allotted time the change in absorbance is determined. All assay reactions are reversible with an exception of glycerol kinase. The NAD and enzyme are in excess compared to the substrate, thus the reactions are essentially taken to completion and the substrate is the rate-limiting component. Therefore, all reactions below are written with a single direction arrow. All reactions are carried out at 23°C.

Alanine

The alanine assay involved the reaction:

$$\text{L-alanine} + NAD^+ + H_2O \xrightarrow[\text{alanine dehydrogenase}]{} \text{Pyruvate} + NADH + NH_4^+ \qquad (1)$$

The enzyme buffer used was 0.05 M trizma base, 2 mM EDTA and 1 mM hydrazine hydrate, pH 10. To 10 ml of enzyme buffer, 4.6 mg of NAD and 3.4 Units (U) of alanine dehydrogenase were added.

ß-hydroxybutyrate

The ß-hydroxybutyrate analysis involved the following reaction:

3-hydroxybutyrate dehydrogenase

ß-hydroxybutyrate + NAD^+ ----------> acetoacteate + NADH + H^+ (2)

The enzyme buffer was 0.2 M monopotassium phosphate, 3 mM EDTA and 1 mM hydrazine hydrate, pH 8.5. To 10 ml of enzyme buffer, 12 mg NAD and 2.1 U ß-hydroxybutyrate dehydrogenase were added.

Glycerol

The glycerol assay involved the following reactions:

glycerol kinase

glycerol + ATP ----------> glycerol-l-phosphate + ADP (3)

glycerol-3-phosphate dehydrogenase

L-glycerol-l-phosphate + NAD^+ -----> dihydroxyacetone phosphate + NADH + H^+ (4)

The enzyme buffer was 0.09 M glycine, 1 mM hydrazine, and 0.01 M $MgC1_2$, pH 9.5. To 10 ml of the enzyme buffer, 15.4 g NAD, 15.4 mg ATP, 0.3 U glycerokinase, and 0.6 U glycerol-3-phosphate dehydrogenase were added.

Lactate

The lactate assay involved the following reaction:

lactate dehydrogenase

lactate + NAD^+ ----------> pyruvate + NADH + H^+ (5)

The enzyme buffer used was 0.24 M glycine and 0.25 M of hydrazine dihydrochloride and 7 mM disodium EDTA, pH 9.6. To 10 ml of enzyme buffer, 4.6 mg NAD and 0.1 U lactate dehydrogenase were added.

Acetoacetate

Blood acetoacetate concentrations were determined by a spectrophotometric method (216) on the samples neutralized as explained in *Collection and Processing of Samples*). 1 ml of neutralized sample was placed into a plastic 4 ml cuvette. 1 ml of enzyme buffer (1:1, vol:vol, of 1 M dipotassium phosphate and 1 M monopotassium phosphate, diluted 1:5, vol:vol with water, pH 7.0) was then added to the cuvette. In addition, 100 ml of 3 mg/ml NADH was added, the solution was mixed, and an initial absorbance reading was taken at 340 nm. Next, 0.05 U of 3-hydroxybutyrate dehydrogenase was added, mixed, and incubated for 1 hour at room temperature. Finally, a last absorbance reading was taken. The difference between the initial and final readings correlates to the acetoacetate level in the samples. Water blanks were used to normalize the data.

The method is the reverse of that used to access β-hydroxybutyrate concentrations (reaction 2). The analysis of acetoacetate involved the following reaction which is based

on the removal of NADH (rather than production in the β-hydroxybutyrate assay), and thus the loss of fluorescence:

$$\text{acetoacetate} + \text{NADH} + H^+ \xrightarrow[\text{3-hydroxybutyrate dehydrogenase}]{} \beta\text{-hydroxybutyrate} + NAD^+ \quad (6)$$

Glutamine and Glutamate

Whole blood glutamine and glutamate concentrations were assessed using methods described by Bernt *et al*. (17) adapted to the Packard Multi Probe Robotic Liquid Handling System. As glutamine breaks down when frozen, glutamine samples were treated with glutaminase (as described in *Collection and processing of samples*) on the day of the study and consequently all glutamine was converted to glutamate. The glutamate samples were not treated with glutaminase and therefore resulted in the loss of glutamine when the samples were frozen. Glutamate concentrations were determined from both sets of samples with the difference in the two equaling the glutamine level. The analysis of glutamate was based on the following reaction:

$$\text{L-glutamate} + NAD^+ + H_2O \xrightarrow[\text{glutamate dehydrogenase}]{} \text{2-oxoglutamate} + \text{NADH} + NH_3^+ \quad (7)$$

The assay buffer consisted of 23 mM Trizma base, 0.22 M hydrazine hydrate, and 0.7 mM EDTA, with a pH of 8.5. The enzyme solution was prepared in a phosphate buffer composed of 0.2 M dibasic sodium phosphate, 0.2 M monobasic sodium phosphate (4:1, v:v), 2 mg/ml NAD, and 36.5 μl/ml glutamate dehydrogenase. The glutaminase-treated sample and the corresponding untreated sample were converted to

concentrations by comparison with the standard curve constructed from monosodium glutamate.

Serine, Glycine and Threonine

The blood gluconeogenic amino acids serine, glycine and threonine were determined by reverse phase HPLC separation using pre-column derivatization with O-phthalaldehyde (OPA) on SSA-treated blood samples (as described in *Collection and Processing of Samples*) (285). The OPA solution (pH 10.4) was prepared by dissolving 12 mg OPA crystals (Pierce, Rockford, IL) in 200 ml of cold HPLC-grade methanol, 4.8 ml of 1.0 M potassium borate buffer, 5 ml of deionized water, and 22 µl of mercaptoethanol. An auto injector withdrew 20 µl of standard, control, or sample and 20 µl of OPA reagent. The sample and reagent were then mixed in the injector loop for 42 s before injection into a 1.5 ml/min mobile phase flow made up of elution buffers A and B. Elution buffer A (pH 7.2) was composed of 0.1 sodium acetate, HPLC grade methanol, and tetrahydorfuran (90:9.5:0.5; v:v:v). Elution buffer B was 100% HPLC grade methanol. The mobile phase flow was shifted from elution buffer A to elution buffer B over 30 min and samples or standards were detected using a fluorometer with an excitation filter of 338 nm and an emission filter of 425 nm. The sample concentration was determined from the standard curve taking into account the two-fold dilution during deproteinization. The detection range is from 5-5000 µmol/l for each amino acid.

Plasma Metabolites

Plasma Glucose

Plasma glucose concentrations were determined by the glucose oxidase method using a Beckman glucose analyzer (Beckman Instruments, Fullerton, CA). The reaction sequence was as follows:

$$\text{ß-D-glucose} + O_2 \xrightarrow{\text{glucose oxidase}} \text{gluconic acid and } H_2O_2 \quad (8)$$

$$H_2O_2 + \text{ethanol} \xrightarrow{\text{catalase}} \text{acetaldehyde} + H_2O \quad (9)$$

$$H_2O_2 + 2H^+ + 2I^- \xrightarrow{\text{molybdate}} I_2 + H_2O \quad (10)$$

The glucose concentration is proportional to the rate of oxygen consumption. The plasma glucose concentration in a sample (10 μl) is determined by comparing of the oxygen consumption in the sample with the oxygen consumed by a standard solution (150 mg/dl). There is no end-product inhibition of the process, as reactions 8 & 9 remove all of the hydrogen peroxide. Thus virtually all of the glucose in the sample is consumed. Glucose was measured a minimum of 4 times at each sampling time point for each vessel and a minimum of 2 times for samples drawn to clamp glucose. The glucose analyzer is accurate to 450 mg/dl.

Plasma 3-[^{3}H]-glucose

For assessment of plasma 3-[^{3}H]-glucose, samples were deproteinized according to the method of Somogyi-Nelson (192, 259, 260) as described in *Collection and Processing of Samples*. For 1-3 days following the experiment the samples were stored at 4°C, after which they were centrifuged at 3000 rpm for 20 min. 5 ml of supernatant were pipetted into a glass scintillation vial and placed into a heated vacuum oven to evaporate $^3H_20$. The residue was reconstituted in 1 ml of deionized water and 10 ml liquid scintillation fluid (EcoLite (+); Research Product Division, Costa Mesa, CA). Tritium in the sample was determined using a Beckman LS 9000 Liquid Scintillation Counter (Beckman Instruments Inc, Irvine, CA) for double label counting. The counter was programmed to correct the counts per minute (cpm) for quenching of the radioactivity in the sample caused by the deproteinization step. Therefore the data were presented in disintegrations per minute (dpm).

To assess for the loss of radioactive glucose during the deproteinization process, a recovery standard was created. The 3-[3H]-glucose infusate was diluted 1:250 (vol:vol) with saturated benzoic acid containing 1 mg/ml cold glucose. Nine 1 ml aliquots of this diluted ^{3}H infusate were placed into 3 sets of glass scintillation vials and were labeled as follows: chemical standard evaporated (CSE), chemical standard (CS), and chemical recovery standard (CRS). The diluted infusate aliquots in the CSE vials were evaporated to dryness in a heated vacuum oven and reconstituted with 1 ml of deionized water. The diluted infusate aliquots in the CS vials were not evaporated. Te aliquots in the CRS vials were treated identical to the plasma samples. 10 ml of scintillation fluid were added to all standard vials and the standards were counted. Comparison of the CS and CSE

determined the loss of ^{3}H counts in the evaporation process. The final amount of radioactivity per sample was determined by generating a recovery factor (ratio of radioactivity in the CSE compared to CRS) which accounted for the radioactivity lost during sample processing.

Plasma Free Fatty Acids (FFAs)

Plasma FFA levels were determined spectrophotometrically using the Packard Multi Probe Robotic Liquid Handling System (Perkin Elmer; Shelton, CT) and a kit from Wako Chemicals (Richmond, VA). In the presence of acyl- Coenzyme A (CoA) synthetase, CoA is acylated by the fatty acids within the plasma sample. The acyl-CoA produced is oxidized by acyl-CoA oxidase, resulting in the production of H_2O_2. The addition of peroxidase, in the presence of H_2O_2, subsequently allows for oxidative condensation of 3-methyl-N-ethyl-N-(β-hydroxyethyl)-aniline with 4- aminoantipyrine (4-AAP) to form a purple colored adduct. The purple color adduct is measured at an optical density of 550 nm and is proportional to the plasma FFA concentration in the sample. The FFA concentrations were calculated using a calibration curve of known amounts of oleic acid. The assay was run at 37ºC. The specific reactions were as follows:

$$\text{FFA} + \text{ATP} + \text{CoA} \xrightarrow{\text{Acyl-CoA synthetase}} \text{Acyl-CoA} + \text{AMP} + \text{Ppi} \quad (11)$$

$$\text{Acyl-CoA} + O_2 \xrightarrow{\text{Acyl-CoA oxidase}} \text{2,3-trans-enoyl-CoA} + H_2O_2 \quad (12)$$

$2\ H_2O_2$ + 3-methyl-N-ethyl-N-(β-hydroxyethyl)-aniline + 4-AAP

Peroxidase

----------→ Purple color adduct (13)

Plasma Triglycerides

Plasma triglyceride levels were assessed by the enzymatic measurement of glycerol, true triglycerides, and total triglycerides in plasma using the Spectramax Plus 384 (Molecular Device Corp. Sunnyvale, CA) and The Serum Triglyceride Determination Kit (Sigma, St Louis, MI). Assay was modified for a 96 well plate. The procedure involves enzymatic hydrolysis of triglycerides by lipoprotein lipase to free fatty acids and glycerol. Glycerol is then phosphorylated by glycerol kinase and adenosine-5'-triphosphate (ATP) resulting in the production of glycerol-1-phosphate (G1P) and adenosine-5'-diphosphate (ADP). G1P is then oxidized by glycerol phosphate oxidase (GPO) to dihydroxyacetone phosphate (DAP) and hydrogen peroxide (H_2O_2). H_2O_2 is then coupled with 4-aminoantipyrine (4-AAP) and sodium N-ethyl-N-(3-sulfopropyl)-anisiden (ESPA) producing quinoneimine dye (absorbance 540 nm). The increase in absorbance is directly proportional to the triglyceride levels of the plasma sample. The assay was run at 37ºC. The triglyceride concentrations were calculated using a calibration curve of known amounts of glycerol. The specific reactions were as follows:

Lipoprotein lipase

Triglycerides ----------→ Glycerol + FFA (14)

Glycerol kinase

Glycerol + ATP ----------→ G-1-P + ADP (15)

GPO

$$G\text{-}1\text{-}P + O_2 \xrightarrow{\text{GPO}} DAP + H_2O_2 \quad (16)$$

peroxidase

$$H_2O_2 + 4\text{-}AAP + ESPA \xrightarrow{\text{peroxidase}} \text{quinoneimine dye} + H_2O \quad (17)$$

Hormones

Epinephrine and Norepinephrine

Plasma epinephrine and norepinephrine levels were determined using a high-performance liquid chromatography (HPLC) method as previously described by Goldstein et al. (112). Catecholamines were measured from the glutathione-treated blood samples as described in *Collection and Processing of Samples*. 400 µl of each sample was partially purified by absorption to 10 mg of acid-washed alumina (Bioanalytical Systems, West Lafayette, IN) in 600 µl of Tris/EDTA(pH 8.6) and 50 µl of an internal standard, dihydroxybenzylamine (DHBA, 500 pg/ml, Sigma Chemical Co.). Samples were shaken for 15 min, centrifuged for 4 min, and aspirated. The alumina pellet was rinsed with 2 ml water, the solution vortexed, centrifuged, and aspirated. This process was repeated 3 times. The catecholamines were then eluted with 200 µl 0.1M perchloric acid (PCA) according to Anton and Sayre (7).

Each sample was injected onto an HR-80, reverse phase, 3 µm octadecylsilane column. The mobile phase consisted of 14.2 g of disodium phosphate, 43 ml of methanol 37 mg of sodium EDTA (pH 3.4), and 440 mg of sodium octyl sulfate. The system employed a Coulchem II Detector, Model 5021 Conditioning Cell, and Model 5011

Analytical Cell (all obtained from ESA, Bedford, MA). Concentrations of epinephrine and norepinephrine were calculated using a linear calibration curve consisting of 5 standards (ranging from 50-1000 pg/ml). Standards were prepared from epinephrine bitartrate and (-)-arterenol bitartrate (norepinephrine) salts (Sigma Chemical Co.). Additionally, known amounts of epinephrine and norepinephrine were added to the first and last samples of each experiment to evaluate recovery, and to ensure precise identification of the peaks.

To identify peaks, data reduction was performed using ESA 500 Chromatograph and data station software. The ratio of the peak height of the internal standard to that of the catecholamine(s) was calculated, and the concentration of catecholamine(s) was determined by comparison with the standard curve. The limit of detection of the assay was 20 pg/ml for epinephrine and 5 pg ml for norepinephrine. There was between 80-100% recovery for both catecholamines. The interassay coefficient of variation (CV) was 3-11 % for epinephrine; the low and high ends of the curve resulted in large variances. For norepinephrine, the interassay CV was 4-6 % .

Cortisol, Glucagon, and Insulin

The plasma levels of cortisol, glucagon, and insulin were measured using radioimmunoassay (RIA) techniques (291). In essence, a plasma sample containing an unknown amount of hormone was incubated with a specific antibody for that hormone. A known amount of radiolabeled hormone was added to the mixture to compete with the antibody binding sites. A double antibody procedure (single antibody procedure for cortisol) which caused precipitation of the bound complex was used to separate unbound

hormone from the antibody-hormone complexes. The radioactivity of the precipitate was measured via a Cobra II Gamma Counter (Packard Instrument Co, Meriden, CT). Binding of the radiolabeled hormone is inversely proportional to the amount of unlabeled hormone present, and a standard curve was constructed using known concentrations of the unlabelled hormone.

Cortisol

Immunoreactive plasma cortisol was measured with a single antibody procedure (101) using a gamma coat RIA (Diagnostic Products Corporation, Los Angeles, CA). 25 µl the plasma sample and 1 ml of ^{125}I-labeled cortisol were pipetted into a cortisol specific antibody-coated tube. The reaction was allowed to continue for 1 hour in a 37°C water bath. The tubes were decanted and rinsed with 1 ml of deionized water. They were allowed to dry and were then counted in the Cobra II Gamma Counter for 1 minute.

The log of the amount of hormone in each sample was inversely proportional to the log of (bound label/free label). The cortisol concentration in each sample was determined by comparison to a standard curve using known amounts of unlabeled hormone. The sample detection range was 0.5-50 ug/dl. The antibody is 100% specific for cortisol, with only slight cross-reactivity with 11-deoxycortisol (6%) and 17-hydroxyprogesterone (1%), and no cross reactivity (<0.4%) with corticosterone (<0.1 %), aldosterone, progesterone, deoxycorticosterone, and tetrahydrocortisone. The recovery for the assay was approximately 90%, and the interassay CV was in the order of 8-10% for the entire range of the dose response curve.

Glucagon

Immunoreactive plasma glucagon was measured using a double antibody RIA (Linco Research Inc., St. Charles, MO) (90). The protocol utilized primary and secondary antibodies specific for glucagon (kit with glucagon antibodies and ^{125}I tracers from Linco). A 100 µl aliquot of the plasma sample and 100 µl of guinea pig specific antibody to glucagon were mixed and incubated for 24 h at 4ºC. 100 µl ^{125}I-labelled glucagon was then added to the solution and incubated for an additional 24 h at 4ºC. Next, the samples were incubated for 2 h at 4ºC with 100 µl goat anti-guinea pig IgG (2nd antibody) and 100 µl IgG carrier. 1 ml of wash buffer was added and the tubes were centrifuged at 3000 rpm. The samples were decanted and the portion of total radioactivity bound to the antibody (pellet) was counted in a Cobra II Gamma Counter.

The log amount of hormone in the samples was inversely proportional to the log of (bound label/free label). The glucagon concentration in each sample was determined by comparison to a standard curve using known amounts of unlabeled hormone. The samples were corrected for non-specific binding, and the sample detection range was 20-400 pg/ml. The antibody is 100% specific for glucagon, with only slight cross reactivity with oxytomodulin (0.01%), and no cross reactivity with glucagon like peptide-1, human C-peptide, human insulin, human proinsulin, pancreatic polypeptide, or somatostatin. A protein effect in the assay causes the 0 pg/ml glucagon standard to read as 15-20 pg/ml. This represents a stable, constant background in all samples. The recovery for the assay was between 80-100%, and the interassay CV was approximately 6-10% for the entire range of the dose response curve.

Insulin

Immunoreactive plasma insulin was also measured using a double antibody RIA as described previously (187). A 100 µl aliquot of the plasma sample, 200 µl of ^{125}I-labeled insulin, and 100 µl of a guinea pig specific antibody to insulin were mixed and incubated for 18 h at 4ºC (both from Linco Research Inc., St. Charles, MO). The samples were incubated for 30 min at 4ºC with 100 µl goat anti-guinea pig IgG (2nd antibody) and 100 µl IgG carrier. One ml of wash buffer was added, and tubes were centrifuged at 3000 rpm. The liquid portion of the samples was decanted and the remaining pellet containing the total radioactivity bound to the antibody was counted in a Cobra II Gamma Counter.

The log of the amount of hormone in the samples was inversely proportional to the log of (bound label/fee label). The insulin concentration in each sample was determined by comparison to a standard curve obtained using known amounts of unlabeled hormone. The samples were corrected for non-specific binding, and the sample detection range was 1-150 µU/ml. The antibody is specific to porcine, canine, and human insulin, but cross-reacts with bovine insulin (90%), human proinsulin (38%), and the split proinsulin products Des 31,32 (47%) and Des 64,65 (72%). In general, less than 15% of the basal insulin level is due to non-insulin material. The antiboby also has no cross-reactivity with C-peptide, glucagon, pancreatic polypeptide, or somatostatin. The recovery for the assay was between 90-100% and the interassay CV was approximately 7-8% for the entire range of the dose response curve.

Hepatic Blood Flow

Blood flow in the hepatic artery and portal vein was determined by use of trasonic flow probes implanted during surgery (as described in *Surgical Procedures*). Total hepatic blood flow (the sum blood flow in hepatic artery and portal vein) was also assessed using the indocyanine green (ICG) dye method, as described by Leevy *et al*. (159). The results presented in this document were calculated using ultrasonic-determined flow (unless stated otherwise), as this method allows for the direct measurement of blood flow in the hepatic artery and portal vein. Whereas the ICG dye method requires an assumption of the percent contribution of each vessel to total hepatic blood flow. ICG-determined flow was used as a backup measurement in the case of ultrasonic flow probe failure. However, the same conclusions were drawn regardless of method used to calculate the data.

Ultrasonic flow measurements represented instantaneous variations in velocity and therefore provided blood flow in the individual vessels of interest. Each probe determined the mean transit time of an ultrasonic signal passed back and forth between two transducers within the probe which were located upstream and downstream of the direction of blood flow in the vessel. The transducers made of a piezoelectric material which is capable of receiving and transmitting an ultrasonic signal. The downstream transducer first emits an ultrasonic pulse into the blood vessel that is received upstream by the second transducer. After the upstream transducer receives the ultrasonic signal, it re-emits the ultrasonic pulse signal back to the downstream transducer. The transit time of each ultrasonic beam as measured by the upstream and downstream transducers (ΔT_{up} and ΔT_{down}, respectively) is defined by the following relationships:

$$\Delta T_{up} = D / (v_o - v_x) \quad (18)$$

$$\Delta T_{down} = D / (v_o + v_x) \quad (19)$$

where D is the distance traveled by the ultrasonic beam within the acoustic window of the probe, v_o is the phase velocity, or the speed of sound, in blood, and v_x represents the component of fluid velocity that is parallel or antiparallel to the phase velocity. The parallel component augments the phase velocity when the signal travels in the same direction of blood flow, while the antiparallel component is subtracted from phase velocity if the ultrasonic signal moves against the flow of blood in the vessel. Combining the two expressions for transit time yielded the following equation:

$$\Delta T_{up} - \Delta T_{down} = (D / (v_o - v_x)) - (D / (v_o + v_x)) \quad (20)$$

Since the transit times measured by both transducers, the distance traveled by the beam, and the speed of sound in blood are all known quantities, this equation is used to calculate v_x. Once v_x is obtained, the transit velocity (V) of blood traveling through the vessel can be determined according to the following equation:

$$V \cos \theta = v_x \quad (21)$$

where θ represents the angle between the centerline of the vessel and the axis of the ultrasonic beam. Lastly, blood flow is the product of the transit velocity and the cross-

sectional area of the vessel. The cross-sectional area of the vessel was pre-determined by the size of the acoustic window according to the probe model. Since transit time is sampled at all points across the diameter of the vessel, volume flow is independent of the flow velocity profile.

If a flow probe failed during the experiment, the missing values were estimated by subtracting the values from the functional flow probe from the ICG determined total hepatic blood flow. For example, values from the arterial flow probe were subtracted from the ICG values to yield estimates of the portal vein flow.

The ICG method is based on the Fick principle, in which the net balance of a substrate across an organ equals the concentration difference of the substrate across the organ multiplied by the blood flow through the organ. The equation can be rearranged to calculate hepatic blood flow by dividing hepatic ICG balance by the arteriovenous difference of ICG across the liver. Because the liver is assumed to be the only site of ICG clearance, hepatic ICG uptake is equal to the ICG infusion rate in steady state conditions. The extraction of ICG across the liver remains constant for brief infusions. However, if ICG is infused for longer than four hours, the level of dye in the plasma gradually increases, resulting in a slight overestimation (5-10%) of hepatic blood flow (125).

Arterial and corresponding hepatic vein plasma samples were centrifuged at 3000 rpm for 30 min using no brake to pellet particulate matter. Absorbance was then measured on a Spectronic spectrophotometer at 810 nm. This process was then repeated, and the values obtained for each sample were averaged. A standard curve was constructed by adding successive 5 μl aliquots of diluted dye (1:10 dilution) to 1 ml of

plasma obtained from the animal before the dye infusion began. Hepatic plasma flow (HPF) was then calculated as follows:

$$HPF = (IR \times 10 \times SCMD)/(\text{dog weight (kg)} \times (0.005) \times (A-H)) \quad (22)$$

where IR is the ICG infusion rate (ml/min), SCMD is the standard curve mean difference per 5 μl increments, and A-H is the difference in absorbance between the hepatic arterial and venous samples. The value of 10 was used to correct for the dilution of ICG used in the standard curve, and 0.005 was the volume in ml used as increments in the standard curve. Hepatic blood flow (HBF) was derived from HPF:

$$HBF = HPF/(1-\text{hematocrit}) \quad (23)$$

Hematocrit was measured at every time point of each in which samples were taken from the hepatic artery and portal and hepatic veins. Because this technique only determines total hepatic blood flow, an assumption was made regarding the contribution of blood flow in the vessels supplying the liver. The normal distribution of flow was assumed to be 20% artery and 80% portal vein at baseline. In fact, the ultratransonic flow probe data obtained (0.22 ± 0.03 and 0.78 ± 0.03 for hepatic artery and portal vein, respectively) confirmed that the ratio of arterial and portal that we used was appropriate.

Tissue Analysis

Hepatic Lipid Content

Approximately 100 mg of tissue was homogenized in chloroform/methanol (2:1 v/v) and the lipids were extracted using a modified method of Folch-Lees (100). The homogenates were then filtered through sharkskin filter paper. 0.1 M potassium chloride was added to separate the chloroform and methanol layers. The chloroform phase was removed, dried down, and the individual classes of lipids were separated by thin layer chromatography using a Silica Gel 60 A plate developed in acetic acid (80:20:1), ethyl ether, and petroleum ether and visualized by rhodamine 6G. Phospholipids and acylglycerols bands were scraped from the plates and methylated using boron trifluoride/methanol as described by Morrison and Smith (188). Methylated fatty acids were extracted and analyzed by gas chromatography. Gas chromatographic analysis were carried out on an HP 5890 gas chromatograph equipped with flame ionization detectors, an HP 3365 Chemstation, and a capillary column (SP2380, 0.25 mm x 30 m, 0.25 μm film, Supelco, Bellefonte, PA). Helium was used as a carrier gas. The oven temperature was programmed from 160ºC to 230ºC at 4ºC/min. Fatty acid methyl esters were identified by comparing the retention times to those of known standards. Inclusion of lipid standards with odd chain fatty acids permitted quantification of the amount of lipid in the sample. Standards used were dipentadecanoyl phosphatidylcholine (C15:0) and trieicosenoin (C20:1).

Histology: Oil Red O Staining

Liver samples from each animal were embedded in OCT and kept at -70°C until sectioning. Serial sections of 10-μm thickness were cut and 3 sections were examined from each animal. Tissues were washed with propylene glycol for 2 minutes and stained with Oil Red O for 1 hour. Tissues were washed briefly (1 min) in 85% propylene glycol and then rinsed in distilled water. Next, the tissues were counterstained with hematoxylin (1 min), rinsed with tap water , and then rinsed again with distilled water. A coverslip was added using an aqueous mounting medium.

Hepatic Adenosine 3', 5'- cyclic monophosphate (cAMP) Content

Hepatic cAMP levels were assessed by a modified high-performance liquid chromatography method developed by Ally et al (5). Liver samples (~500mg) frozen in liquid nitrogen were homogenized in ice cold 0.4 M perchloric acid containing 0.5 mM ethylene glycol-bis (β-aminoethyl ether) tetraacetic acid (EGTA). After 1 min on ice, the acid extract was centrifuged at 2,500 g for 10 min at 4°C. The supernatant, neutralized with ~360 μl of 0.5 M K_2CO_3 to pH 6.8 was centrifuged at 4°C for 5 min to precipitate insoluble $KClO_4$. The mobile phase consisted of elution buffer A (90:10, 100 mM potassium phosphate, pH 6.0, adjusted with K_2PO_4/methanol) and buffer B (80:20, 100 mM potassium phosphate, pH 6.0, adjusted with K_2PO_4/methanol). The chromatographic separation was carried out via auto-injection of 200 ul of sample onto a LC18-T column (25 cm x 4.6 mm I.D., 5 μm particle size, Supelco, Bellefonte, PA) protected with a C_{18} guard column (Supelco, Bellefonte, PA). Elution occurred at a flow rate of 0.8 ml/minute

and a column temperature of 30°C. Detection of cAMP was achieved with UV detection at 254nm (0.1 AUFS) and a retention time of ~20.0 min.

Basal hepatic cAMP levels were assessed from 18-h fasted dogs with basal glucagon and insulin concentrations.

Body Composition Assessment

Magnetic Resonance Imaging (MRI)

Prior to imaging, the dog will be anesthesized by a 1mg/lb dose of Telazol (Tiletimine/Zolzapam/Fort Dodge). To maintain anesthesia, 2% Aerrane (isoflurane/Baxter) will be used while on the ventilator. Magnetic imaging scans will be performed. 3 plane abdominal slices (30cm x 5mm), 3D in-phase and out-of-phase axial abdominal slices will be obtained using a 3 Tesla whole–body General Electric/Magnex magnetic resonance imaging and spectroscopy system (Signa® Edipse 3.0T M4 Release software). Images will be analyzed using software program designed for the quantification of fat tissue and other tissue in each slice. Total abdominal fat and tissue will be estimated as the integrated fat or tissue across all slices. Percent fat will then be calculated as the total abdominal fat divided by the total abdominal tissue. In addition, visceral and subcutaneous distributions of fat will be quantified. Visceral fat will be defined as intraabdominal fat bound by parietal peritoneum or transversalis fascia. Subcutaneous fat will be defined as the fat superficial to the abdominal and back muscles. Subcutaneous fat will be calculated by subtracting the intraabdominal fat area from the total fat area.

Magnetic Resonance Spectroscopy (MRS)

All MRS data will be collected on a 3-Tesla whole–body General Electric/Magnex magnetic resonance imaging and spectroscopy system (Signa® Edipse 3.0T M4 Release software). A localized volume MR technique has on a PRESS sequence without water suppression will be used. Prior to volume localization, an imaging protocol (as described above) will be performed that will include acquisition of anatomical images and positioning of the spectroscopic voxel in the area of the liver. Both the anatomical images and the spectroscopic data will be obtained while the dog is forced to hold its breath (the ventilator is turned off). Three 2 x 2 x 2 ($8cm^3$) voxels were examined in each time point during the study protocol. 64 transients with a repetition of 2 seconds and an echo time (TE) of 25 ms will be acquired from each voxel and used to evaluate the spin density for water and fat contributions.

The water and fat time-domain signals will each be modeled as a sum of exponentially decaying sinusoids. The amplitude and frequency of each sinusoid will be optimally estimated (along with the decay rate and phase). All frequencies (chemical shifts) will be measured relative to the principal water ^1H resonance of ~4.7 ppm. The water ^1H resonance is a large peak located at ~4.5 ppm. The lipid signal results from multiple chemically shifted ^1H resonances corresponding to methyl and methylene groups occupying different positions on lipid molecules with frequencies found at around (0.9 – 2.4 ppm) with a major peak at ~1.5 ppm corresponding to methylene groups $(CH_2)n$ chains. The resonances are used to calculate a ratio/percent change in fat content in the liver.

Calculations

Glucose Turnover

Glucose turnover is the rate at which old glucose is replaced with new glucose. Tracer-determined total glucose production (R_a) and glucose utilization (R_d) were calculated using an isotope dilution method described by Wall (286), as simplified by DeBodo (71), and using a two-compartmental model described by Mari (63) with canine parameters established by Dobbins (78). The glucose pool was initially primed with an injection of 3-[^{3}H]-glucose followed by a constant infusion of the tracer. By the beginning of the control period, the tracer (3-[^{3}H]-glucose) and tracee (cold glucose) were in equilibrium so that the specific activity of glucose (SA = dpm/mg) was in a steady state. R_a and R_d were calculated according to the following equations:

$$R_a = [I - N\,(dSA/dt)]/SA, \text{ and} \quad (24)$$

$$R_d = R_a - (dN/dt) \quad (25)$$

where I is tracer infusion rate (dpm/min), N is the size of the glucose pool (mg) and t is time (min) (175). In a steady state, when $dSA/dt = 0$, the R_a equation is simplified to:

$$R_a = I/SA \quad (26)$$

This method utilizes a one-compartment model of glucose kinetics as described by Steele (6). The one-compartment model assumes one compartment of glucose that consists of both a rapidly and slowly mixing pool of glucose. Therefore, when rapid changes in cold glucose are induced in the system, the consequent changes in glucose specific activity would be unevenly distributed throughout the entire glucose compartment. To compensate for this non-uniform mixing, a correction factor for the pool size is calculated as:

$$N = pVC \quad (27)$$

where p is the pool fraction, V is the volume of distribution of glucose (ml) and C the cold glucose concentration (mg/dl). The pool fraction (the rapidly mixing component of the glucose compartment) was estimated to be 0.65 (219), while V was assumed to be the extracellular volume, which is approximately 22% of the dog weight (65).

The major limitation of the one-compartment model is that a rapid change in SA invalidates the method, so that a fall in SA, which occurs either by endogenous glucose production or exogenous glucose infusion in the presence of a constant 3-[^{3}H]-glucose infusion, the change in SA would cause an error in the estimation of R_a (underestimation if SA drops, overestimation if SA increases) (62). In order to overcome this problem in the present studies, the data were calculated using a two-compartment model (171). This model describes the glucose system more accurately under non-steady-state conditions. Ra was calculated as the sum of three terms: a steady-state term, a term for the first compartment, and a term for the second compartment. The principle equations are as follows, where the expression of R_a, calculated at the equally spaced time instants t_0, $t_1,\ldots, t_k, t_{k+1}$, is determined from the following formulas:

$$R_a(t_k) = (R^*_{inf})(t_k)/SA(t_k) - V_1[C(t_k)dSA(t_k)/dt] / SA(t_k) - V_2k_{22}[SA(t_k)G(t_k) - G^*(t_k)]/SA(t_k) \quad (28)$$

$$G(t_{k+1}) = b_1G(t_k) + b_2C(t_k) + b_3C(t_{k+1}) \quad (29)$$

$$G^*(t_{k+1}) = b_1G^*(t_k) + b_2C^*(t_k) + b_3C^*(t_{k+1}) \quad (30)$$

$$V_2 = V_1k_{12}k_{21}/k^2_{22} \quad (31)$$

where t_k and t_{k+1} are time parameters, respectively; $R_a(t_k)$ and $R^*_{inf}(t_k)$ are the rate of appearance calculated with approximate two-compartment model (mg/kg/min) and tracer

infusion rate (dpm/kg/min), respectively; $SA(t_k)$ and $dSA(t_k)$ are specific activity (dpm/mg) and derivative of specific activity (dpm/mg/min), respectively. V_1 and V_2 (ml/kg) are the volumes of the first and second compartments, respectively; $C^*(t_k)$ and $C(t_k)$ are tracer and tracee concentrations, respectively; k_{12}, k_{21}, and k_{22} are constant rate parameters of the first and second compartments, respectively; $G(t_k)$ and $G^*(t_k)$ are variables calculated recursively from tracee and tracer concentrations, respectively; b_l, b_2, and b_3 are coefficients of recursive equations for calculating $G(t_k)$ and $G^*(t_k)$. Canine parameters were used for V_l, V_2, and k_{22} in the present studies were those determined by Dobbins *et al*. (78). It has been reported (78) that under non-steady state conditions where specific activity changes dramatically, glucose appearance determined using the two-compartment model is more accurate than the Steele equation (one-compartment model).

When glucose was infused, endogenous glucose production (endo R_a) was determined by subtracting the glucose infusion rate (GIR), from total glucose production (Ra).

Of note, there are two major assumptions that are made when using this particular isotope dilution method to determine glucose kinetics. First, the labeled and unlabeled glucose molecules are assumed to be metabolized in the same manner. Secondly, the label is assumed be irreversibly lost (293).

It should also be noted that, as the liver and the kidneys both produce glucose, whole body tracer-determined glucose production is slightly higher than the rate of hepatic glucose production. Although net kidney glucose balance in the postabsorptive state is near zero, the kidney has been estimated to contribute 5-15% to whole body

glucose production. However, studies have suggested that the kidney is only a minor contributor to total glucose production (88).

Net Hepatic Substrate Balance

The net balance of a substrate across an organ, otherwise known as the arteriovenous (A-V) difference technique, utilized the Fick principle as described for the ICG-determination of blood flow (as described in *Sample Analysis* under *Hepatic Blood Flow*). Briefly, net hepatic balance of a substrate (NHSB) was calculated as the difference between the substrate load leaving the liver ($Load_{out}$) and the substrate load entering the liver ($Load_{in}$), as shown in the equation below:

$$NHSB = Load_{out} - Load_{in} \quad (32)$$

The $Load_{out}$ was calculated according to the equation:

$$Load_{out} = [S]_{HV} \times HBF \quad (33)$$

where $[S]_{HV}$ is the substrate concentration in the hepatic vein, and HBF is the total hepatic blood flow.

The $Load_{in}$ was calculated according to the equation:

$$Load_{in} = ([S]_{A} \times HABF) + ([S]_{PV} \times PVBF) \quad (34)$$

where $[S]_{A}$ and $[S]_{PV}$ are arterial and portal venous substrate concentrations, respectively, and HABF, PVBF are hepatic artery and the portal vein blood flows, respectively. For all

glucose balance calculations, plasma glucose concentrations were converted to whole blood values using a previously determined correction factor (131, 201) which assumes blood glucose to be 73% of the plasma glucose values. Blood flows were used for all substrate balance calculations except FFA balances. FFA balances were calculated using plasma flow, determined by multiplying blood flow by (1-hematocrit). A positive value for NHSB indicates net substrate production by the liver, whereas a negative value represents net hepatic substrate uptake. In some cases, uptake is presented rather than balance, and when such is the case positive values are used.

Limitations of the A-V difference technique include: 1) imprecision in the measurement of local blood flow, 2) measurement of net rather than absolute flux across the organ and 3) variability of vascular anatomy and heterogeneity of tissue structure and function. In addition, transit time through the organ must be taken into account. Because the A-V difference represents net flux across an organ, it is most valid during steady-state conditions.

Hepatic Gluconeogenesis and Glycogenolysis

Net hepatic gluconeogenic (NHGNG) flux and net hepatic glycogenolysis (NHGLY) were estimated in the present studies. The synthesis and subsequent release of glucose from non-carbohydrate precursors is classically known as gluconeogenesis. All carbon produced by the gluconeogenic pathway is not necessarily released by the liver. Some of the carbon may be stored as glycogen, oxidized, or released as lactate. Therefore, we made a distinction between gluconeogenic flux to glucose-6-phosphate (G-6-P) and net hepatic gluconeogenic flux.

Hepatic gluconeogenic flux to G-6-P was determined by dividing the sum of net hepatic uptake of gluconeogenic precursors (alanine, glutamate, glutamine, glycerol, glycine, lactate, pyruvate, serine, and threonine) by two to account for the incorporation of the three-carbon precursors into the six-carbon glucose molecule. The net hepatic balance of pyruvate was assumed to be 10% of net hepatic lactate balance. This method assumes that there is 100% conversion of gluconeogenic precursors taken up by the liver into G6P and that intrahepatic GNG precursors do not contribute significantly to GNG flux. When net hepatic output of any precursor occurred, rather than uptake, the precursor was considered to be a product of the liver, and thus uptake was set to zero.

NHGNG flux was determined by subtracting the sum of net hepatic output rates (when such occurred) of gluconeogenic precursors (in glucose equivalents) and hepatic glucose oxidation from the gluconeogenic flux to G-6-P. When NHGNG flux is positive, there is net flux to glucose-6-phophate (G6P), whereas a negative number indicates net flux to pyruvate, or net glycolysis. In the present studies, glucose oxidation was assumed to be 0.2 $mg \cdot kg^{-1}min^{-1}$ in all groups (56, 121). This parameter was not directly measured because it is difficult to differentiate between the small signal and the high inherent noise in the measurement. However, our lab has found glucose oxidation after an overnight fast to range from 0.1 to 0.2 $mg \cdot kg^{-1}min^{-1}$. While using this value may slightly overestimate or underestimate the absolute rate glucose oxidation, it is unlikely to differ by more than 0.1 mg/kg/min from the true value. In previous studies hepatic GO did not change appreciably under euglycemic/hyperinsulinemic states (184). Additionally, it seems unlikely that glucagon would change hepatic glucose oxidation significantly. Although, glucagon has been shown to inhibit pyruvate dehydrogenase,

and thus pyruvate oxidation(107, 221), the basal oxidation is so low that the noise of the measurement would be larger than the magnitude of the potential fall. NHGLY was estimated by subtracting NHGNG flux from net hepatic glucose balance. A positive value for NHGLY indicates net glycogen breakdown, whereas a negative value represents net glycogen synthesis.

When using the A-V difference technique to estimate fluxes of NHGNG and NHGLY it is necessary to consider the limitations of this approach. There is little to no hepatic production of gluconeogenic amino acids or glycerol however, such is not the case for lactate. Our estimate of the rate of gluconeogenic flux to G-6-P will only be quantitatively accurate only if lactate flux is unidirectional at a given moment. It has been suggested that there is spatial separation of metabolic pathways in that, gluconeogenic periportal hepatocytes primarily consume lactate and other non-carbohydrate precursors for the synthesis of glucose and glycogen, while glycolytic perivenous hepatocytes predominantly consume plasma glucose which can be incorporated into glycogen, oxidized, or released as lactate or other glycolytic substrates (142, 220). Therefore, in a net sense it is possible that hepatic gluconeogenic and glycolytic flux occur simultaneously, with lactate output and uptake occurring in different cells. To the extent that flux occurs in both directions simultaneously, the net hepatic balance method will result in an underestimation of gluconeogenic flux to G-6-P. Of note, net hepatic gluconeogenic flux and net hepatic glycogenolytic flux can be calculated accurately without concern for the assumptions related to whether or not simultaneous gluconeogenic and glycolytic substrate flux occur. Ideally the gluconeogenic flux rate would be calculated using unidirectional hepatic uptake and

output rates for each substrate, but this would be difficult, as it would require the simultaneous use of multiple stable isotopes which could themselves induce a mild perturbation of the metabolic state.

Non-Hepatic Glucose Uptake

Non-hepatic glucose uptake (non-HGU) was calculated over time intervals by the following formula:

$$\text{Non-HGU} = \text{average total glucose infusion between T1 and T2} + (T1_{NHGB} + T2_{NHGB})/2) - \text{glucose mass change in the pool} \quad (35)$$

where T1 and T2 indicates the time points for which glucose is being measured. The $((T1_{NHGB} + T2_{NHGB})/2)$ term will be a negative number in the presence of net hepatic glucose uptake. The glucose mass change in the pool is calculated using the following equation:

$$\text{Glucose mass change in the pool} = ((([G_A]_{T2} - [G_A]_{T1}) / 100) * ((0.22 * \text{body wt in kg} * 1000 * 0.65) / \text{body wt in kg})) / (T2-T1) \quad (36)$$

where $[G_A]$ is the plasma glucose concentration, T1 and T2 are the time points of the interval, 0.22 represents the volume of extracellular fluid (the volume of distribution) or 22% of the dog's weight (6), and 0.65 represents the fraction of the pool (65).

Sinusoidal Hormone Concentrations

Because the liver is supplied by blood flow from both the hepatic artery and the portal vein, neither represents the true inflowing hepatic blood flow supply. For this reason, hepatic sinusoidal hormone levels (of insulin and glucagon) were calculated as follows:

$$\text{Hepatic Sinusoidal Hormone Level} = [S]_A \times (APF/TPF) + [S]_P \times (PPF/TPF) \qquad (37)$$

where A and P are arterial and portal vein plasma substrate concentration; APF and PPF are the arterial and portal vein plasma flow measured by the ultrasonic flow probes; TPF (total hepatic plasma flow) = APF + PPF. Note this calculation represent the average inflowing hepatic sinusoidal hormone level, rather than the average sinusoidal level.

Statistical Analysis

Data are expressed as means ± standard error (SE). Data were analyzed for differences both among groups and within groups (i.e. change from individual baselines). Statistical comparisons for time course data were made by two-way ANOVA with repeated measures design run on SigmaStat (SPSS Science, Chicago, IL). Post hoc analysis was performed with Tukey's test. When only two values were compared an independent t-test was used (SigmaStat, SPSS Science, Chicago, IL). For Specific Aim I,

statistical comparisons of β-OHB and individual and total gluconeogenic amino acid data were made by two-way ANOVA. Statistical significance was accepted at $P < 0.05$.

CHAPTER III

THE EFFECT OF AN ACUTE ELEVATION OF FFA LEVELS ON GLUCAGON-STIMULATED HEPATIC GLUCOSE PRODUCTION

Aim

As β-cell function is impaired in overt type 2 diabetes, lower plasma insulin levels during the postprandial period should result in a decreased insulin response at both the pancreatic α-cell and adipocyte and therefore cause glucagon and FFA levels to be elevated. Indeed, in subjects with type 2 diabetes, it has been shown that glucagon secretion from α-cells is not suppressed and has even been shown to be elevated (75, 243). Additionally, FFA normally fall during the postprandial period, but in individuals with type 2 diabetes FFA levels remain elevated (223, 224). As an insufficient decrease in HGP is involved in the postprandial hyperglycemia observed in type 2 diabetes, it is possible that elevated levels of glucagon and FFA could be responsible for the increase in hepatic glucose production by the liver in these patients. Although it is well established that both glucagon and FFA are essential regulators of glucose production by the liver, it is unclear how they interact to acutely regulate HGP.

Like glucagon, epinephrine directly stimulates HGP by increasing GLY. However, the indirect actions of epinephrine alter the mechanisms (stimulate GNG/inhibit GLY) by which glucose is produced by the liver. This results from its ability to release FFA from adipose tissue. Since the direct actions of both epinephrine and glucagon on HGP are mediated by cAMP, it could be hypothesized that the elevated

FFA, as seen postprandially in type 2 diabetes, would alter hepatic glucagon action in a similar manner to that seen with epinephrine. Therefore the goal of ***Specific Aim I*** was to determine the effects of physiological incremental increases in glucagon and FFA on the contributions of GLY and GNG of HGO.

Experimental Design

First Study

Each experiment consisted of a tracer and dye equilibration period (-140 to -40 min), a basal period (-40 to 0 min), and an experimental period (0 to 195 min). At -140 min, a priming dose of [3-^{3}H] glucose (33.3 μCi) was given and a constant infusion of [3-^{3}H] glucose (0.35 μCi/min) was begun to allow the assessment of hepatic glucose production. Constant infusions of indocyanine green (0.077 mg/min), to assess hepatic blood flow, and somatostatin (0.8 μg/kg/min), to inhibit endogenous insulin and glucagon secretion were also started at -140 min. A constant intraportal infusion of glucagon (0.55 ng/kg/min) was given (t = -140 min) to replace basal endogenous glucagon secretion. Endogenous insulin was replaced intraportally at a variable rate beginning at -140 min. The plasma glucose level was monitored every 5 min, and euglycemia was maintained by adjusting the rate of insulin infusion. Once the plasma glucose level had been stabilized at euglycemia for 30 min, basal sampling was started (-40 min) and the infusion rate of insulin remained unchanged thereafter. The average insulin infusion rate was 234 ± 23 μU/kg/min.

The first study included five protocols:

Protocol 1 (GGN, n = 6): At 15 min, the intraportal glucagon infusion was increased from 0.55 ng/kg/min to three times the basal rate (1.65 ng/kg/min).

Protocol 2 (HG, n = 5): To control for the effects of hyperglycemia on HGO, a hyperglycemic clamp was performed. 20% dextrose was infused via a leg vein to clamp the arterial glucose at the levels seen in the groups receiving three times basal glucagon.

Protocol 3 (FFA + GGN, n = 7): A constant Intralipid (0.02 ml/kg/min, 20% fat emulsion; Baxter Healthcare Corporation, Deerfield, IL) plus heparin (0.5 U/kg/min) infusion was started at 0 min via a leg vein. After a FFA/glycerol equilibration period (15 min), the intraportal glucagon infusion was increased from 0.55 ng/kg/min to 1.65 ng/kg/min as seen in protocol 1.

Protocol 4 (GLYC + GGN, n = 5): To control for the rise in glycerol, a constant glycerol infusion (via a leg vein) of 0.95 mg/kg/min was started at 0 min. After a glycerol equilibration period (15 min), the intraportal glucagon infusion was increased from 0.55 ng/kg/min to 1.65 ng/kg/min as seen in protocol 1.

Protocol 5 (FFA + HG, n= 5): In order to control for the increase in FFA, glycerol, and glucose, a constant 20% Intralipid (0.02 ml/kg/min) plus heparin (0.5 U/kg/min) infusion was started at 0 min in the presence of a hyperglycemic clamp. 20% dextrose was infused via a leg vein to clamp the arterial glucose at the levels seen in the groups receiving three times basal glucagon.

The glucagon infusion rate was increased by 7% every hour in groups 1, 3, and 4 to compensate for aggregation occurring in the infusion syringe.

Arterial blood samples were taken every 10 min during the basal period and every 15 min during the experimental period. In the FFA + HG and HG groups, arterial blood

samples were also taken every 5 minutes in order to monitor glucose levels. The total blood volume withdrawn did not exceed 20% of the dog's total blood volume and each volume of blood was replaced with two volumes of saline.

Second Study

The equilibration period (-140 to -40 min) and basal period (-40 to 0 min) in the second study were identical to those in the first study (described above). The average insulin infusion rate for this study was 264 ±28 μU/kg/min. The experimental period (0 to 45 min) was not only shortened to 45 min but the FFA/glycerol equilibration period was extended 15 min and the glucagon and Intralipid/heparin infusion rates were increased by 33% and 50%, respectively, compared to the first study.

The second study included only two protocols:

Protocol A (GGN, n = 3): At 30 min, the intraportal glucagon infusion was increased from 0.55 ng/kg/min to four times the basal rate (2.2 ng/kg/min).

Protocol B (FFA + GGN, n = 3): A constant Intralipid (0.03 ml/kg/min, 20% fat emulsion; Baxter Healthcare Corporation, Deerfield, IL) plus heparin (0.75 U/kg/min) infusion was started at 0 min via a leg vein. After a FFA/glycerol equilibration period (30 min), the intraportal glucagon infusion was increased from 0.55 ng/kg/min to 2.2 ng/kg/min as seen in protocol A.

Arterial blood samples were taken every 10 min during the basal period, every 10 min during the FFA/glycerol equilibration (0 to 30 min), and every 5 min after the glucagon infusion was increased to four times the basal rate (30 to 45 min). The total blood volume withdrawn did not exceed 20% of the dog's total blood volume and each volume of blood was replaced with two volumes of saline.

Immediately following the final blood sample, each animal was anesthetized with pentobarbital sodium. The animal was then removed from the harness while the hormones and Intralipid/heparin continued to be infused. A midline laporotomy incision was made, and clamps cooled in liquid nitrogen were used to freeze sections of left and right central and left lateral lobes of the liver in situ. The hepatic tissue was then cut free, placed in liquid nitrogen, and stored at –70°C. Approximately 2 min elapsed between the time of anesthesia and the time of tissue clamping. All animals were then euthanized.

Results

Hormone levels and hepatic blood flow. Arterial plasma levels of insulin remained basal in all groups throughout the study (Tables 3.1 and 3.2). During the basal period, arterial and portal vein plasma glucagon levels were ~45 ± 2 and 60 ± 2 pg/ml, respectively (data not shown). During the experimental period, glucagon infusion at three times the basal rate (1.65 ng/kg/min) caused increases of ~ 40 and 100 pg/ml in arterial and portal vein plasma glucagon levels, respectively (all $P < 0.05$; Fig. 3.1, Table 3.2). In the HG and FFA + HG groups, arterial and portal vein plasma glucagon levels remained basal and stable during the experimental period (Fig. 3.1). Arterial plasma cortisol, arterial blood epinephrine and norepinephrine, and hepatic blood flow remained basal in all groups throughout the study (data not shown).

Arterial levels and net hepatic uptakes of plasma FFA and blood glycerol. Peripheral infusions of Intralipid and heparin increased the arterial plasma FFA level from ~ 545 to ~ 1650 μmol/l by the end of the study ($P < 0.05$, Fig. 3.2). The arterial plasma FFA level remained unchanged in the GLYC + GGN (Table 3.2), GGN, and HG groups (Fig. 3.2).

Net hepatic uptake of FFA increased from ~ 2 to ~ 4 - 5 μmol/kg/min by the last hour in the FFA+GGN and FFA + HG groups ($P < 0.05$, Fig. 3.2). Net hepatic uptake of FFA remained basal and unchanged in the GLYC + GGN (Table 3.2), GGN, and HG groups (Fig. 3.2).

Peripheral infusions of Intralipid and heparin increased the arterial blood glycerol level from ~ 70 to ~ 200 μmol/l by the end of the study in the FFA + GGN and FFA + HG groups, respectively ($P < 0.05$, Fig. 3.2). In the GLYC + GGN group, a peripheral glycerol infusion of 0.95 mg/kg/min increased the arterial blood glycerol level from 74 ± 9 to 195 ± 21 μmol/l ($P < 0.05$, Table 3.2). The arterial blood glycerol level remained basal and unchanged in the GGN and HG groups (Fig. 3.2). Net hepatic glycerol uptake increased from ~ 1.5 to 3.5 μmol/kg/min in the FFA + GGN, GLYC + GGN, and FFA + HG groups (all $P < 0.05$; Fig. 3.2, Table 3.2). Net hepatic uptake of glycerol remained basal and unchanged in the GGN and HG groups (Fig. 3.2).

Glucose metabolism. In all five groups, plasma glucose levels rose from just over 100 to ~ 200 mg/dl (Fig. 3.3, Table 3.2). In response to a portal infusion of glucagon (1.65 ng/kg/min), net hepatic glucose output (NHGO) increased by 5.4 ± 1.6 and 4.8 ± 1.0 mg/kg/min (both $P < 0.05$, NS between groups) in GGN and GLYC + GGN groups, respectively, by 15 min of glucagon infusion (min 30, Fig. 3.3, Table 3.2). In the presence of Intralipid and heparin infusions, glucagon-stimulated NHGO only increased by 3.2 ± 1.1 mg/kg/min ($P < 0.05$ vs. GGN and GLYC + GGN groups, Fig. 3.3). Hyperglycemia alone (HG) and peripheral infusions of Intralipid and heparin in the presence hyperglycemia (FFA+HG) resulted in a decrease in NHGO from 1.6 ± 0.3 to -0.4 ± 0.5 and 2.2 ± 0.2 to 0.2 ± 0.7 mg/kg/min, respectively, by the last hour of the

experimental period (Fig. 3.3). Changes in tracer-determined endogenous glucose production (R_a) paralleled the changes in NHGO (Table 3.3, Table 3.2). Elevation in circulating FFA blunted glucagon-stimulated endogenous glucose production by 50% (Δ 2.2 mg/kg/min, $P< 0.05$, GGN minus HG vs. FFA + GGN minus FFA + HG at min 30, Table 3.3).

Net hepatic glycogenolysis and gluconeogenesis. In response to a portal infusion of glucagon (1.65 ng/kg/min), net hepatic glycogenolysis (NHGLY) had increased by 5.4 ± 1.6 and by 5.7 ± 1.4 mg/kg/min in GGN and GLYC + GGN groups, respectively, 15 min after initiation of the glucagon infusion (min 30, both $P < 0.05$, Fig. 3.4, Table 3.2). In the FFA + GGN group, NHGLY had only increased by 3.2 ± 1.1 mg/kg/min by 15 min (min 30, $P < 0.05$ vs. GGN and GLYC + GGN groups, Fig. 4). In the HG and FFA + HG groups, NHGLY decreased from 2.2 ± 0.5 to -0.03 ± 0.4 and 3.0 ± 0.5 to 0.08 ± 0.4 mg/kg/min (last 30 minutes of the experimental period; Fig. 3.4).

Net hepatic gluconeogenic (NHGNG) flux had fallen by 0.9 ± 0.2, 0.7 ± 0.4, and 0.8 ± 0.4 15 min after the start of glucagon infusion (min 30) in the GGN, FFA + GGN, and GLYC + GGN groups, respectively (Fig. 4). By the last 30 min of the study, NHGNG flux had returned to basal rates in the GGN and GLYC + GGN groups (Fig. 4, Table 3.2). However, in the FFA + GGN and FFA + HG groups, peripheral infusions of Intralipid and heparin resulted in an increase in NHGNG flux of 0.8 ± 0.2 and 0.8 ± 0.3 mg/kg/min, respectively, by the end of the study ($P < 0.05$, Fig. 3.4). NHGNG flux fell slightly in response to hyperglycemia alone (NS, Fig. 3.4).

Arterial blood levels and net hepatic balances of β–OHB and acetoacetate. Peripheral infusions of Intralipid and heparin tended to cause a rise in arterial blood β-

hydroxybutyrate (β-OHB) levels (~20 to 27 μmol/l, last h) even though there was no significant increase in net hepatic β-OHB output (NS, data not shown). In the absence of elevated FFA, there was no significant change in arterial levels or net hepatic output of β-OHB (data not shown). The arterial blood levels of acetoacetate remained unchanged regardless of treatment despite the tendency for net hepatic output of acetoacetate to increase over time in the GGN, FFA + GGN, and FFA + HG groups (~ Δ 0.5 μmol /kg/min) and decrease in the GLYC + GGN and HG groups (~Δ -0.2 μmol /kg/min, NS, data not shown).

Arterial blood levels and net hepatic outputs of lactate. After the first 75 min of the experimental period, three times basal glucagon caused an initial modest increase in arterial blood lactate levels, due to an rise in net hepatic lactate output (NHLO, Fig. 3.5, Table 3.2). An elevation in plasma FFA decreased NHLO by the end of the study in both the FFA + GGN and FFA + HG groups ($P < 0.05$, Fig. 3.5). In the presence of hyperglycemia (HG), arterial blood lactate levels rose significantly (716 ± 176 to 1142 ± 269 μmol/l; 195 min, $P < 0.05$) over time as a result of an increase in NHLO (Fig. 3.5).

Arterial blood levels, net hepatic balances, and fractional extraction of gluconeogenic amino acids. Portal infusion of glucagon (1.65 ng/kg/min), had no effect on arterial blood levels, net hepatic balance, or fractional extraction of individual or total amino acids by 30 min after the initiation of glucagon infusion (data not shown). By the end of the study, individual (excluding glutamine and glutamate) and total amino acid fractional extraction increased in response to three times basal glucagon ($P < 0.05$, data not shown). This in turn resulted in a fall in arterial blood levels and some decrease in net hepatic uptake of the gluconeogenic amino acids (NS, data not shown). However, an elevation of

FFA levels did not alter glucagon's effect on amino acid fractional extraction at any time point throughout the experiment (data not shown). In the HG and FFA + HG groups, individual and total amino acid arterial blood levels, net hepatic balances, and fractional extractions remained constant throughout the study.

Hepatic cAMP levels at the peak of glucagon action. To determine if elevated plasma FFA inhibit the rise in cAMP caused by glucagon *in vivo*, we repeated the GGN and FFA + GGN protocols (n=3/group) and terminated the experimental period at the peak of glucagon action (15 min after the increase in the glucagon infusion rate) and collected tissue to assess hepatic cAMP levels. In addition to shortening the experimental period, we extended the FFA/glycerol equilibration period by 15 min and the glucagon and Intralipid/heparin infusion rates were increased by 33% and 50%, respectively, compared to the first study.

Arterial plasma levels of insulin remained basal (~6.0 μU/ml) in both groups throughout the study. Arterial and portal plasma glucagon levels (pg/ml) increased by ~ 50 and 140 pg/ml in both groups, respectively ($P < 0.05$, Fig. 3.6). Arterial plasma cortisol, arterial blood catecholamines, and hepatic blood flow remained basal in both groups (data not shown). Arterial plasma FFA (570 ± 36 μmol/l) and blood glycerol (55 ± 7 μmol/l) remained basal in the GGN group throughout the study. In the FFA + GGN group, peripheral infusions of Intralipid and heparin increased the arterial plasma FFA and blood glycerol levels from 419 ± 51 to 1482 ± 241 and 42 ± 9 to 252 ± 47 μmol/l, respectively ($P < 0.05$). Arterial glucose levels (mg/dl) rose from 106 ± 4 to 125 ± 2 in the GGN group and from 108 ± 2 to 135 ±7 in the FFA + GGN group ($P < 0.05$).

In response to a portal infusion of glucagon (2.2 ng/kg/min), NHGO increased from 1.9 ± 0.2 (0 to 30 min) to 10.1 ± 1.8 (min 45) mg/kg/min ($P < 0.05$ vs basal, Fig. 3.6). However, in the FFA + GGN group, elevated FFA and glycerol blunted glucagon stimulated NHGO, where NHGO rose from 1.9 ± 0.5 (0 to 30 min) to 8.0 ±1 mg/kg/min (min 45, $P < 0.05$ vs basal, Fig. 3.6). Similarly, four times basal glucagon increased NHGLY (mg/kg/min) from ~2.0 (0 to 30 min) to 12.3 ± 2.5 in the GGN group and to only 8.4 ±1.7 in the FFA + GGN group at min 45 ($P < 0.05$ vs. basal, Fig. 3.6). NHGNG flux (mg/kg/min) decreased from -0.6 ± 0.4 to -2.2 ± 0.7 after 15 min of four times basal glucagon infusion ($P < 0.05$, Fig. 3.6). However, in the FFA + GGN group, NHGNG flux did not change in response to glucagon (Fig. 3.6).

In the GGN group, there was a slight increase in arterial lactate levels from 721 ± 254 to 1103 ± 247 μmol/l due to a dramatic rise in NHLO (μmol/kg/min) from 9.7 ± 4 to 31 ± 8 ($P < 0.05$, Fig. 3.6). Elevated FFA and glycerol completely inhibited glucagon's increase in NHLO (Fig. 3.6). Hepatic cAMP levels (ng/mg of tissue) increased from a basal level of 96 ± 16 to 178 ± 9 and 176 ± 24 in the GGN and FFA + GGN groups, respectively (n=3/group, data not shown).

Discussion

The present study determined the effects of physiological increments in glucagon and FFA on HGO in the presence of basal insulin and matched glycemia in the conscious dog. Glucagon was elevated to levels approximately one-half those needed for the hormone's maximal effect on HGO (266) so that we would be able to detect any change caused by FFA. Intralipid and heparin were infused at rates needed to achieve FFA levels identical to those seen in our previous studies in which we assessed the ability of a simulated rise in lipolysis to alter epinephrine's hepatic glycogenolytic and gluconeogenic effects (265, 266). Since the direct actions of both glucagon and epinephrine on HGO are mediated by cAMP, we hypothesize that elevated FFA will alter glucagon-stimulated HGO as it does on epinephrine action at the liver. Although the results from the present studies showed that an increase in FFA did in fact limit the initial increase in glucagon-stimulated HGO by blunting glycogenolysis, the elevation of FFA did not increase gluconeogenic flux.

The present studies confirmed previous findings that stimulation of HGO by glucagon primarily results from an initial rapid, potent, and time-dependent increase in glycogenolysis (48, 49, 116, 117, 169). In the first and second studies, the increments in portal glucagon levels increased NHGLY by 5.5 ± 1.6 mg/kg/min and 7.2 ± 1.4 mg/kg/min, respectively, within 15 min (Figs. 4 and 6). However, in the first study, combined Intralipid and heparin infusion blunted glucagon's initial increase in NHGO (40%) and NHGLY (40%, $P < 0.05$, Figs. 3.3 and 3.4). A trend for the inhibition of NHGO (20 %) and NHGLY (30%) was also observed in the second study but the small number of animals used prevented statistical significance from being achieved

(n=3/group, Fig. 6). In the presence of an isolated rise in glycerol equivalent to that seen with Intralipid (0.02 ml/kg/min) and heparin (0.5 U/kg/min), the rise in portal glucagon stimulated a similar increase in NHGLY (5.6 ± 1.4 mg/kg/min) by 15 min to that seen with glucagon administration alone in study one (Table 3.2 and Fig. 3.4). Thus, the inhibition of glycogenolysis and consequently HGO seen in response to Intralipid and heparin must have been solely due to elevated plasma FFA. As expected, hyperglycemia suppressed NHGLY and NHGO to approximately zero in the HG and FFA + HG groups (Fig. 3.3 and 3.4). Therefore, these findings indicate that elevated FFA inhibit the glycogenolytic effects of glucagon as they do those of epinephrine. However, this effect was short-lived (1 h) compared to that of increased FFA on epinephrine-induced net hepatic glycogenolysis, which lasted for a 2 h period (53).

Consistent with our earlier findings (48, 116, 117) glucagon administration resulted in an immediate but brief decrease in NHGNG flux in the GGN and GLYC + GGN groups (Table 3.2 and Fig. 3.4 and 3.6). The initial decrease corresponds to and presumably results from the hormone's rapid effect on NHGLY, in which some of the glucose produced by the breakdown of glycogen enters the glycolytic pathway and exits the liver as lactate (48, 49). In fact, the increase in net hepatic lactate output mirrored the initial increase in NHGLY in the GGN and GLYC + GGN groups (Table 3.2 and Fig. 3.4, 3.5, and 3.6). Over the first 75 min of the experimental period, Intralipid and heparin infusion showed a tendency to blunt the increase in net hepatic lactate output caused by glucagon (Fig. 3.5). Lack of statistical significance of this blunting effect was due to one outlier. If this particular dog was omitted, the initial change in net hepatic lactate output

(μmol/kg/min) would be 3.8 ± 1.5 in the FFA + GGN group as opposed to 10.4 ± 1.1 in the GGN group (min 30). In the second study, the fall in NHGNG flux and rise in net hepatic lactate output was completely inhibited in the FFA + GGN group ($P < 0.05$, n=3/group, Figs. 3.6). Thus, the glucose and lactate data from both the first and second studies collectively indicate that elevated FFA blunt glucagon-stimulated NHGO by inhibiting NHGLY.

Because overall NHGNG flux did not change in the GGN group (Fig. 3.4), the present data are consistent with our previous findings that glucagon has little to no acute effect on hepatic gluconeogenesis. On the other hand, NHGNG flux increased from -0.08 ± 0.4 to 0.67 ± 0.3 mg/kg/min by the end of the study in the FFA + GGN group (Fig. 3.4). Although an increase in NHGNG was observed in this group, it cannot be interpreted as an augmentation of glucagon action since an identical increase in NHGNG flux was observed in the FFA + HG group (Fig. 3.4). In both Intralipid/heparin protocols, the almost three-fold rise in blood glycerol levels (Fig. 3.2), giving rise to increases in net hepatic glycerol uptake, contributed to the increase in hepatic gluconeogenesis. However, the rate of NHGNG flux in the GLYC + GGN group was identical to that seen with glucagon treatment alone. Arterial NHGNG flux did not significantly change in the presence of hyperglycemia alone. It seems most likely, therefore, that the rise in hepatic gluconeogenesis was largely due to the increase in hepatic FFA uptake. In contrast to the interaction of FFA and epinephrine (53), elevated plasma FFA did not augment glucagon's ability to stimulate hepatic gluconeogenesis.

Elevated FFA blunt the early response of hepatic glycogenolysis to both glucagon and epinephrine. A rise in plasma FFA has been shown to result in an increase in fatty

acid metabolites (fatty acyl CoA, diacylglycerol, ceramides) in liver and muscle (42), which have been suggested to activate protein kinase C (PKC, (115, 156, 241). Bouscarel et al have shown that activated PKC inhibits glucagon-induced cAMP formation in hepatocytes (30). Activated PKC can also phosphorylate and inactivate G_s (126), resulting in a subsequent desensitization of the glucagon or β_2-adrenergic receptor (206). Therefore it could be hypothesized that an increase in fatty acid metabolites directly inhibit the glucagon and epinephrine signaling pathways via the activation of PKC, which would inactivate $G_{s,}$ and in turn inhibit adenlyate cyclase, resulting in a decrease in cAMP. Our finding that hepatic cAMP content at the peak of glucagon-stimulated glycogenolysis was not blunted by high levels of FFA (data not shown) does not support this hypothesis.

FFA have been shown to directly inhibit glucose-6-phophatase (180, 181), which subsequently increases glucose-6-phosphate (G6P) which can stimulate glycogen synthase and inhibit hepatic glycogenolysis. Using liver samples from the first study, Hornbuckle et al have shown that FFA did not alter mRNA expression of the catalytic subunit or transporter of glucose-6-phosphatase (129). However, these liver samples were collected at the end of the study, when FFA had no effect on HGO. It remains possible that FFA could directly inhibit glucose-6-phosphatase activity, thereby blunting the initial response to glucagon.

A more likely hypothesis is that elevated FFA blunted the early rise in hepatic glycogenolysis by inhibiting glycolysis. It has been proposed (132, 186, 221) that increased FFA levels could raise intracellular citrate levels leading to an inhibition of phosphofructokinase, thus at the same time limiting glycolysis, and consequently

increasing G6P, which would in turn blunt NHGLY. Our current studies, particularly the second, of the two sets of experiments show that a rise in FFA blunted glucagon's immediate, brief increase in net hepatic lactate output, suggesting inhibition of net hepatic glycolysis. In response to hyperglycemia or glucagon- and epinephrine-stimulated glycogenolysis, an increase in net hepatic lactate output occurs (49, 53, 84, 116, 117, 193, 265), most likely because some of the glucose taken up by the liver and produced by glycogen breakdown, respectively, enters the glycolytic pathway and exits the liver as lactate. Intralipid and heparin infusions result in net hepatic lactate uptake consistent with inhibition of glycolysis or stimulation of gluconeogenesis (54). In agreement with this, hyperinsulinemia which reduces plasma FFA results in an increase in net hepatic lactate output (84, 255) that is not evident when the FFA level is clamped (255). Additionally, in the present (Fig. 3.5) and previous studies (53, 54), an elevation of plasma FFA decreased the ability of hyperglycemia to cause net hepatic lactate output. Although it has been suggested that elevated FFA results in an increase in hepatic gluconeogenesis which then inhibits hepatic glycogenolysis (44, 54, 59, 60, 158, 217), these and other studies have shown that by the time the rise in glycogenolysis was fully manifest (30 min) a small decrease had occurred in hepatic gluconeogenic flux (53, 116, 117).

Although FFA have a similar effect on the initial action of both glucagon and epinephrine on HGO, FFA temporally affect each hormone differently. With time, an elevation in plasma FFA did not alter the overall rate of epinephrine-mediated HGO but enhanced the hormone's ability to stimulate gluconeogenesis and inhibited its action on glycogenolysis (53). In contrast, by the end of the present study the rise in FFA did not

alter glucagon-stimulated glucose production by the liver or the mechanisms by which it was produced. Thus, the autoregulation, which took place in presence of epinephrine, did not occur in the presence of glucagon. One possible explanation for this lies in that the potency of glucagon to stimulate glycogenolysis and thus force carbon down the glycolytic pathway is greater than that of epinephrine. This would override FFA's ability to inhibit glycolysis or fuel gluconeogenesis. When epinephrine is administered peripherally, and therefore has both direct and indirect (i.e. stimulation of lipolysis) effects on the liver, hepatic lactate uptake occurs (57, 116, 117, 265), whereas net hepatic lactate output takes place following portal administration of epinephrine (53, 56, 57).

In conclusion, these findings indicate that elevated FFA inhibit the glycogenolytic effects of glucagon, as they do the glycogenolytic effect of epinephrine. However, this effect is short-lived compared to epinephrine. In contrast to epinephrine, an increase in FFA does not augment glucagon-stimulated hepatic gluconeogenesis. Although postprandial levels of glucagon and FFA are elevated in individuals with type 2 diabetes, our results suggests that their interaction alone does not potentiate HGO nor does FFA alter the mechanisms by which glucagon stimulates HGO.

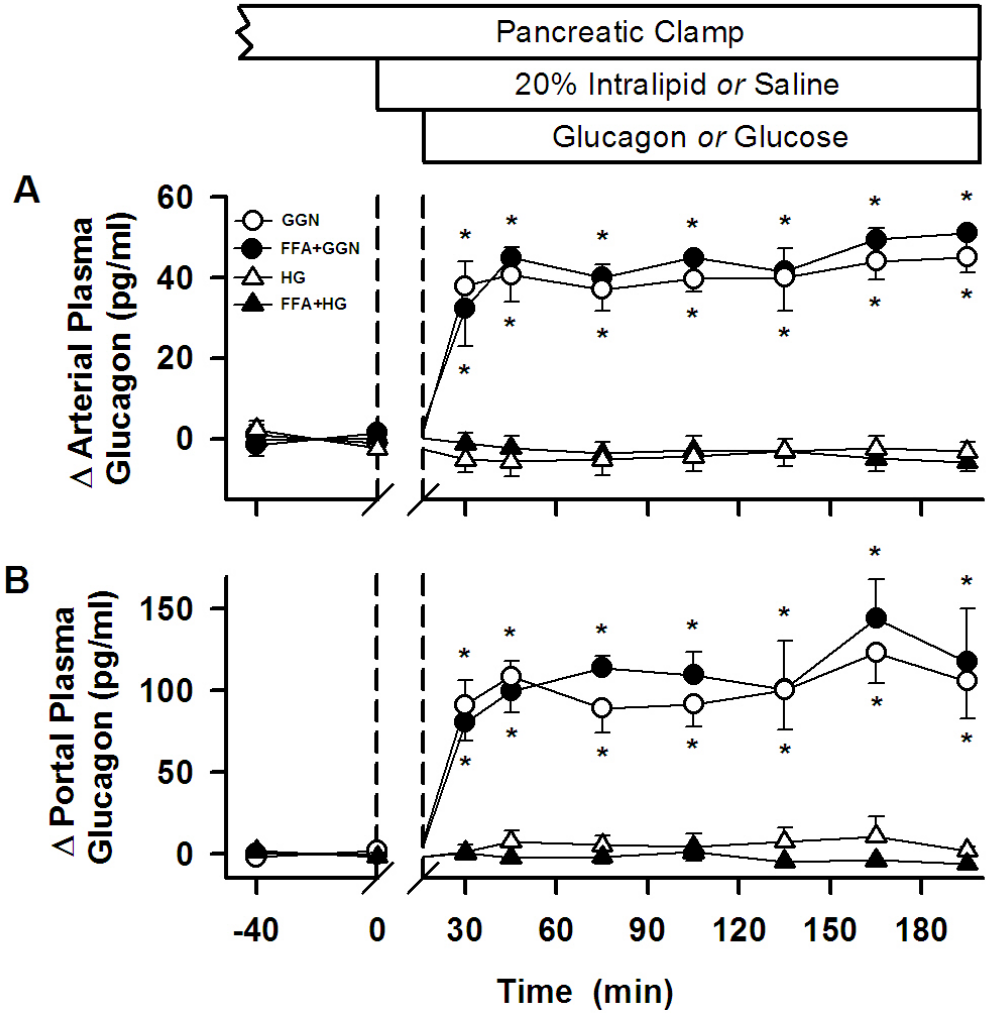

Figure 3.1: Arterial and portal vein levels of plasma glucagon. Change in arterial plasma (A) and portal vein (B) glucagon levels during basal (-40 to 0 min) and experimental (0 to 195 min) periods in the presence of a pancreatic clamp. A break was set in the x axis between 0 and 16 min. Protocols were performed in conscious 18 h fasted dogs. Values are means ± SE. * $P < 0.05$ vs. respective basal levels for both groups receiving three times basal glucagon (GGN and FFA + GGN).

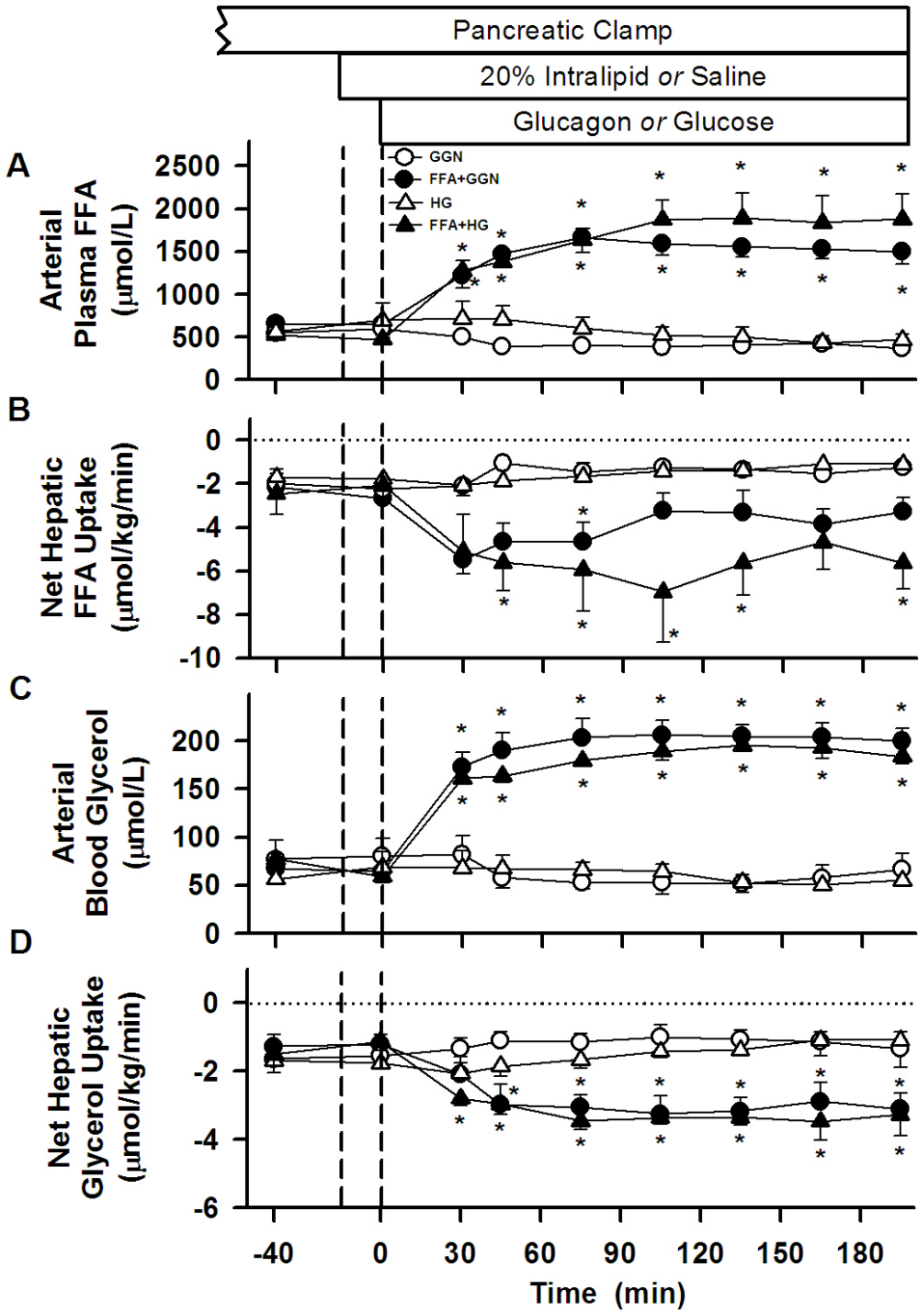

Figure 3.2: Arterial plasma FFA and blood glycerol levels and net hepatic uptake. Arterial plasma FFA levels (A), net hepatic FFA uptake (B), arterial blood glycerol levels (C), and net hepatic glycerol uptake (D) during basal (-40 to 0 min) and experimental (0 to 195 min) periods in the presence of a pancreatic clamp. Protocols were performed in conscious 18 h fasted dogs. Values are means ± SE. * $P < 0.05$ vs. respective basal levels for both groups receiving 20% Intralipid plus heparin infusions (FFA+GGN and FFA+HG).

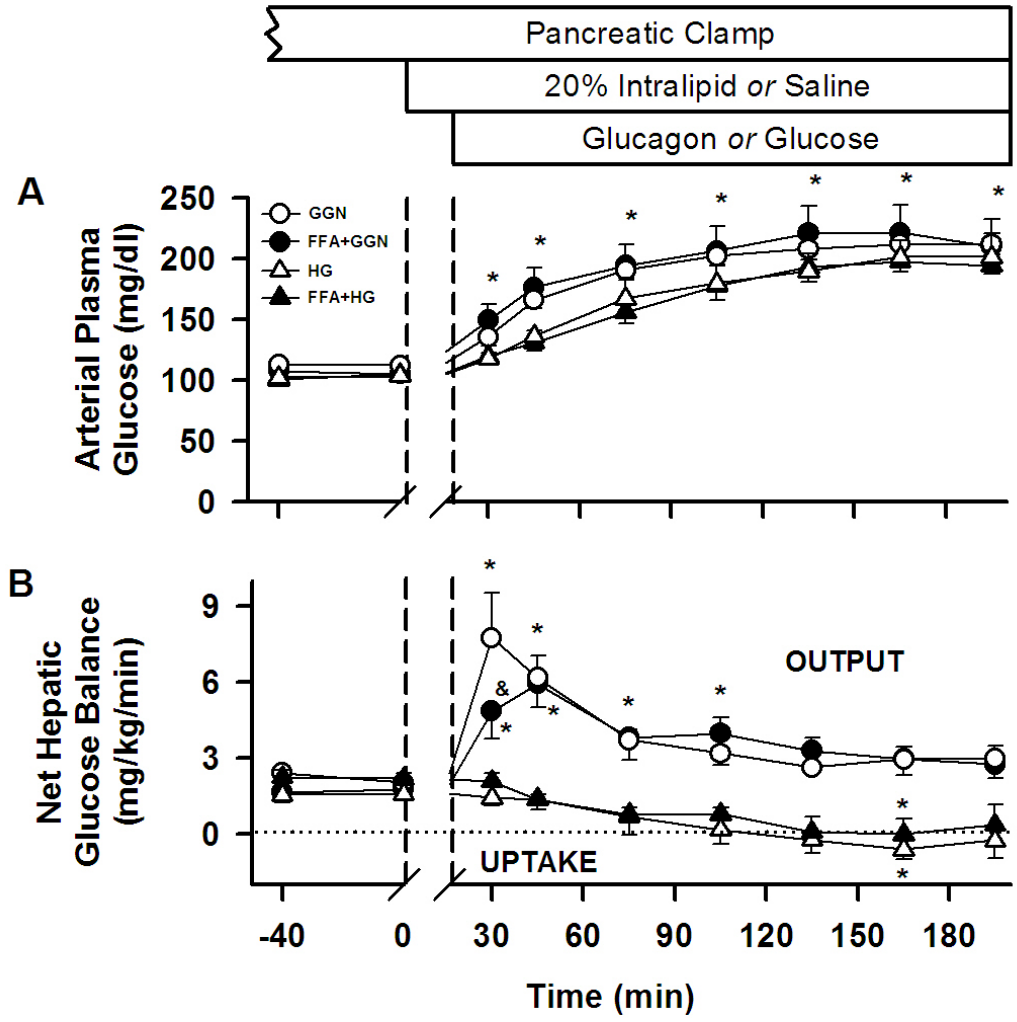

Figure 3.3: Arterial plasma levels of glucose and net hepatic glucose balance. Arterial plasma levels of glucose (A) and net hepatic glucose balance (B) during basal (-40 to 0 min) and experimental (0 to 195 min) periods in the presence of a pancreatic clamp. A break was set in the x axis between 0 and 16 min. Protocols were performed in conscious 18 h fasted dogs. Negative and positive values of net hepatic balance represent net hepatic uptake and output, respectively. Values are means ± SE. * $P < 0.05$ vs. respective basal values for all groups. There were no significant differences between the groups for arterial plasma glucose. & $P < 0.05$ FFA+GGN vs. GGN.

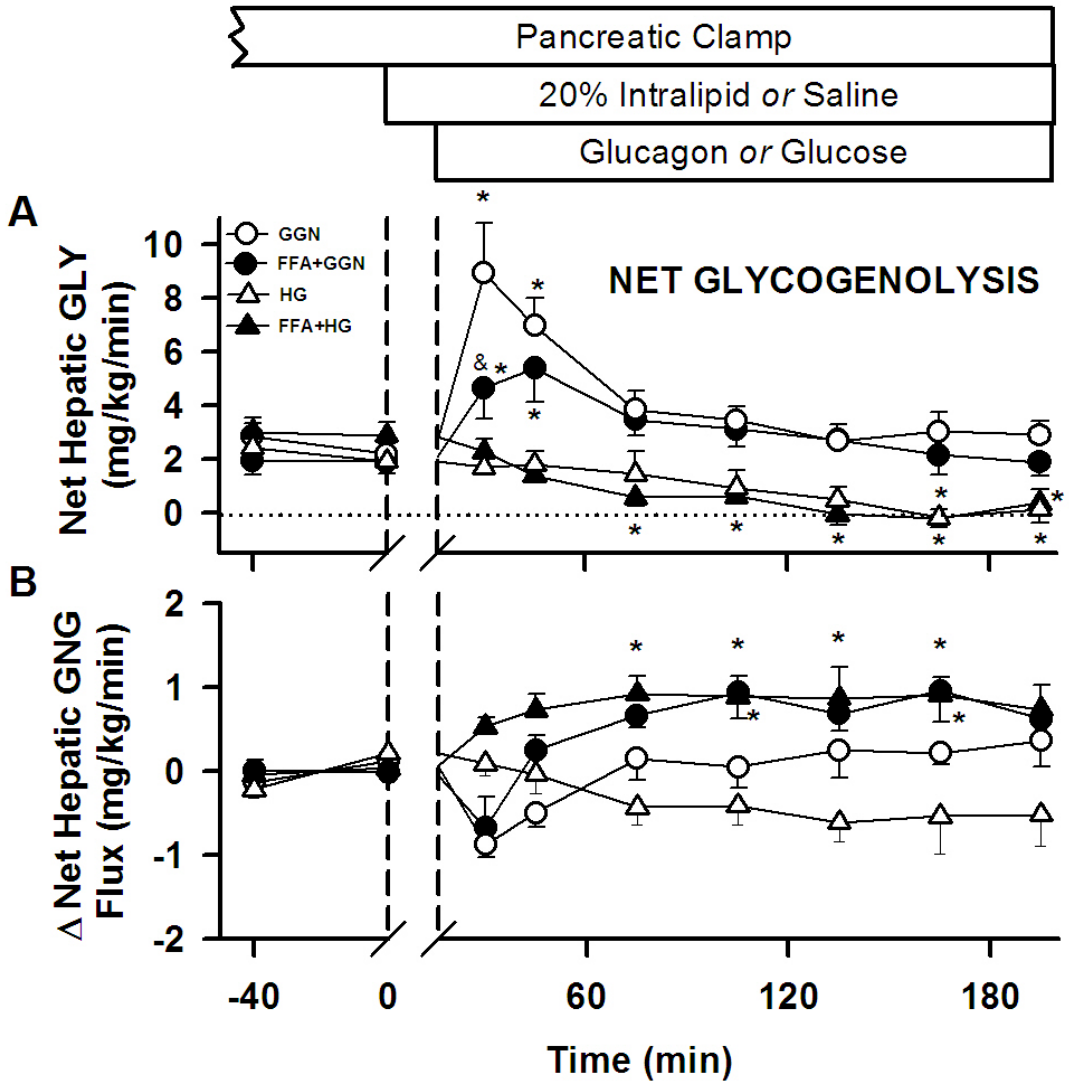

Figure 3.4: Net hepatic glycogenolysis (GLY) and gluconeogenic (GNG) precursor flux. Net hepatic glycogenolytic (A) and gluconeogenic flux (B) during basal (-40 to 0 min) and experimental (0 to 195 min) periods in the presence of a pancreatic clamp. A break was set in the x axis between 0 and 16 min. Protocols were performed in conscious 18 h fasted dogs. Negative and positive values of net hepatic GNG flux represent net glycolysis and net gluconeogenesis, respectively. Values are means ± SE. * $P < 0.05$ vs. respective basal values for all groups. & $P < 0.05$ FFA+GGN vs. GGN.

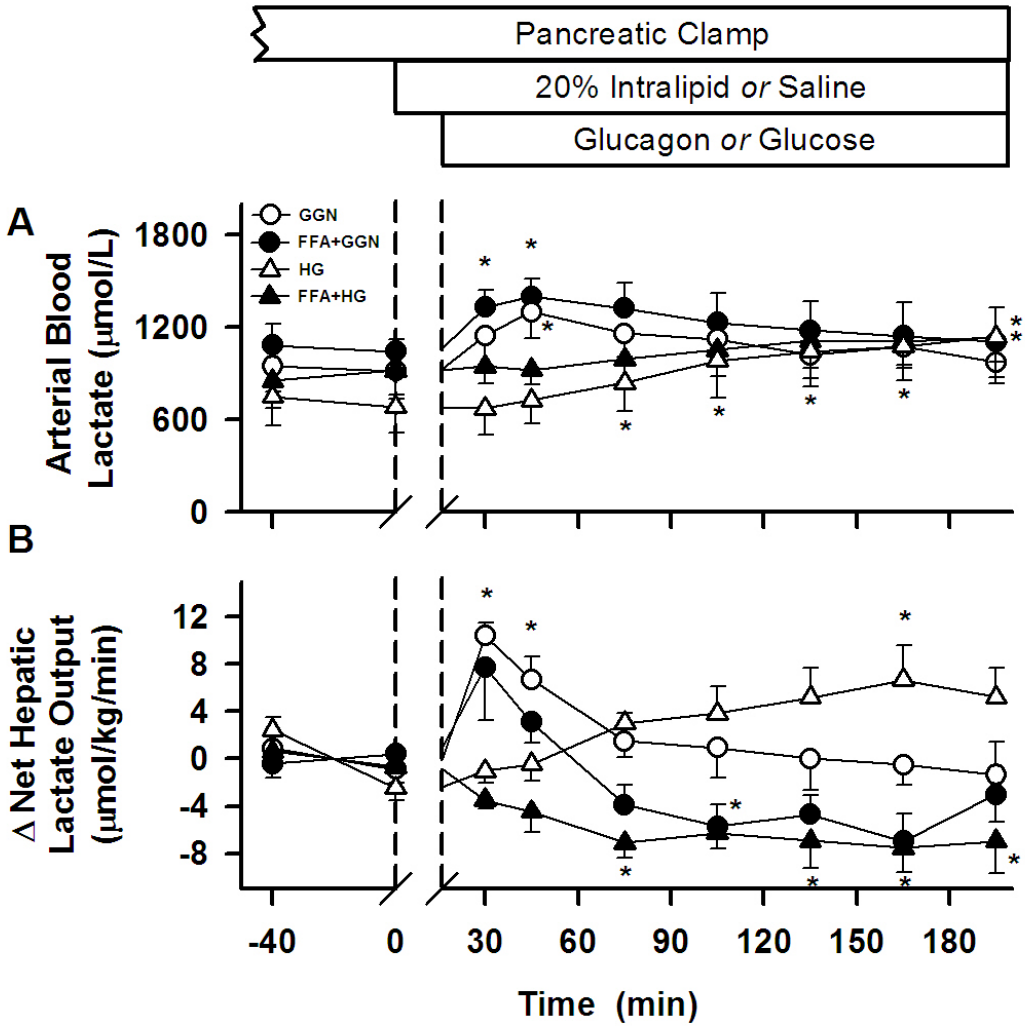

Figure 3.5: Arterial blood levels and net hepatic output of lactate. Arterial blood levels (A) and change in net hepatic balance (B) of lactate during basal (-40 to 0 min) and experimental (0 to 195 min) periods in the presence of a pancreatic clamp. A break was set in the x axis between 0 and 16 min. Protocols were performed in conscious 18 h fasted dogs. Values are means ± SE. * $P < 0.05$ vs. respective basal levels.

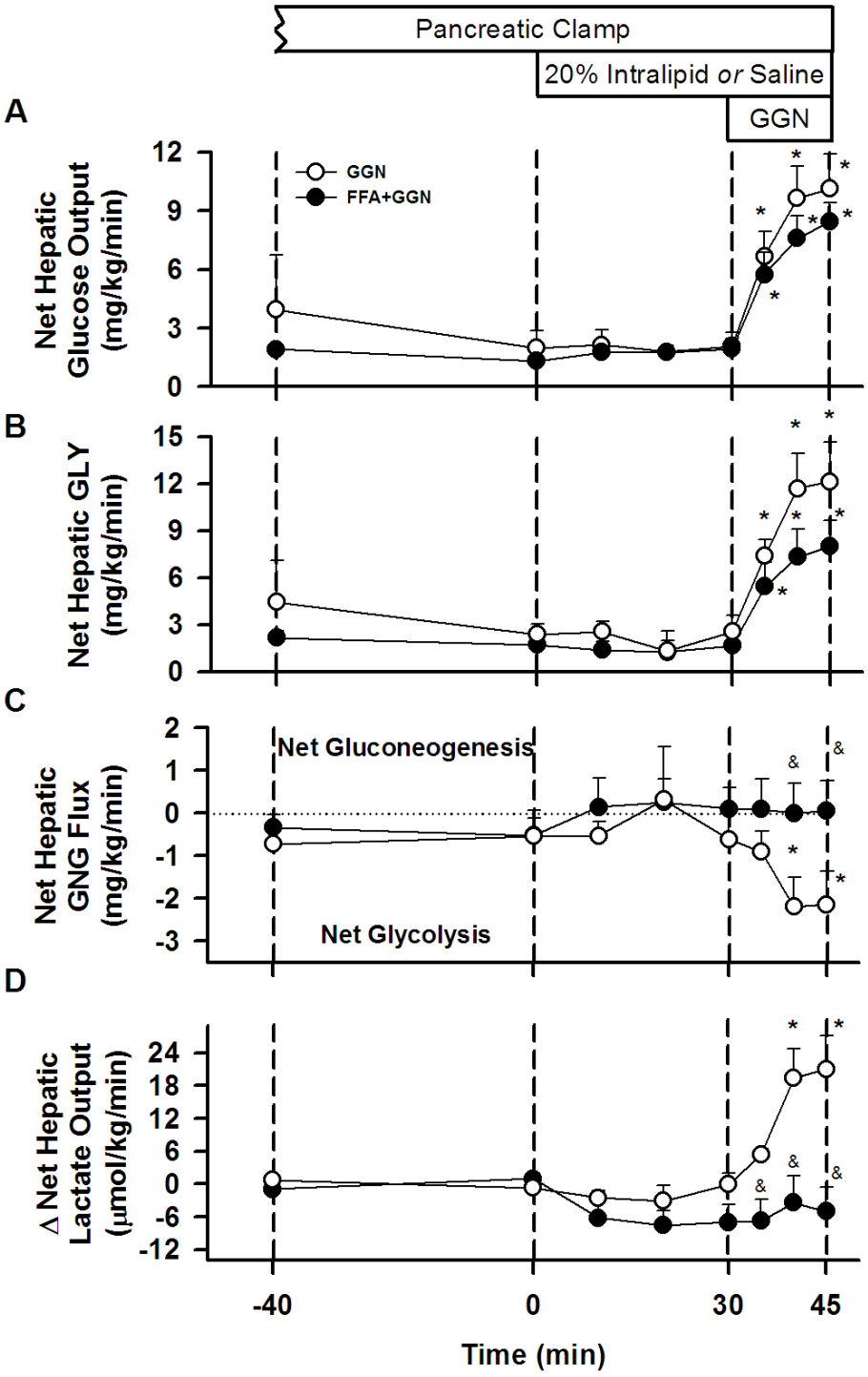

Figure 3.6: Net hepatic glucose balance, glycogenolysis (GLY) and gluconeogenic (GNG) flux, and lactate balance in the second study. Net hepatic glucose balance (A), glycogenolysis (B), gluconeogenic flux (C), and lactate balance (D) during basal (-40 to 0 min) and experimental (0 to 45 min) periods in the presence of a pancreatic clamp. Protocols were performed in conscious 18 h fasted dogs. Values are means ± SE. * $P <$ 0.05 vs. respective basal levels. & $P < 0.05$ FFA+GGN vs. GGN.

TABLE 3.1

Arterial plasma concentrations of insulin during basal (-40 to 0 min) and experimental (0 to 195 min) periods in the presence of a pancreatic clamp in conscious 18 h fasted dogs.

	Basal period	Experimental period (min)						
	-40 - 0	30	45	75	105	135	165	195
Arterial Plasma Insulin (μU/ml)								
GGN	6 ± 1	6 ± 1	6 ± 1	6 ± 1	6 ± 2	6 ± 2	6 ± 2	6 ± 2
FFA + GGN	5 ± 1	6 ± 1	6 ± 1	6 ± 1	6 ± 1	6 ± 1	6 ± 1	7 ± 1
HG	5 ± 1	5 ± 1	5 ± 1	5 ± 1	5 ± 1	6 ± 2	5 ± 1	6 ± 1
FFA + HG	4 ± 1	4 ± 1	4 ± 1	4 ± 1	5 ± 1	5 ± 1	5 ± 1	5 ± 1

Values are means ± SE. Basal period values are an average of samples taken at -40 and 0 min. There were no significant differences among groups.

TABLE 3.2

Plasma hormone levels, arterial concentrations and net hepatic uptakes of plasma FFA and blood glycerol, arterial blood concentrations and net hepatic output of lactate, glucose metabolism, and net hepatic glycogenolysis and gluconeogenic flux for the GLYC+GGN group during basal (-40 to 0 min) and experimental (0 to 195 min) periods in the presence of a pancreatic clamp in conscious 18 h fasted dogs.

	Basal period	Experimental period (min)						
	-40 - 0	30	45	75	105	135	165	195
Plasma Hormone Concentrations								
Insulin (μU/ml)								
Arterial	4 ± 1	3 ± 1	3 ± 1	3 ± 1	3 ± 1	3 ± 1	3 ± 1	3 ± 1
Δ Glucagon (pg/ml)								
Arterial	0 ± 1	37 ± 12*	43 ± 14*	39 ± 11*	41 ± 10*	41 ± 12*	37 ± 11*	41 ± 12*
Portal	0 ± 1	90 ± 18*	85 ± 26*	90 ± 21*	89 ± 23*	77 ± 24*	85 ± 20*	87 ± 30*
Arterial Concentrations and Net Hepatic Uptakes of Plasma FFA and Blood Glycerol								
Arterial Plasma FFA (μmol/l)	615 ± 82	471 ± 43	364 ± 45	349 ± 51	334 ± 60	347 ± 61	397 ± 64	427 ± 63
Net Hepatic FFA Balance (μmol/kg/min)	-2.5 ± 0.4	-1.9 ± 0.3	-1.5 ± 0.3	-1.7 ± 0.3	-1.4 ± 0.5	-1.3 ± 0.4	-1.7 ± 0.6	-1.5 ± 0.6
Arterial Blood Glycerol (μmol/l)	74 ± 9	198 ± 27*	181 ± 19*	191 ± 18*	188 ± 24*	198 ± 25*	206 ± 25*	203 ± 15*
Net Hepatic Glycerol Balance (μmol/kg/min)	-2.2 ± 0.4	-4.1 ± 0.4*	-3.7 ± 0.4*	-3.8 ± 0.4*	-3.8 ± 0.5*	-4.0 ± 0.6*	-4.3 ± 0.5*	-4.3 ± 0.6*
Arterial Blood Concentrations and Net Hepatic Output of Lactate								
Arterial Blood Lactate (μmol/l)	1027 ± 243	1342 ± 256	1470 ± 234	1429 ± 238	1370 ± 278	1440 ± 277	1396 ± 280	1369 ± 299
Δ Net Hepatic Lactate Output (μmol/kg/min)	0.0 ± 0.3	12.0 ± 2.5	10.2 ± 2.6	6.0 ± 3.4	5.5 ± 2.6	4.4 ± 3.2	2.0 ± 2.9	1.6 ± 2.8
Glucose Metabolism								
Arterial Plasma Glucose (mg/dl)	93 ± 1	110 ± 4*	142 ± 8*	168 ± 10*	176 ± 10*	183 ± 11*	187 ± 11*	193 ± 13*
Net Hepatic Glucose Output (mg/kg/min)	1.4 ± 0.2	6.3 ± 1.0	4.8 ± 0.8	2.5 ± 0.4	2.1 ± 0.5	2.3 ± 0.3	2.2 ± 0.6	1.5 ± 0.5
R_a (mg/kg/min)	3.1 ± 0.4	6.9 ± 0.6*	7.2 ± 0.7*	6.0 ± 0.5*	4.6 ± 0.5	3.9 ± 0.4	4.2 ± 0.6	4.4 ± 0.8
Net Hepatic Glycogenolysis and Gluconeogenesis								
Net Hepatic GLY (mg/kg/min)	1.9 ± 0.4	7.5 ± 1.4*!	5.9 ± 0.8*	3.3 ± 0.4	2.6 ± 0.4	2.8 ± 0.2	2.4 ± 0.5	1.7 ± 0.4
Δ Net Hepatic GNG Flux (mg/kg/min)	0.0 ± 0.1	-0.81 ± 0.4*	-0.66 ± 0.2	-0.25 ± 0.4	-0.12 ± 0.3	-0.03 ± 0.3	0.24 ± 0.2	0.25 ± 0.2

Values are means ± SE. Basal period values are an average of samples taken at -40 and 0 min. * $P < 0.05$ vs. respective basal concentrations. $ $P < 0.05$ FFA+HG. ! $P < 0.05$ FFA+GGN. FFA+GGN, n=6. GGN, n=6. FFA+HG, n=5. HG, n=5. Negative values indicate net uptake. R_a, tracer determined endogenous glucose production. GLY, glycogenolysi. GNG, gluconeogenesis.

TABLE 3.3

Tracer determined endogenous glucose production (R_a) during basal (-40 to 0 min) and experimental (0 to 195 min) periods in the presence of a pancreatic clamp in conscious 18 h fasted dogs.

	Basal period	Experimental period (min)						
	-40 - 0	30	45	75	105	135	165	195
R_a (mg/kg/min)								
GGN	2.8 ± 0.1	6.5 ± 0.7*	6.5 ± 0.7*	5.1 ± 0.5*	4.0 ± 0.3	3.8 ± 0.3	3.8 ± 0.4	3.9 ± 0.5
FFA + GGN	2.5 ± 0.2	5.5 ± 1.0*	5.6 ± 0.9*	4.8 ± 0.4*	3.9 ± 0.2	3.6 ± 0.3	3.4 ± 0.3	3.3 ± 0.3
HG	2.4 ± 0.2	2.0 ± 0.3	1.7 ± 0.2	2.0± 0.1	1.4 ± 0.4	2.1 ± 0.3	1.2 ± 0.3	1.3 ± 0.3
FFA + HG	2.4 ± 0.2	3.2 ± 0.4	2.5 ± 0.2	1.8 ± 0.4	1.5 ± 0.2	1.6 ± 0.3	1.3 ± 0.2	1.1 ± 0.3

Values are means ± SE. Basal period values are an average of samples taken at -40 and 0 min. * $P < 0.05$ vs. respective basal rates. & $P < 0.05$ FFA+GGN vs. GLYC+GGN and GGN. FFA+GGN, n=7. GGN, n=6. FFA+HG, n=5. HG, n=5.

CHAPTER IV

INDUCTION OF HEPATIC STEATOSIS IN A CANINE MODEL

Aim

Specific Aim II was to induce fatty liver (hepatic steatosis) in the dog. The net content of triglyceride in the liver depends on the relative activities of enzymes involved in lipid metabolism that influence fatty acid uptake and synthesis versus those that influence fatty acid oxidation and export. When input (uptake or *de novo* lipogenesis) of fatty acids to hepatocytes exceeds their output (degradation or export), triglycerides accumulate within the liver. Therefore, in an attempt to induce fatty liver in the dog, lipid metabolism was altered by 3 different treatments: 1) a 10% fructose diet, 2) elevating hepatic FFA flux, or 3) elevating hepatic FFA flux while simultaneously inhibiting triglyceride export from the liver using the microsomal triglyceride transfer protein inhibitor, CP-346086.

Experimental Treatment Regimens

Treatment 1: 10% fructose diet. A 10% fructose diet was used to stimulate an increase in hepatic *de novo* lipogenesis. Male mongrel dogs were fed once daily either a standard (SD, as described in Chapter II, n=2), a 10% fructose (FD, n=2) or carbohydrate (CD, 10% increase, n=2) diet for 4 months. In the FD and CD groups, either 95g of fructose or maltodextrin was added to the standard meat/chow diet, respectively. The daily caloric intake increased from ~1800 kcal/ to ~2200 kcal/d in both the HF and HC

groups. Magnetic resonance imaging (MRI) and magnetic resonance spectroscopy (MRS) were performed at 0, 6, 12, and 16 weeks. Approximately 24-h after the final feeding, a midline laparotomy incision was made following a two-step hyperinsulinemic-euglycemic clamp (described in Chapter V). Clamps cooled in liquid nitrogen were used to freeze sections of left and right central and left lateral lobes of the liver and skeletal muscle of the right sartorius *in situ*. The tissue was placed in liquid nitrogen and stored at –70°C. Approximately 2 min elapsed between the time of anesthesia and the time of tissue excision. All animals were then euthanized. Tissue lipids were separated by TLC and then quantitated by gas chromatography as described in Chapter II.

Treatment 2: Increased hepatic FFA flux. An intraportal infusion of 20% Intralipid (0.02 ml/kg/min) plus heparin (0.5 U/kg/min) or saline (0.02 ml/kg/min) was administered at ~2 PM immediately after feeding for 3-h/d for 15-d (n=7/group). Approximately 24-h after the final treatment, the same tissue sampling technique described above was carried out following a two-step hyperinsulinemic-euglycemic clamp. Tissue lipids were separated by TLC and then quantitated by gas chromatography. For histological examination, liver samples were frozen in embedding medium (Tissue-Tek, O.C.T. Compound) and stored at -70°C.

In order to determine the metabolic and hormonal changes that occurred during the daily intraportal infusions, a subset of dogs received only one 3-h treatment. Following a basal period (-40 to 0 min), the dogs were fed a meal, and an intraportal infusion of Intralipid/heparin (n=4) or saline (n=4) was administered from 0 to 180 min. Arterial, portal vein, and hepatic vein samples were taken at -40, 0, 15, and 30 min and every 30 min thereafter. Immediately following the study, the same tissue sampling

technique described above was carried out. Tissue lipids were separated by TLC and then quantitated by gas chromatography.

Treatment 3: Increased hepatic FFA flux + inhibited VLDL secretion. A 12 mg/kg dose of microsomal triglyceride transfer protein inhibitor, CP-346086, was administered orally (gelatin capsules No.00; Eli Lilly, Indianapolis, IN) 2-h prior to feeding (12 AM) for 17 days. Starting on day 3, an intraportal infusion of 20% Intralipid (0.02 ml/kg/min) plus heparin (0.5 U/kg/min) was administered at ~2 PM immediately after feeding for 3-h/d for 15-d (n=5). Approximately 24-h after the final treatment, the same tissue sampling technique described above was carried out following a two-step hyperinsulinemic-euglycemic clamp. Tissue lipids were separated by TLC and then quantitated by gas chromatography. For histological examination, liver samples were frozen in embedding medium (Tissue-Tek, O.C.T. Compound) and stored at -70°C.

The daily intraportal infusions were administered via the vascular access port using a Huber point needle (22 gauge, right angle, 1/2" tip-to-end; 6" tubing; Access Technologies, Inc., Skokie, IL) and aseptic accessing techniques as recommended by the manufacturer. Each animal rested quietly in a Pavlov harness during the 3-h daily treatment.

Results

Treatment 1: 10% fructose diet. A 10% fructose diet did not result in an increase in triglyceride content after four months as determined by gas chromatography (Fig. 4.1). Despite numerous contacts to the Vanderbilt University Institute of Imaging Science we were unable to obtain the MRI and MRS data for analysis.

Treatment 2: Increased hepatic FFA flux.

Metabolic and hormonal changes following one 3-h treatment.

Hepatic blood flow. Hepatic blood flow increased significantly ($P < 0.05$), in response to the meal primarily because of increase portal vein blood flow ($P < 0.05$ Lipid vs. control period, Table 4.1). The increase in hepatic artery flow over control period rates reached statistical significance in the Saline but not Lipid groups, despite the fact the absolute increase was the same (Table 4.1).

Arterial levels and net hepatic uptakes of plasma FFA and blood glycerol. Intraportal infusions of Intralipid and heparin increased the arterial and portal plasma FFA levels from 536 ± 275 to 1842 ± 231 and 560 ± 280 to 2022 ± 202 μmol/l, respectively, by 90 min and they remained elevated at these levels until the end of the study ($P < 0.05$ vs. control period, Fig. 4.2). In the Saline group, after the meal, arterial and portal plasma FFA levels rapidly fell from ~630 to ~180 μmol/l by 30 minutes and remained unchanged thereafter ($P < 0.05$ vs. control period, Fig. 4.2). Therefore, the hepatic FFA load (μmol/kg/min) increased by 46 ± 4 in the Lipid group and decreased by 5 ± 2 in the Saline group (last h, Fig. 4.2, $P < 0.05$ between groups). Rates of net hepatic FFA uptake paralleled levels of plasma FFA throughout the study in both groups (Fig. 4.2). Hepatic FFA fractional extraction did not differ between groups (Fig. 4.2).

Intraportal infusions of Intralipid and heparin rapidly (15 min) increased portal blood glycerol levels from 66 ± 22 to 184 ± 33 μmol/l, whereas arterial levels gradually rose from 56 ± 17 to 98 ± 8 μmol/l respectively by 90 min and remained elevated at that level until the end of the study ($P < 0.05$, Fig. 4.3). In the Saline group, arterial and portal blood glycerol levels after the meal rapidly fell (15 min), reaching a nadir at one-half their control period values and not changing significantly change thereafter ($P < 0.05$, Fig. 4.3). Therefore, the hepatic glycerol load (μmol/kg/min) increased by 6.7 ± 0.8 in the Lipid group and decreased by 0.5 ± 0.4 in the Saline group (last h, Fig. 4.3). Rates of net hepatic glycerol uptake paralleled levels of portal blood glycerol throughout the study in both groups (Fig. 4.3). Hepatic glycerol fractional extraction was not significantly different between groups (Fig. 4.3).

Of note, levels of plasma FFA and blood glycerol returned to basal values within an hour of terminating the lipid infusion (data not shown, n=1).

Glucose metabolism. Arterial and portal plasma glucose levels increased rapidly after feeding, peaking at min 15 and remaining significantly elevated for the duration of the study ($P < 0.05$, Fig. 4.4). The mean hepatic glucose load doubled as a consequence of the increases in the blood glucose level and blood flow ($P < 0.05$, Fig. 4.4). In both the Lipid and Saline groups net hepatic glucose output was ~2.6 mg/kg/min during the control period; however, an hour after the meal, the liver had converted to net glucose uptake (~-1.7 mg/kg/min, Fig. 4.4). Net hepatic uptake continued at approximately the same rate for the remainder of the study in the Saline group, whereas it tended to decrease in the Lipid group. Hepatic glucose fractional extraction mirrored net hepatic glucose balance throughout the study in both groups (Fig. 4.4).

Hormone levels. Arterial and portal plasma levels of insulin and glucagon rapidly (15 min) increased following the meal and remained elevated throughout the postprandial period (Table 4.2). Of note, the initial rise in arterial plasma insulin levels (μU/ml) tended to be 2-fold higher in the Lipid group (Δ 26 ± 9) compared to the Saline control (Δ 11 ± 5). Due to the low statistical power and the apparent variability following the meal, few significant differences were observed. Arterial plasma cortisol levels remained basal in both groups throughout the study (data not shown).

Tissue lipids. Following a single 3-h infusion, hepatic triglycerides were 66% higher in the Lipid group than the Saline Control whereas muscle triglycerides were similar in both groups (Fig. 4.5).

Tissue lipids following repeated brief elevations of FFA. One day following the final infusion of the 15-d treatment regimen, liver triglyceride content (μg/mg tissue) was similar in the Saline (0.9 ± 0.1) and Lipid (1.3 ± 0.5) groups (Fig. 4.6). Triglyceride content in skeletal muscle was similar in both groups (Fig. 4.6). Additionally, there were no significant differences in liver or skeletal muscle diacylglyceride or phospholipid levels among groups(data not shown).

Treatment 3: Increased hepatic FFA flux + inhibited VLDL secretion. Repeated elevations of FFA in the presence of the MTP inhibitor, CP-346086 for 3-h/d for 15-d resulted in nearly a 2-fold increase in liver triglycerides (1.9 ± 0.6 μg/mg tissue, $P < 0.05$ vs. Saline, Fig.4.6). Liver sections stained with oil red O confirmed that chronic treatment with Intralipid/heparin in the presence of CP-346086 resulted in hepatic lipid accumulation (Fig. 4.6). Triglyceride content (μg/mg tissue) in skeletal muscle tended to be lower in the Lipid + CP-346086 group (8 ± 3) compared to Saline (15 ± 5) and Lipid

(11 ± 2). Additionally, there were no significant differences in liver and skeletal muscle diacylglyceride or phospholipid levels (data not shown).

Discussion

Although there is a strong correlation with lipotoxicity (152, 195, 202) and type 2 diabetes it is unclear as to whether the accumulation of intracellular lipid in liver and muscle is a cause or an effect of a decreased insulin response. The putative role of triglyceride accumulation in non-adipose tissues is based solely upon correlative results. Therefore, one remains unconvinced regarding the importance of triglyceride accumulation as a direct cause of insulin resistance and a contributor to the pathogenesis of diabetes. Thus the aim of the present study was to create a canine model of hepatic steatosis.

When input (uptake or synthesis) of fatty acids to hepatocytes exceeds their output (degradation or export), triglycerides accumulate within the liver. The conventional explanation for lipotoxicity is that an impairment of fat deposition in adipose tissue due to either over storage of lipid or decreased storage ability results in increased release of FFA from adipocytes. FFA must then be partitioned for storage in other tissues such as the liver, skeletal muscle, and pancreas. However, in the liver, increases in dietary substrates for lipogenesis (FFA and carbohydrates) and decreases in VLDL export are also thought to contribute to the increased hepatocelluar lipid content.

Dietary substrates are particularly relevant given the increased consumption of energy-dense diets (214). The dietary substrate, fructose, is of particular interest as it has been suggested that its consumption (essentially in soft drinks) may be a causal factor for

the development of insulin resistance (32). Fructose can directly contribute to hepatic lipid content via stimulation of *de novo* lipogenesis by two mechanisms: it increases hepatic glucose uptake (an effect likely to be mediated by increased translocation of glucokinase) (198, 250) and bypass the regulated conversion of F6P to $F1,6P_2$ (119) . It is thus a relatively unregulated source of substrate for triglyceride synthesis. In fact, it has been shown that rats placed on a 10% fructose diet for one month had significant increases in hepatic fatty acid synthase, *de novo* fatty acid synthesis, fatty acid re-esterification, and liver triglycerides (151). Thus, our first attempt to induce hepatic steatosis was the use of a 10% fructose diet. The 10% fructose diet did not increase liver triglycerides even after four months of treatment. The protocol was terminated due to the insignificant effect on hepatic lipid metabolism.

Parks and colleagues have elegantly demonstrated, using a multiple-stable-isotope approach, that plasma FFA account for 60% of the hepatic triglyceride accumulation in obese patients with hepatic steatosis (79). Furthermore, it has been shown that insulin does not suppress lipolysis in patients with NAFLD to the same extent it does in healthy individuals (238). Taken together, these findings suggest that elevated FFA flux to the liver results in an accumulation of hepatic triglycerides. Therefore, in our second attempt to induce the fatty liver in the dog, hepatic FFA flux was repeatedly elevated for 3-h/d for 15-d. The lipid infusion was administered at the time of feeding to maximally increase rates of lipogenesis. The rise in insulin which occurs in response to a meal should result in the stimulation of lipogenic enzymes and thus further promote the accumulation of triglyceride within the liver.

In order to determine the acute metabolic and hormonal changes that occurred during the daily intraportal infusions, a subset of dogs received only one 3-h treatment (Lipid, n=4; Saline, n=4). Intraportal infusion of Intralipid and heparin resulted in a 4-fold increase in plasma FFA levels in both the portal and arterial circulations. In contrast, intraportal infusion of Intralipid and heparin resulted in a 3-fold rise in the blood glycerol level in the portal circulation and a 2-fold rise in the arterial circulation. Plasma insulin levels increased, as expected, in response to the meal in both groups (69). The increments in hepatic glucose load were identical in the Saline and Lipid groups following the meal. Within sixty minutes of meal consumption, a switch from net glucose output to uptake was observed. Thus as plasma insulin, FFA, and glucose were elevated during the 3-h lipid infusion, hepatic lipogenesis should have been increased.

Boden et al. (27) have shown that an acute elevation of FFA levels in humans increased intramyocellular triglyceride in a time- and dose-dependent manner. In the present study, we demonstrated for the first time that an acute rise in FFA during the postprandial period results in a nearly 2-fold increase in hepatic triglycerides. Interestingly, no differences were observed in skeletal muscle triglycerides, despite the significant rise in arterial plasma FFA and insulin.

Following the 15-d treatment regimen (elevated FFA for 3-h/d) neither hepatic nor muscle triglyceride levels were significantly higher in the Lipid group compared to the Saline group. Since liver triglycerides were elevated following a single treatment but not after 15-d of lipid infusion, it seems that the liver compensated for the daily elevations of hepatic FFA flux and/or triglyceride synthesis by removing any excess hepatic lipids via increased β-oxidation or VLDL production. In fact, when we inhibited

VLDL secretion by the liver using the MTP inhibitor, CP-346086, liver triglycerides were increased 2-fold following the 15-d lipid treatment.

MTP is thought to play a pivotal, if not an obligatory, role in the assembly and secretion of triglyceride-rich apoB containing lipoproteins (VLDL and chylomicrons) from the liver and intestine. In fact, the genetic manipulation of liver-specific MTP demonstrates its key functions in regulating liver triglyceride concentrations (279). Liver-specific MTP knockout mice exhibit hepatic steatosis and decreased hepatic triglyceride secretion, while mice over-expressing hepatic MTP show an increase in *in vivo* hepatic triglyceride secretion (218). The human recessive disease abetalipoproteinemia, which is characterized by near complete absence of apoB-containing lipoproteins, is caused by a variety of mutations in the gene for a subunit of MTP (191, 226, 244, 290). Interestingly, polymorphisms of MTP are found with increased frequency in patients with NAFLD (190). Therefore, our findings support the hypothesis that MTP plays a significant role in the regulation of hepatic triglycerides and that its inhibition may contribute to the accumulation of lipids in patients with hepatic steatosis. (Of note, due to the discontinuation of CP-346086 manufacture, we were unable to determine the metabolic and hormonal changes that occurred during the daily intraportal lipid infusions in the presence of the inhibitor.)

The goal of ***Specific Aim II*** was to induce fatty liver (hepatic steatosis) in the dog. In attempt to do so, lipid metabolism was altered by 3 different treatments: 1) a 10% fructose diet, 2) elevating hepatic FFA flux, or 3) elevating hepatic FFA flux while simultaneously inhibiting triglyceride export from the liver using the microsomal triglyceride transfer protein inhibitor, CP-346086. A 10% fructose diet given over a four

month period and repeated elevations of FFA (3-h/d for 15-d) were not successful in elevating hepatic triglycerides. However, as triglyceride levels were elevated 2-fold following the combined lipid and CP-346086 treatment. We were thus successful in creating a canine model of hepatic steatosis. This model would provide an excellent research tool to determine the effects of elevated liver triglycerides on the actions of glucoregulatory hormones. As hepatic steatosis has a very strong association with hepatic insulin resistance, it has of particular interest to determine whether the accumulation of intracellular lipid is a cause or an effect of a decreased insulin response.

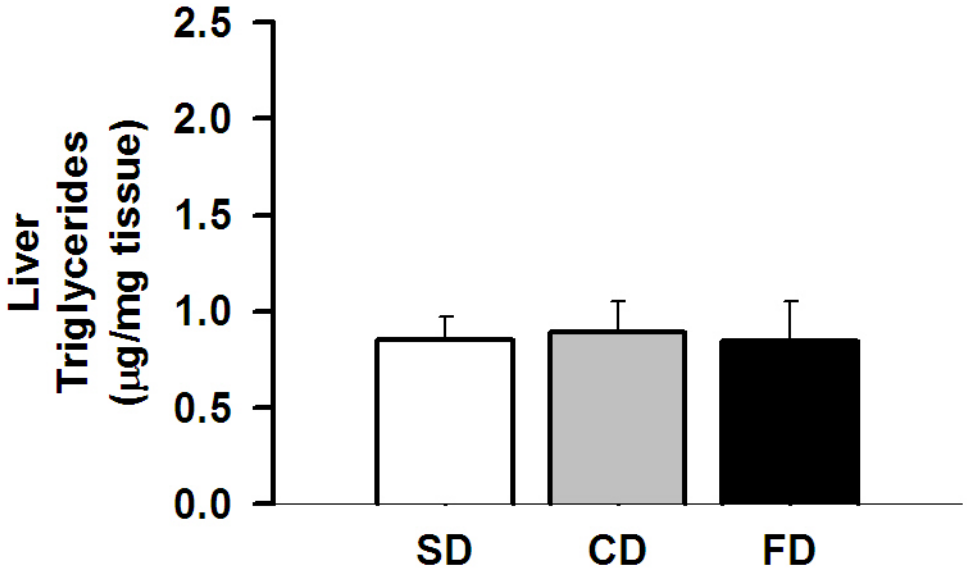

Figure 4.1: Hepatic triglycerides. Hepatic triglyceride content in male mongrel dogs that were fed once daily either a standard (SD), a 10% fructose (FD) or carbohydrate (CD, 10% increase) diet for 4 months. n=2/group

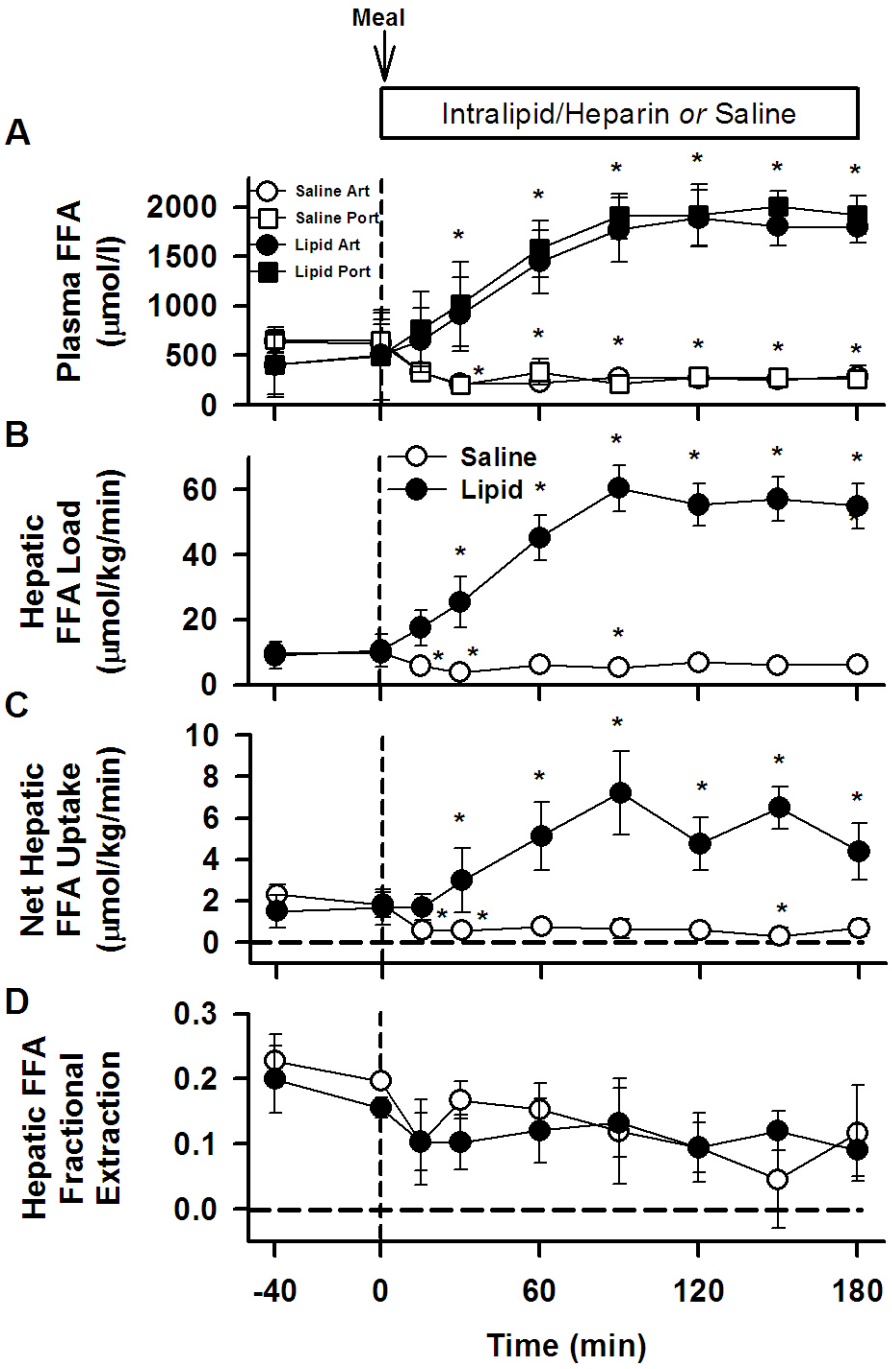

Figure 4.2: Arterial and portal plasma levels, hepatic load, net hepatic uptake, and hepatic fractional extraction of FFA. Arterial and portal plasma levels (A) hepatic load (B), net hepatic balance (C), and hepatic fractional extraction of FFA during control period (-40 to 0 min) and postprandial period (0 to 180 min). An intraportal infusion of either Intralipid/heparin or saline was infused from 0 to 180 min. Fractional extraction was calculated as net hepatic balance per load in. Values are means ± SE. * $P < 0.05$ vs. respective control period

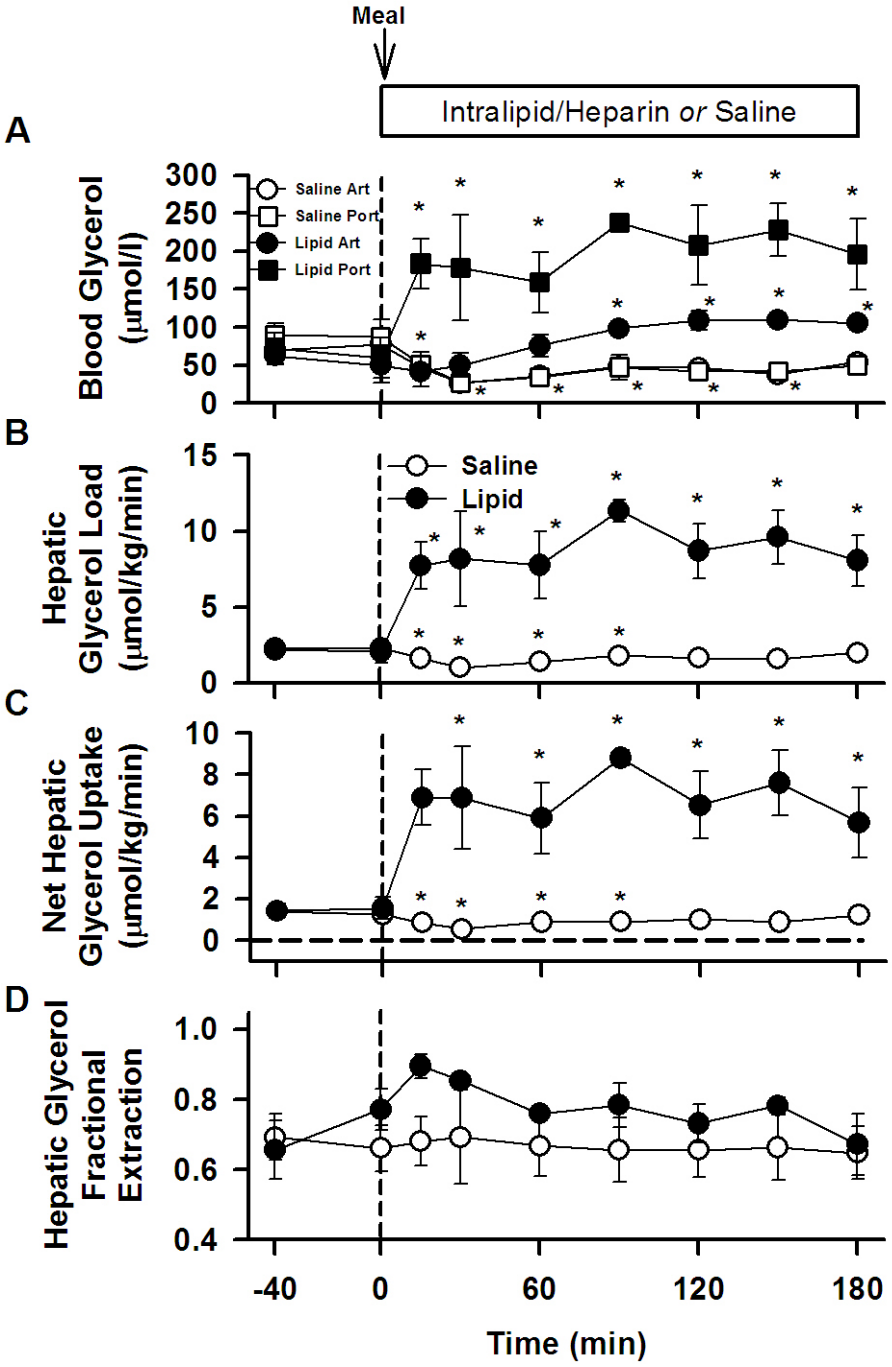

Figure 4.3: Arterial and portal blood levels, hepatic load, net hepatic uptake, and hepatic fractional extraction of glycerol. Arterial and portal plasma levels (A) hepatic load (B), net hepatic balance (C), and hepatic fractional extraction of glycerol during control period (-40 to 0 min) and postprandial period (0 to 180 min). An intraportal infusion of either Intralipid/heparin or saline was infused from 0 to 180 min. Fractional extraction was calculated as net hepatic balance per load in. Values are means ± SE.
* $P < 0.05$ vs. respective control period

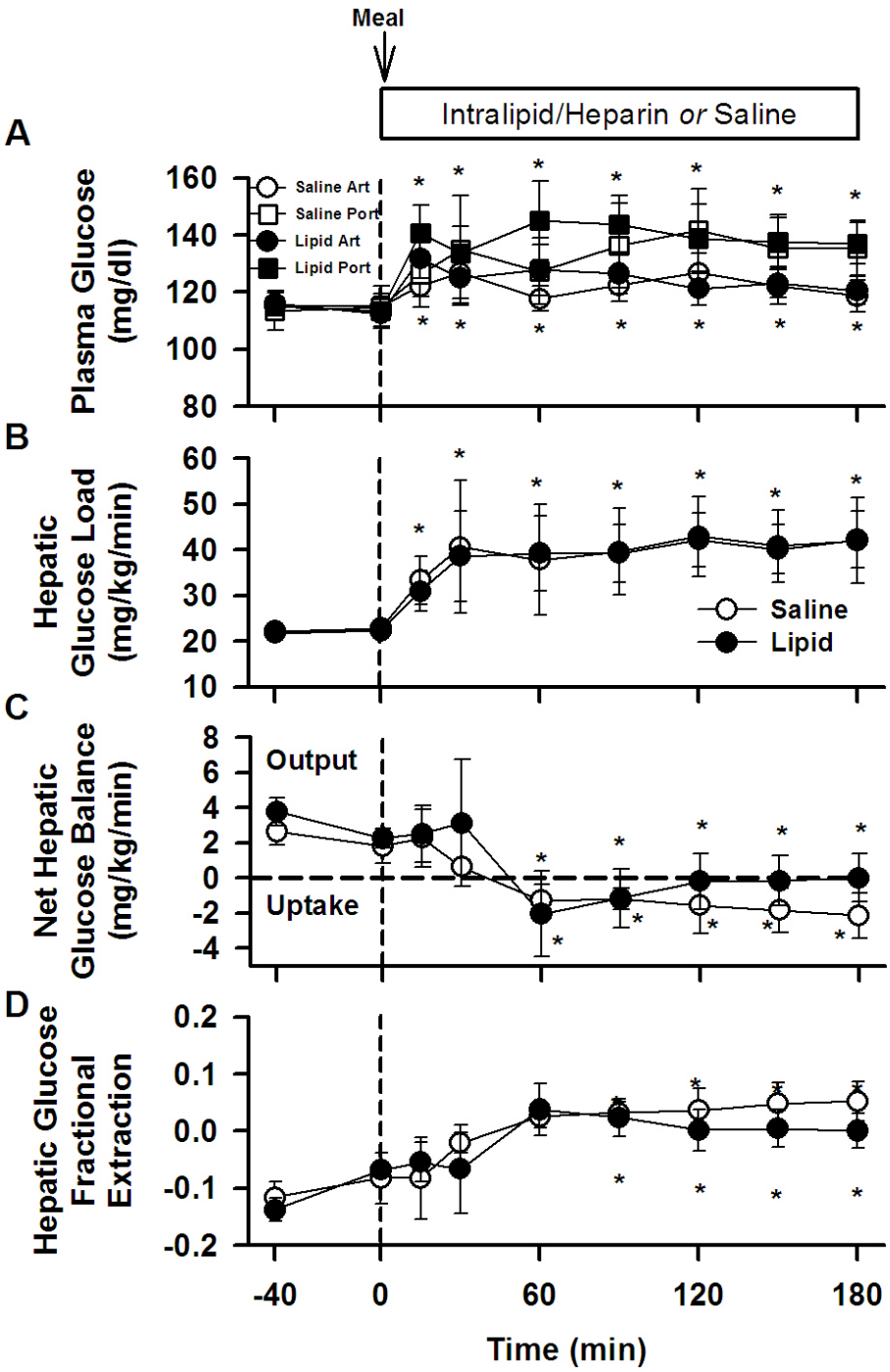

Figure 4.4: Arterial and portal plasma levels, hepatic load, net hepatic balance, and hepatic fractional extraction of glucose. Arterial and portal plasma levels (A) hepatic load (B), net hepatic balance (C), and hepatic fractional extraction of glucose during control period (-40 to 0 min) and postprandial period (0 to 180 min). An intraportal infusion of either Intralipid/heparin or saline was infused from 0 to 180 min. Positive and negative values of net hepatic glucose balance represent net output and net uptake, respectively. Fractional extraction was calculated as net hepatic balance per load in. Values are means ± SE. * $P < 0.05$ vs. respective control period

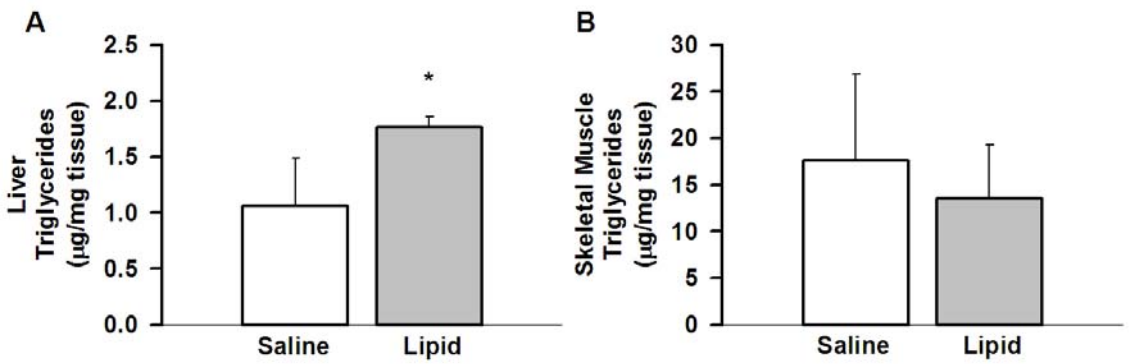

Figure 4.5: Tissue triglycerides after a single infusion. Liver (A) and skeletal muscle (B) triglycerides. Tissue was excised immediately following a 3-h intraportal infusion of either Intralipid/heparin or saline which was administered during the postprandial state. * $P < 0.05$ vs. Saline

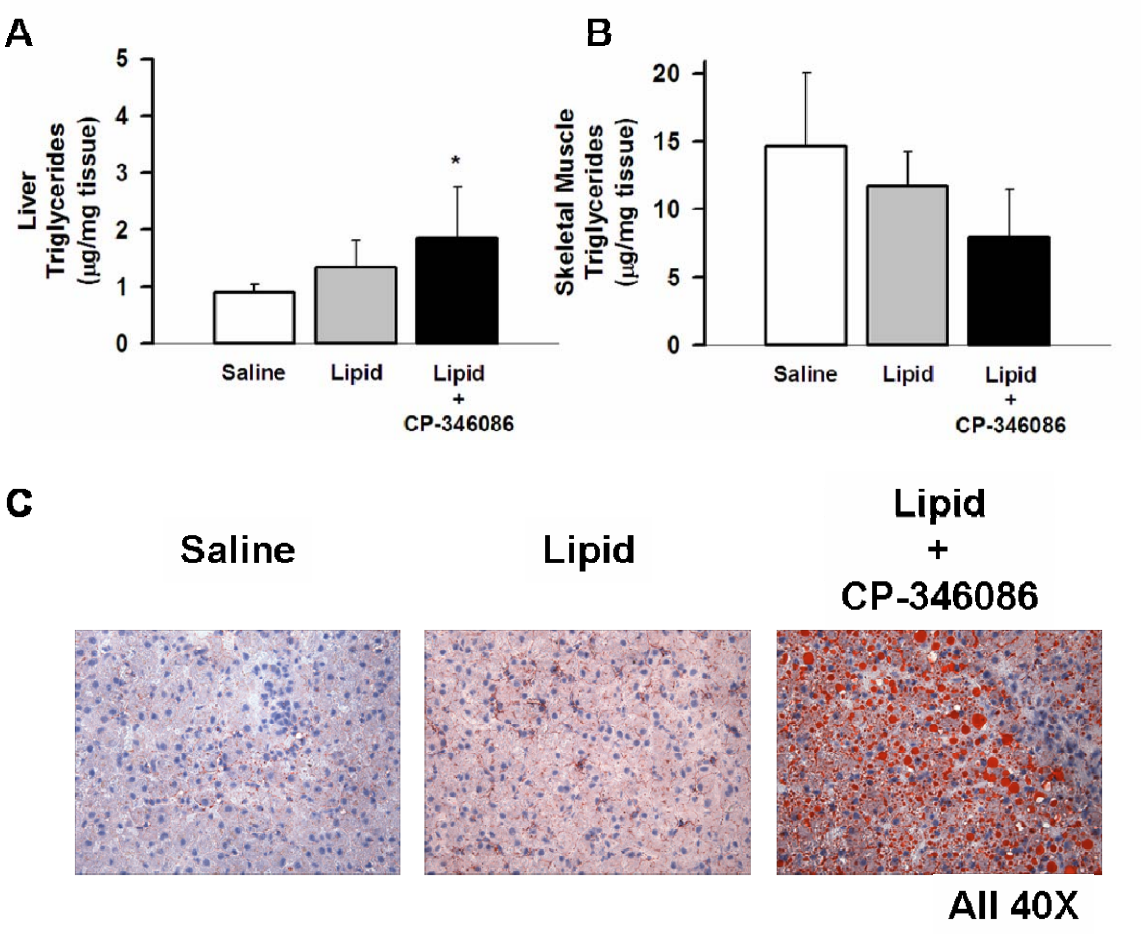

Figure 4.6: Tissue lipids after repeated infusion. Liver (A) and skeletal muscle (B) triglyceride levels and oil red O staining of representative liver sections (C) following treatment with saline, Intralipid/heparin (Lipid), or Intralipid/heparin in the presence of a microsomal triglyceride transfer protein inhibitor, CP-346086 for 3-h/d for 15-d. Tissue was excised immediately following a 2-step hyperinsulinemic-euglycemic clamp. Values are means ± SE. * $P < 0.05$ vs. Saline.

TABLE 4.1

Hepatic blood flow during control period (-40 to 0 min) and postprandial period (0 to 180 min). An intraportal infusion of either Intralipid/heparin or saline was infused from 0 to 180 min.

	Control period	Experimental period (min)						
	-40 - 0	15	30	60	90	120	150	180
Hepatic Blood Flow								
Arterial								
Saline	5 ± 0	6 ± 0*	6 ± 1*	6 ± 1	6 ± 1	6 ± 1	7 ± 2	6 ± 2
Lipid	5 ± 1	6 ± 0	6 ± 0	8 ± 2	8 ± 2	7 ± 2	7 ± 3	8 ± 2
Portal								
Saline	22 ± 1	28 ± 4	32 ± 7	34 ± 7	33 ± 5	33 ± 5	32 ± 5	35 ± 6
Lipid	29 ± 3	40 ± 3*	44 ± 3*	44 ± 2*	45 ± 4*	39 ± 3*	38 ± 2*	38 ± 5*

Values are means ± SE. Basal period values are an average of samples taken at -40 and 0 min. * $P < 0.05$ vs. respective control levels.

TABLE 4.2

Plasma hormone levels during control period (-40 to 0 min) and postprandial period (0 to 180 min). An intraportal infusion of either Intralipid/heparin or saline was infused from 0 to 180 min.

	Control period	Experimental period (min)						
	-40 - 0	15	30	60	90	120	150	180
Plasma Hormone Concentrations								
Insulin (μU/ml)								
Arterial								
Saline	8 ± 1	19 ± 5*	33 ± 17	19 ± 7	25 ± 10	43 ± 10	36 ± 15	22 ± 5*
Lipid	9 ± 1	36 ± 8*	25 ± 8	34 ± 17	35 ± 18*	33 ± 18*	36 ± 18	31 ± 19
Portal								
Saline	27 ± 11	50 ± 16	112 ± 54	32 ± 9	94 ± 29	133 ± 35	129 ± 64	54 ± 15
Lipid	19 ± 6	75 ± 32	52 ± 24	53 ± 19	100 ± 55	82 ± 56	95 ± 53	74 ± 58
Glucagon (pg/ml)								
Arterial								
Saline	35 ± 7	83 ± 32*	80 ± 27	88 ± 45	80 ± 45	56 ± 21	55 ± 21	71 ± 41
Lipid	51 ± 11	95 ± 5*	86 ± 12*	74 ± 7	74 ± 12	69 ± 13	65 ± 7	66 ± 7
Portal								
Saline	60 ± 19	143 ± 56	110 ± 50	124 ± 75	119 ± 68	104 ± 71	80 ± 38	103 ± 58
Lipid	70 ± 9	126 ± 18*	101 ± 13	99 ± 9*	100 ± 14	85 ± 9	93 ± 20	96 ± 17

Values are means ± SE. Basal period values are an average of samples taken at -40 and 0 min. * $P < 0.05$ vs. respective control levels.

CHAPTER V

THE EFFECTS OF REPEATED ELEVATIONS OF FFA AND INCREASED LIVER TRIGLYCERIDES ON HEPATIC AND PERIPHERAL INSULIN SENSITIVITY

Aim

The goal of Specific Aim III was to examine whole body insulin sensitivity following treatment regimens to induce hepatic steatosis (see Chapter IV): a 10% fructose diet (4-mo), repeated elevations of FFA for 3-h/d for 15-d, or repeated elevations of FFA (3-h/d for 15-d) in the presence of a MTP inhibitor, CP-346086. The 10% fructose diet did not increase liver triglycerides even after four months of treatment; thus the protocol was terminated due to the insignificant effect on hepatic lipid metabolism. Although whole body insulin sensitivity was assessed after 4-mo of treatment, the statistical power (n=2/group) was too low to draw any conclusions.

As demonstrated in Specific Aim II, repeated elevations of FFA for 3-h/d for 15 d (*Treatment 1,* Lipid) did not chronically alter hepatic triglyceride content; however, simultaneous elevation of hepatic FFA flux and inhibition of hepatic triglyceride export (*Treatment 2, Lipid* + CP-346086) resulted in a two-fold increase in liver triglycerides. Although it is well established that both acute and chronic increases of FFA cause insulin resistance, it remains unclear if recurring elevations of plasma FFA levels, such as might occur during the postprandial period in type 2 diabetes, can alter insulin sensitivity. For that reason, even though repeated elevations of FFA did not result in a rise in hepatic triglycerides, it was of interest to evaluate insulin sensitivity following the treatment regimen. To assess whole body insulin sensitivity, a two-step hyperinsulinemic-

euglycemic clamp was performed on the day immediately following completion of the 15-d treatment period used to induce hepatic steatosis in the dog.

Experimental Design

Nineteen male mongrel dogs received treatment with saline (n=7), 20% Intralipid + heparin for 3-h/d for 15-d (Lipid, n=7), or 20% Intralipid + heparin for 3-h/d for 15-d in the presence of an MTP inhibitor, CP-346086 (Lipid + CP-346086). Approximately 15-h following the final infusion (18 h after feeding), a two step hyperinsulinemic-euglycemic clamp was performed. Each experiment consisted of a tracer and dye (ICG) equilibration period (-140 to -40 min), a basal period (-40 to 0 min), and an experimental period (0 to 240 min). At -140 min, a priming dose of [3-^{3}H] glucose (33.3 μCi) was given and a constant infusion of [3-^{3}H] glucose (0.35 μCi/min) was begun to allow the assessment of hepatic glucose production. At the same time a constant infusion of ICG (0.07 mg/min) was started to assess hepatic blood flow. A somatostatin infusion (0.8 $\mu g \cdot kg^{-1}min^{-1}$) was started at 0 min to inhibit endogenous insulin and glucagon secretion. A constant intraportal infusion of glucagon (0.55 ng/kg/min; Bedford Laboratories, Bedford, OH) was given (t = 0 min) to replace endogenous glucagon secretion. Endogenous insulin secretion was replaced by two rates of insulin infusion, 600 μU/kg/min from 0 to 120 min and 2000 μU/kg/min from 120 to 240 min. In a normal overnight fasted dog under euglycemic conditions, 600 μU/kg/min of insulin should reduce net hepatic glucose output to approximately zero mg/kg/min while 2000 μU/kg/min should shift the liver to a low rate of net hepatic glucose uptake (NHGU) (). It should also cause a significant

increase in non-hepatic glucose uptake of ~12 mg/kg/min. A fifty percent solution of dextrose was administered peripherally during the experimental period in order to maintain euglycemia. Plasma glucose concentrations were measured every 5 minutes to assess the need for glucose infusion. Arterial blood samples were taken every 10 min during the basal period and every 15 min during the experimental period for the assessment of glucose and [3-^{3}H]- glucose. For the measurement of acetoacetate, FFA, and glucagon, arterial, portal vein, and hepatic vein samples were taken at -40 and 0 min during the basal period and every hour during the experimental period. For all other parameters, arterial, portal vein, and hepatic vein samples were taken at -40 and 0 min during the basal period and every 30 min for the last 90 min of each step of the experimental period. The total blood volume withdrawn did not exceed 20% of the dog's total blood volume and each volume of blood taken was replaced with two volumes of 0.9% saline.

Immediately following the last blood withdrawal, each animal was anesthetized with pentobarbital sodium. The animal was then removed from the harness while the hormones and glucose continued to be infused. A midline laparotomy incision was made, and clamps cooled in liquid nitrogen were used to freeze sections of all seven hepatic lobes *in situ*. Each hepatic biopsy was placed in liquid nitrogen and stored at –70°C. For histological examination, liver samples were frozen in embedding medium (Tissue-Tek, O.C.T. Compound) and stored at -70°C. Approximately 2 min elapsed between the time of anesthesia and the time of tissue excision. All animals were then euthanized.

Results

Hormone levels and hepatic blood flow. Hepatic sinusoidal levels of plasma glucagon remained basal throughout the study in all groups (Fig. 5.1). Arterial plasma insulin levels increased from basal values of ~ 7 ± 1 to ~11 ± 0.5 as a result of a 600 μU/kg/min insulin infusion in Step 1 of the experimental period in all groups (Fig. 5.2). During Step 2, a 2000 μU/kg/min insulin infusion increased arterial plasma insulin levels to 51 ± 4, 42 ± 4, and 40 ± 6 μU/ml in the Saline, Lipid, and Lipid + CP-346086 groups, respectively (P = 0.049 Lipid vs. Saline, P = 0.017 Lipid + CP-346086 vs. Saline, Fig. 5.2). Despite the moderate differences in arterial plasma insulin levels, there were no significant differences in hepatic sinusoidal insulin levels among the groups (Fig. 5.2). Arterial plasma cortisol, plasma epinephrine and norepinephrine, and hepatic blood flow remained basal and unchanged in all groups throughout the study (data not shown).

Glucose levels and glucose infusion rates. In all three groups, arterial plasma glucose (mg/dl) was successfully clamped in Step 1 (~110) and Step 2 (~109) of the experimental period at levels similar to those observed during the control period (~112, Fig. 5.3). In the Saline group, the glucose infusion rate required to maintain euglycemia in response to an insulin infusion rate of 600 μU/kg/min was 2.2 ± 0.2 mg/kg/min. That rate rose significantly to 15.3 ± 1.5 mg/kg/min when the insulin infusion was increased to 2000 μU/kg/min (Step 2, Fig. 5.3). However, in the Lipid group, the glucose infusion (mg/kg/min) only reached rates of 1.3 ± 0.3 in Step 1 and 11.1 ± 1.4 in Step 2 of the experimental period (both $P < 0.05$ vs. Saline and Lipid + CP-346086, Fig. 5.3). Interestingly, the glucose infusion rates required to maintain euglycemia in the Lipid +

CP-346086 group (3.0 ± 0.7 and 16.5 ± 2.7 mg/kg/min in Step 1 and Step 2, respectively, Fig. 5.3) were not different from those seen in the Saline group.

Glucose metabolism. Basal rates of net hepatic glucose output (NHGO, mg/kg/min) were similar in all three groups (Saline= 2.2 ± 0.6, Lipid= 1.9 ± 0.3, Lipid + CP-346086= 1.9 ± 0.4, Fig. 5.4). In the Saline group, 600 μU/kg/min of insulin suppressed NHGO to 0.0 ± 0.3 mg/kg/min while infusion of insulin at 2000 μU/kg/min of insulin stimulated net hepatic glucose uptake (NHGU) of -1.2 ± 0.5 mg/kg/min (Fig. 5.4). Insulin only suppressed NHGO in Step 1 of the Lipid and Lipid + CP-346086 groups to 0.9 ± 0.4 and 0.7 ± 0.2 mg/kg/min, respectively (both $P < 0.05$ vs. Saline, Fig. 5.4). Likewise, high levels of insulin tended to cause less NHGU in the lipid treated groups (~ -0.3 ± 0.2 mg/kg/min) than in the Saline group ($P< 0.01$, Step 2, Fig. 5.4). Thus, repeated brief elevations in FFA resulted in decreased insulin sensitivity in the liver.

Basal net hepatic glycogenolytic (NHGLY) flux rates were 2.7 ± 0.6, 2.0 ± 0.5, and 1.6 ± 0.6 mg/kg/min in the Saline, Lipid, and Lipid + CP-346086 groups, respectively (Fig. 5.4). Increases in insulin, in the Saline group, resulted in a fall in net NHGLY flux (mg/kg/min) by 2.4 ± 0.7 in Step 1 and actually caused net glycogen synthesis in Step 2 (both $P < 0.05$ vs. control period, Fig. 5.4). In contrast, in the Lipid group, increases in plasma insulin levels only decreased NHGLY flux by 1.0 ± 0.8 mg/kg/min in Step 1 and barely caused net glycogen synthesis in Step 2 ($P < 0.05$ vs. Saline, Fig. 5.4). A similar trend was also observed in the Lipid + CP-346086 group, in which NHGLY flux decreased by 1.0 ± 0.5 mg/kg/min in Step 1 and minimum net glycogen synthesis occurred in Step 2 (Fig. 5.4).

In the Saline group, basal net hepatic gluconeogenic (NHGNG) flux was -0.5 ± 0.3 mg/kg/min, a rate signifying a state of net glycolysis. In contrast, in both of the lipid treated groups, rates of basal NHGNG flux (mg/kg/min) represented a state of net gluconeogenesis with a rate of 0.1 ± 0.3 in the Lipid group and 0.3 ± 0.3 in the Lipid + CP-346086 (both $P < 0.05$ vs. Saline, Fig. 5.4). In response to low dose insulin, rates of NHGNG flux were not significantly altered. All groups exhibited net gluconeogenesis during Step 2. The positive values obtained for NHGNG flux in the Saline group in response to high levels of insulin were likely due to the inhibition NHGLY flux such that carbon in the glycolytic pathway was reduced.

Non-hepatic glucose uptake (non-HGU) was basal (~2.0 mg/kg/min) in all three groups during the control period (Fig. 5.4). Insulin infusion at 600 μU/kg/min did not alter non-HGU (mg/kg/min) in the Saline (2.4 ± 0.2) or Lipid (2.1 ± 0.2) groups but surprisingly increased it in the Lipid + CP-346086 group (3.6 ± 0.7, $P < 0.05$ vs. Saline and Lipid, Fig 5.4). In Step 2, hyperinsulinemia significantly increased non-HGU to 14.4 ± 1.8 mg/kg/min in the Saline group. However, in the Lipid group, non-HGU only increased to 9.9 ± 1.0 mg/kg/min ($P < 0.05$ vs. Saline and Lipid + CP-346086, Fig. 5.4), whereas it was similar to that seen in the Saline group in the presence of Lipid and the MTP inhibitor (17.9 ± 4.8 mg/kg/min, $P < 0.05$ vs. Lipid, Fig. 5.4).

Arterial blood levels and net hepatic balance of lactate. In the Saline group, basal arterial blood lactate levels and net hepatic lactate output (NHLO) were 653 ± 83 μmol/l and 7.5 ± 2.9 μmol/kg/min, respectively (Fig. 5.5). Basal arterial lactate levels (μmol/l) were significantly decreased in the Lipid (433 ±33) and Lipid + CP-346086 (347 ± 51, $P < 0.05$ vs. Saline), groups in association with decreased basal NHLO ($P < 0.05$ vs. Saline,

Fig. 5.5). In fact, repeated lipid treatment in the presence of CP-346086 resulted in net uptake of lactate by the liver (-1.5 ± 3.4 μmol/kg/min, $P < 0.05$ vs. Saline, Fig. 5.5). Arterial blood lactate levels were not significantly altered by elevated insulin levels in any group throughout the experimental period. NHLB was suppressed by high dose insulin in the Saline group but no appreciable change was observed in the other two groups.

Arterial plasma FFA and triglycerides and blood glycerol levels and net hepatic uptake. In the Saline group, arterial plasma FFA levels (μmol/l) fell from 545 ± 103 to 187 ± 26 in response to an insulin infusion rate of 600 μU/kg/min (Step 1), and to 46 ± 5 when the insulin infusion was increased to 2000 μU/kg/min (Step 2, Fig. 5.6). However, in the Lipid group, plasma FFA levels (μmol/l) decreased from 711 ± 124 to 407 ± 122 ($P < 0.05$ vs. Saline) in Step 1 and 76 ± 25 in Step 2 (Fig. 5.6). Interestingly, FFA levels in the Lipid + CP-346086 group (564 ± 89 μmol/l) tended to drop to those seen in the Saline group with levels of 230 ± 89 and 45 ± 14 μmol/l in Step 1 and Step 2, respectively (Fig. 5.6). Rates of net hepatic FFA uptake fell in parallel with the decline in plasma FFA levels in all three groups (Fig. 5.6).

Arterial blood glycerol levels (μmol/l) fell from 62 ± 9 to 30 ± 4 and 17 ± 3 due to increased insulin infusion rates in the Saline group (Fig. 5.6). However, in the Lipid group, glycerol levels (μmol/l) decreased from 79 ± 14 to 55 ± 9 ($P < 0.05$ vs. Saline) in Step 1 and 33 ± 8 in Step 2 (Fig. 5.6). Blood glycerol levels in the Lipid + CP-346086 group (69 ± 13 μmol/l) tended to drop to those seen in the Saline group with levels of 38 ± 5 and 20 ± 3 μmol/l in Step 1 and Step 2, respectively (Fig. 5.6). Rates of net hepatic

glycerol uptake fell in parallel with the decline in plasma glycerol levels in all three groups (Fig. 5.6).

Basal arterial plasma triglycerides were ~500 ± 40 μmol/l in the Saline and Lipid group and fell modestly in response to increased plasma insulin (Fig. 5.7). Interestingly, basal triglycerides were higher in the Lipid + CP-346086 group (740 ± 92 μmol/l, $P < 0.05$ vs. Saline and Lipid, Fig. 5.7), and fell significantly fell during the experimental period to levels similar to those seen in the other two groups.

Arterial blood levels and net hepatic balances of β-OHB and acetoacetate. Basal arterial blood β-hydroxybutyrate (β-OHB) levels were not significantly different among the Saline and Lipid groups (Fig. 5.8). However, there was a tendency for basal arterial blood β-OHB levels to be higher in the Lipid + CP-346086 group compared to the Saline group (Fig. 5.8). Rates of basal net hepatic β-OHB output (μmol/kg/min) in the Lipid (0.8 ± 0.2) and Lipid + CP-346086 (1.1 ± 0.3) groups, on the other hand, were significantly elevated compared to those in the Saline group (0.4 ± 0.04, $P < 0.05$, Fig. 5.8). Arterial blood levels and net hepatic outputs of β-OHB fell in response to increases in plasma insulin so that eventually they were no different from those in the Saline control (Fig. 5.8). Arterial blood levels of acetoacetate were comparable among all groups. Basal net hepatic output of acetoacetate tended to be higher in the Lipid + CP-346086 group than in the Saline and Lipid groups. Although rates of net hepatic outputs of acetoacetate fell in response to elevated insulin in all groups, rates remained higher in the Lipid + CP-346086 (NS) compared to the other groups (Fig. 5.8). Thus, lipid treatment resulted in increased ketogenesis, particularly in the presence of the MTP inhibitor, consistent with excessive FA breakdown.

Arterial blood levels, net hepatic balances, and fractional extraction of gluconeogenic amino acids. Basal arterial blood levels of total gluconeogenic amino acids were similar among all groups despite lower levels of the individual amino acids alanine and serine in the Lipid group and alanine alone in the Lipid + CP-346086 (Table 5.1). Additionally, no differences in net hepatic balance or fractional extraction of individual or total amino acids were observed among groups during the control period (Table 5.1). Interestingly, hepatic fractional extraction of total gluconeogenic amino acids was higher in the Lipid + CP-346086 group in response to low dose insulin than the other groups ($P < 0.05$ vs. Saline and Lipid, Table 5.1). By Step 2 of the experimental period, net hepatic balance and fractional extraction of total gluconeogenic amino acids increased in response to elevated insulin levels regardless of treatment ($P < 0.05$, Table 5.1). This in turn resulted in a fall in arterial blood levels of each gluconeogenic amino acid ($P < 0.05$, Table 5.1).

Discussion

The aim of the present study was to determine the effect of repeated elevations of circulating FFA on insulin sensitivity in the liver and peripheral tissues in the presence or absence of an MTP inhibitor. Repeated elevations of FFA for 3-h/d for 15-d did not chronically alter hepatic triglyceride content (see Chapter IV); however, simultaneous elevations of hepatic FFA flux and inhibition of hepatic triglyceride export with CP-346086 resulted in a two-fold increase in liver triglycerides. Although it is well established that both acute and chronic increases of FFA cause insulin resistance, it remains unclear if a meal associated (3-h) elevation in plasma FFA levels can alter insulin sensitivity. Thus we examined whole body insulin sensitivity following treatment

with saline, Intralipid/heparin (Lipid), or Intralipid/heparin in the presence of a microsomal triglyceride transfer protein inhibitor, CP-346086, for 3 h/d for 15 d.

Approximately 15 h after the final treatment (18 h fast), a 2 step hyperinsulinemic-euglycemic clamp was performed to assess insulin sensitivity. In the presence of basal glucagon and euglycemia, insulin was administered intraportally at 600 μU/kg/min in step 1 (0 to 120 min) and 2000 μU/kg/min in step 2 (120 to 240 min). In the normal overnight-fasted dog, 600 μU/kg/min of insulin should fully suppress net hepatic glucose output, while 2000 μU/kg/min should induce a low rate of net hepatic glucose uptake and marked non-HGU (47). Our findings were three-fold: 1) brief 3-h elevations in FFA given daily for 3-h/d for 15-d can impair insulin action in liver, adipose tissue, and skeletal muscle, 2) the accumulation of hepatic triglycerides brought about by inhibition of VLDL export does not worsen the effects of repeated elevations of FFA on the liver, and 3) the peripheral insulin resistance brought about by repeated elevations of FFA is not observed when the lipid treatment is administered in the presence of the MTP inhibitor, CP-346086.

The present study confirmed previous findings that acute suppression of NHGO by insulin results from inhibition of glycogenolysis (Fig. 5.4, (25, 83, 106). Boden et al. (25) showed in humans that, by 3-h, an acute administration of Intralipid and heparin reduced insulin suppression of glycogenolysis and therefore endogenous glucose production by 66 and 64%, respectively. Here we show that repeated brief elevations of FFA daily over a 15-d period chronically reduced insulin suppression of net hepatic glucose production by ~40 % in the Lipid and Lipid + CP-3460686 groups compared to Saline control (Fig. 5.3). This reduction resulted from insulin's inability to suppress

NHGLY (Fig. 5.4). Furthermore, higher insulin levels (~130 μU/ml) were less effective in stimulating NHGU in the lipid treated groups (both $P \leq 0.1$ vs. Saline, Fig. 5.4). As hepatic sinusoidal levels of plasma insulin and glucagon were successfully controlled throughout the study, the reduction in hepatic insulin action was due to the 15-d lipid treatments.

Repeated brief elevations of FFA altered basal NHGNG flux in both lipid treated groups. As expected in a 18-h fasted dog, net hepatic glycolysis was present during the basal period in the Saline group (117). Interestingly, following 15-d of lipid treatment, NHGNG flux had shifted to net gluconeogenesis. A possible explanation for this difference in basal NHGNG flux is suggested by the higher rates of hepatic production of ketone bodies observed in both Lipid groups compared to the Saline group (Fig. 5.8). It has been proposed (132, 186, 221) that increased fatty acid oxidation subsequently raises intracellular citrate levels, leading to decreased PFK-1 and increased $P1,6P_2$ase activities, and thus suppression of glycolysis and/or stimulation of gluconeogenesis. When glucose is being produced via glycogenolysis, as seen here in the basal period, some of the glycogenolytically-derived carbon enters the glycolytic pathway and exits the liver as lactate, and an increase in net hepatic lactate output occurs (49, 117). In the present study, an increase in hepatic ketone production was associated with suppressed hepatic lactate output during the basal period of both of the lipid treated groups. Thus, as increased basal hepatic ketone production positively correlated with changes in basal NHGNG flux in both of the lipid groups, it is likely a new steady state had been achieved, whereby the daily elevated hepatic FFA load was compensated for by an

increase in the removal of hepatic lipids via mitochondrial β-oxidation and ketogenesis, which in turn inhibited glycolysis and/or stimulated gluconeogenesis.

Insulin resistance was also induced in peripheral tissues following 15-d of repeated brief elevations of FFA. In response to an insulin infusion of 600 μU/kg/min, arterial blood glycerol levels fell to a significantly lesser degree in the Lipid group than in the Saline group. Interestingly, arterial blood glycerol levels remained elevated in Step 2 despite such high levels of insulin. This observation is of particular significance as suppression of lipolysis is the most sensitive response to the action of insulin (270). Although glycerol is a better indicator of lipolysis, arterial plasma FFA levels also fell less in response to low dose insulin in the Lipid group than they did in the Saline group. Levels were comparable during high insulin infusion (Fig. 5.6). These findings suggest that insulin's ability to suppress lipolysis in adipose tissue was significantly impaired. As FFA have been shown to mediate insulin inhibition of hepatic glucose production, the lack of their suppression might explain the defect in insulin action at the liver in response to low dose insulin.

Additionally, non-hepatic glucose uptake was reduced by ~30 % in the Lipid group compared to Saline group in response to high dose insulin (Fig. 5.4). Of note, the lower arterial plasma insulin levels observed in the Lipid group than in the Saline group in Step 2 (Fig. 5.2) are presumably due to two outliers. If these particular dogs are omitted from data analysis, plasma insulin levels (μU/ml) would be 46 ± 2 in the Lipid compared to 51 ± 4 in the Saline group. In that case, non-HGU (mg/kg/min) would be 9.9 ± 1.3 (Lipid) as opposed to 14.4 ± 1.8 (Saline). Therefore, differences in non-HGU

are most likely attributable to repeated elevations of FFA and not to the apparent reduction in circulating insulin.

Interestingly, the induction of insulin resistance in both adipose tissue and skeletal muscle brought about by repeated elevations of FFA was not observed when the lipid infusion was administered in the presence of the MTP inhibitor, CP-346086. Arterial plasma FFA and blood glycerol levels in the group receiving the inhibitor fell to levels similar to those seen in the Saline group in response to insulin throughout the experimental infusion (Fig. 5.6). Furthermore, non-hepatic glucose uptake was comparable between the Lipid + CP-346086 and Saline groups. It should be noted that, in Step 2 of the experimental period, arterial plasma insulin levels were slightly lower (Fig. 5.2) in the Lipid + CP-346086 group than in the Saline group, strengthening the conclusion that the MTP inhibitor prevented loss of peripheral insulin sensitivity.

The lack of peripheral insulin resistance observed following combined treatment of lipid and CP-346086 was most likely a result of a less pronounced increase in FFA during the lipid infusion, compared to lipid treatment alone. Simultaneous infusion of Intralipid and heparin is a common research tool used to acutely raise circulating FFA. Heparin administration increases plasma levels (over 100-fold) of the lipolytic enzyme, lipoprotein lipase (LPL), which results in hydrolysis of triglycerides from chylomicrons and VLDL particles and consequently increases circulating levels of FFA (170). LPL does not distinguish between exogenous and endogenous triglycerides. Therefore, the level of FFA observed during combined Intralipid and heparin infusions is the result of hydrolysis of triglycerides from both sources. As MTP is thought to play a pivotal role in the assembly and secretion of apoB-containing lipoproteins, and CP-346086 was

administered at the time of feeding, both VLDL and chylomicron secretion were presumably inhibited postprandially in the liver and small intestine, respectively. Therefore, it is possible that inhibition of apo-B lipoprotein secretion by CP-346086 during the lipid infusion resulted in a blunting of the elevation of FFA, such that it was not sufficient to induce insulin resistance. In keeping with this possibility, there was no evidence for elevation of FFA, glycerol, or triglycerides in the fasting state in the Lipid group, suggesting that the daily infusions of lipid and heparin had no prolonged effect on these parameters. Morover, in the single dog examined following an acute infusion of Intralipid, FFA and glycerol levels returned to basal within an hour after the infusion ceased (Chapter IV).

An alternative explanation could be that over a 24-h period, reduction of circulating lipoprotein triglycerides and subsequent lipid uptake by peripheral tissues prevented the FFA-induced insulin resistance observed in adipose tissue and skeletal muscle. We have no data regarding the full 24-h response, but the elevation of plasma triglycerides in the basal state and the fact that the basal FFA levels were not reduced in the group receiving the inhibitor suggest that the latter alternative is unlikely.

There is a large body of evidence which strongly suggests that elevated plasma FFA levels are a major cause of insulin resistance in obesity and type 2 diabetes. It has been hypothesized that acute elevations in FFA impair insulin action via oxidative and/or non-oxidative mechanisms. As alluded to above, FFA compete with glucose for substrate oxidation which consequently leads to the inhibition of glycolysis and could therefore reduce peripheral glucose uptake and/or stimulate hepatic gluconeogenesis. An alternative hypothesis, as proposed by Shulman (252) and Boden (19), is that elevations

of intracellular FA metabolites (diacylglycerol, fatty acyl CoA, and ceramides) following increased FFA delivery activate PKC. PKC then leads to decreased activity of the insulin receptor and IRS-1 and consequently results in decreased PI3K activity and reduced insulin-stimulated muscle glucose transport. Although this mechanism has primarily been established in muscle, studies have indicated that a similar mechanism may also occur in liver (28, 156) and adipose tissue (104).

More recently, it has been suggested that FFA-induced hepatic (28, 36) and peripheral (194, 208) insulin resistance is associated not only with elevations of intracellular FFA metabolites but also activation of proinflammatory signaling pathways (JNK and IkB/NFκB) and increased expression of proinflammatory cytokines such as TNF-α and IL-6. Activation of an inflammatory state is thought to play an important role in insulin resistance and is thus an important link to the pathogenesis of type 2 diabetes. As increases in proinflammatory gene expression are associated with insulin resistance in the liver and peripheral tissues, it is probable that a sub-acute inflammatory response was induced following repeated lipid treatment. Indeed, IKK-β activation in insulin resistant hepatocytes and adipocytes is associated with macrophage infiltration and proinflammatory cytokine release which could promote local and potentially systemic inflammation. Additionally, acute infusion of Intralipid has been shown to activate the NFκB pathway in mouse (36, 150) and human (150, 302), and the associated insulin resistance has been shown to be ameliorated by salicylate. Thus, it would be of particular interest to assess markers of inflammation following repeated elevations of FFA. Although markers of inflammation were not evaluated in the current study, it is possible

that recurring elevations of FFA induced a sub-acute inflammatory response that resulted in chronic insulin resistance.

Accumulation of intracellular triglycerides in liver and skeletal muscle has been strongly implicated in the development of insulin resistance; however to date, their putative role is based solely upon correlative results. It is proposed that the triglycerides themselves do not alter insulin action but rather provide a reservoir of FFA and/or FA metabolites that arise during lipid synthesis or hydrolysis and thus impair insulin signaling via activation of PKC, JNK, and/or IKK-β. The present study supports this hypothesis, given that the accumulation of hepatic triglyceride content in the Lipid + CP-346086 group did not result in a greater reduction of hepatic insulin action compared to the Lipid group (Fig. 5.4). Moreover, as a single 3-h treatment of elevated FFA resulted in a two-fold rise in hepatic triglycerides (Chapter IV, Fig. 4.5) that was not present following the 15-d treatment regimen, it is possible that a compensation of the liver during the chronic treatment allowed it to remove accumulated hepatic lipids that would have impaired insulin suppression of NHGO. The fact that basal hepatic β-OHB production was elevated in both of the lipid groups following the 15-d treatment, albeit in the presence of normal basal plasma FFA levels, strongly suggests that the liver does indeed compensate for a positive triglyceride balance. Therefore, it is possible that hepatic triglyceride hydrolysis and subsequent increases in intracellular FFA and/or FA metabolites and impaired insulin signaling via activation of PKC, JNK, and/or IKK-β contribute to the insulin resistance associated with steatosis.

In conclusion, the present study is the first to show that repeated brief daily elevations of FFA induce insulin resistance in liver, skeletal muscle, and adipose tissue. This

finding suggests that recurring elevations of FFA, such as might occur during the postprandial period in type 2 diabetes, could progressively lead to chronic insulin resistance. In addition, we show that accumulation of hepatic triglycerides does not worsen the effects of repeated elevations of FFA. We speculate that it is rather the compensatory mechanism(s) of the liver to remove excess lipids that results in hepatic insulin resistance. And lastly, peripheral insulin resistance was not present following combined lipid and CP-346086 treatment which was likely owing to a less significant rise in FFA during the lipid infusion as less lipoprotein-associated triglycerides were available for hydrolysis. However, it could be that accumulation of hepatocellular triglycerides reduce circulating lipids and thus serve to prevent induction of peripheral insulin resistance. Although we can not draw any definitive conclusions from this particular finding, it raises the question as to whether normalization of the increased postprandial VLDL production observed in type 2 diabetes would improve insulin sensitivity.

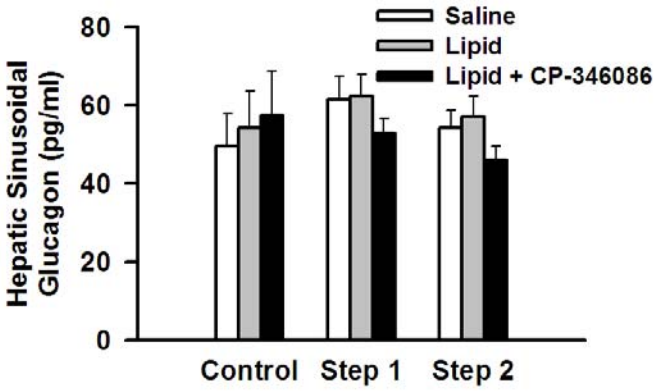

Figure 5.1: Hepatic sinusoidal levels of plasma glucagon. Hepatic sinusoidal levels of plasma glucagon during a 2 step hyperinsulinemic-euglycemic clamp in conscious 18 h fasted dogs. Insulin was infused intraportally at 600 μU/kg/min in Step 1 and 2000 μU/kg/min in Step 2. The clamp was performed following treatment with saline, Intralipid/heparin (Lipid), or Intralipid/heparin in the presence of a MTP inhibitor, CP-346086 for 3h/d for 15-d. Values are means ± SE. Control period values are an average of samples taken at -40 and 0 min. Values for Steps 1 and 2 of the experimental period are an average of the 3 samples taken during the last h of each step at 30 min intervals.

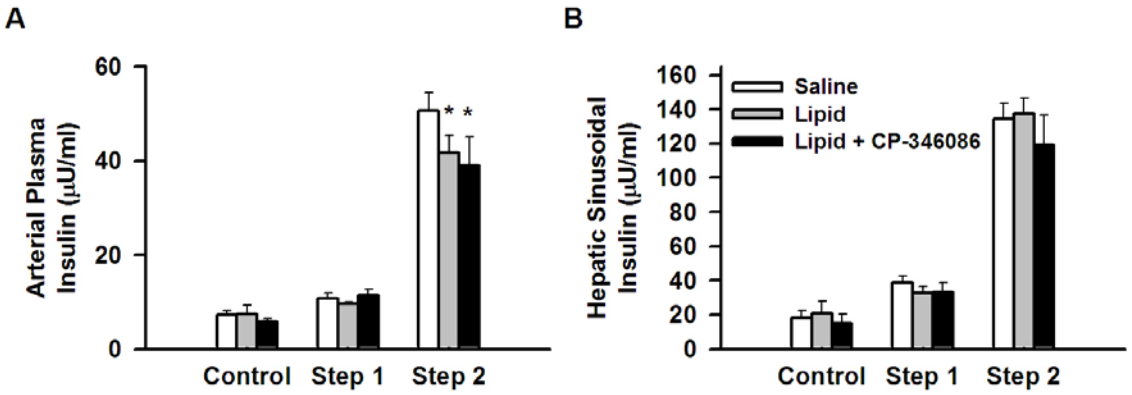

Figure 5.2: Arterial and hepatic sinusoidal levels of plasma insulin. Arterial (A) and hepatic sinusoidal levels (B) of plasma insulin during a 2-step hyperinsulinemic-euglycemic clamp in conscious 18 h fasted dogs. Insulin was infused intraportally at 600 μU/kg/min in Step 1 and 2000 μU/kg/min in Step 2. The clamp was performed following treatment with saline, Intralipid/heparin (Lipid), or Intralipid/heparin in the presence of a MTP inhibitor, CP-346086 for 3h/d for 15-d. Values are means ± SE. Control period values are an average of samples taken at -40 and 0 min. Values for Steps 1 and 2 of the experimental period are an average of the 3 samples taken during the last h of each step at 30 min intervals. * $P < 0.05$ vs. Saline

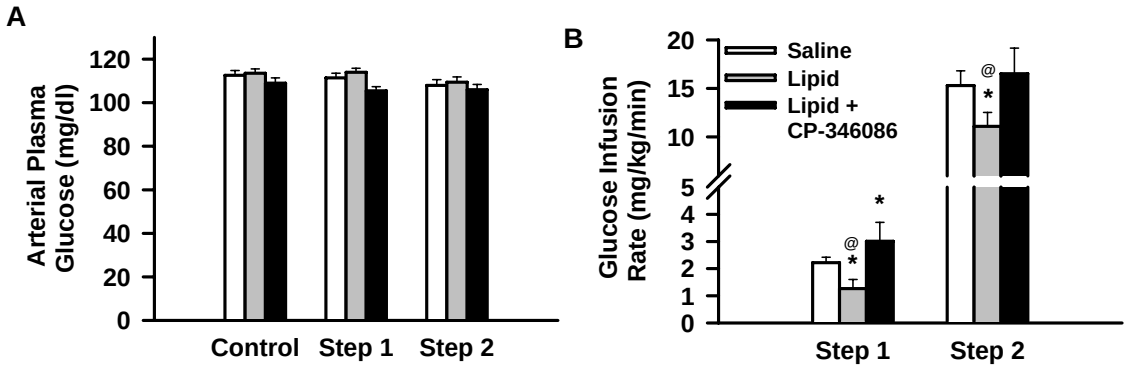

Figure 5.3: Arterial plasma levels of glucose and glucose infusion rates. Arterial plasma levels of glucose (A) and glucose infusion rates (B) during a 2-step hyperinsulinemic-euglycemic clamp in conscious 18 h fasted dogs. Insulin was infused intraportally at 600 μU/kg/min in Step 1 and 2000 μU/kg/min in Step 2. The clamp was performed following treatment with saline, Intralipid/heparin (Lipid), or Intralipid/heparin in the presence of a MTP inhibitor, CP-346086 for 3 h/d for 15-d. Values are means ± SE. Control period values are an average of samples taken at -40 and 0 min. Values for Steps 1 and 2 of the experimental period are an average of the 3 samples taken during the last h of each step at 30 min intervals. * $P < 0.05$ vs. Saline @ $P < 0.05$ vs. Lipid

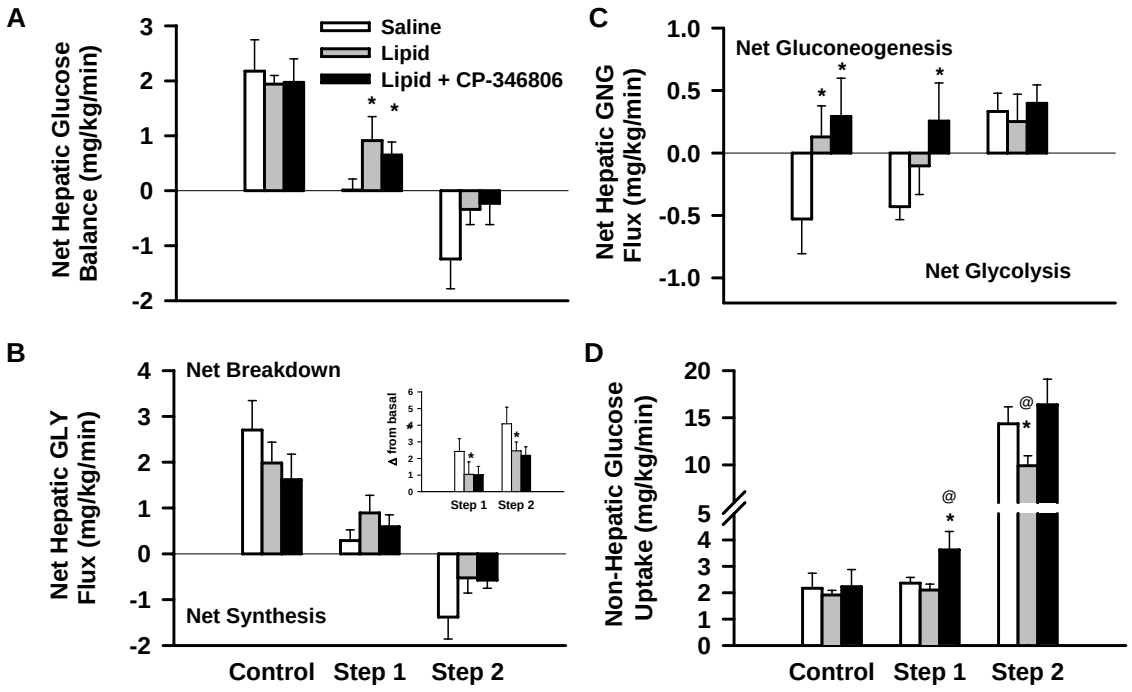

Figure 5.4: Net hepatic glucose balance, glycogenolytic (GLY) and gluconeogenic (GNG) fluxes, and non-hepatic glucose uptake. Net hepatic glucose balance (A) and glycogenolytic flux (B), gluconeogenic flux (C), and non-hepatic glucose uptake (D) during a 2-step hyperinsulinemic-euglycemic clamp in conscious 18 h fasted dogs. Insulin was infused intraportally at 600 μU/kg/min in Step 1 and 2000 μU/kg/min in Step 2. The clamp was performed following treatment with saline, Intralipid/heparin (Lipid), or Intralipid/heparin in the presence of a MTP inhibitor, CP-346086 for 3 h/d for 15-d. Positive and negative values of net hepatic glucose balance represent net output and net uptake, respectively. Positive and negative values of net hepatic GLY flux represent net glycogenolysis and net synthesis, respectively. Positive and negative values of net hepatic GNG flux represent net gluconeogenesis and net glycolysis, respectively. *Inset:* Change in net hepatic GLY from control period during hyperinsulinemic-euglycemic clamp. Values are means ± SE. Control period values are an average of samples taken at -40 and 0 min. Values for Steps 1 and 2 of the experimental period are an average of the 3 samples taken during the last h of each step at 30 min intervals. * $P < 0.05$ vs. Saline @ $P < 0.05$ vs. Lipid

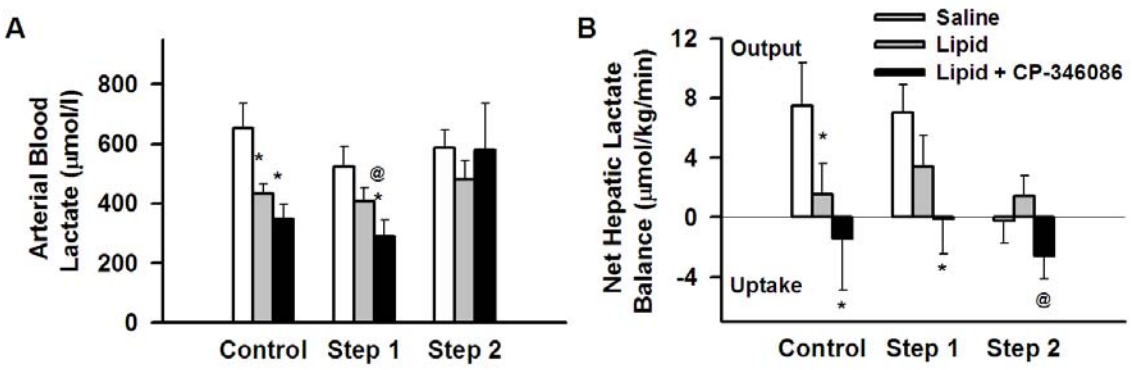

Figure 5.5: Arterial blood levels and net hepatic balance of lactate. Arterial blood levels (A) and net hepatic balance (B) of lactate during a 2-step hyperinsulinemic-euglycemic clamp in conscious 18 h fasted dogs. Insulin was infused intraportally at 600 μU/kg/min in Step 1 and 2000 μU/kg/min in Step 2. The clamp was performed following treatment with saline, Intralipid/heparin (Lipid), or Intralipid/heparin in the presence of a MTP inhibitor, CP-346086 for 3 h/d for 15-d. Positive and negative values of net hepatic lactate balance represent net output and net uptake, respectively. Control period values are an average of samples taken at -40 and 0 min. Values for Steps 1 and 2 of the experimental period are an average of the 3 samples taken during the last h of each step at 30 min intervals. * $P < 0.05$ vs. Saline @ $P < 0.05$ vs. Lipid.

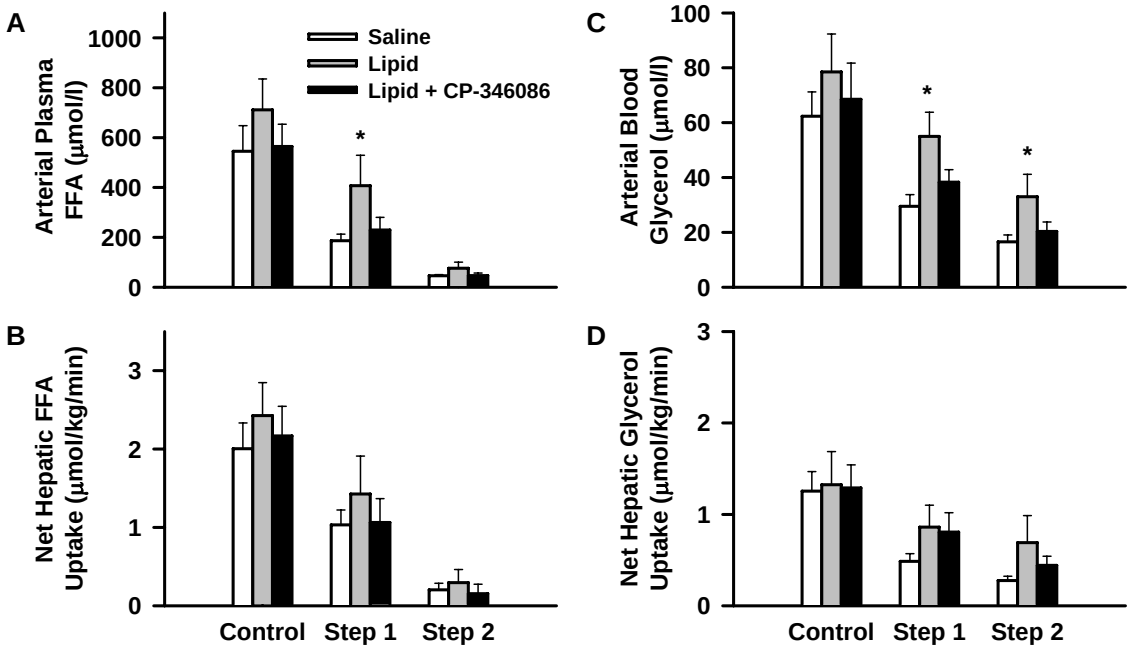

Figure 5.6: Arterial plasma FFA and blood glycerol levels and net hepatic uptakes. Arterial plasma FFA levels (A), net hepatic FFA uptake (B), arterial blood glycerol levels (C), and net hepatic glycerol uptake (D) during a 2-step hyperinsulinemic-euglycemic clamp in conscious 18 h fasted dogs. Insulin was infused intraportally at 600 μU/kg/min in Step 1 and 2000 μU/kg/min in Step 2. The clamp was performed following treatment with saline, Intralipid/heparin (Lipid), or Intralipid/heparin in the presence of a MTP inhibitor, CP-346086 for 3 h/d for 15-d. Control period values are an average of samples taken at -40 and 0 min. Values for Steps 1 and 2 of the experimental period are an average of the 3 samples taken during the last h of each step at 30 min intervals.
* $P < 0.05$ vs. Saline.

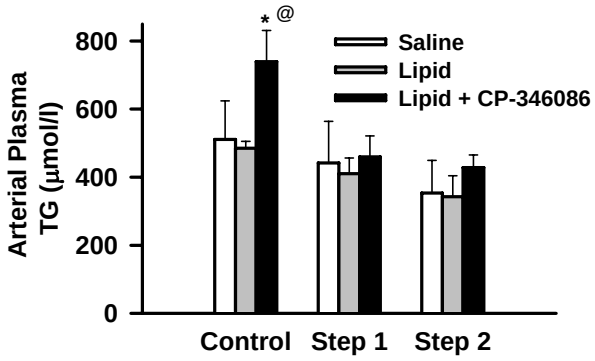

Figure 5.7: Arterial plasma triglyceride levels. Arterial plasma triglyceride levels during a 2-step hyperinsulinemic-euglycemic clamp in conscious 18 h fasted dogs. Insulin was infused intraportally at 600 µU/kg/min in Step 1 and 2000 µU/kg/min in Step 2. The clamp was performed following treatment with saline, Intralipid/heparin (Lipid), or Intralipid/heparin in the presence of a MTP inhibitor, CP-346086 for 3 h/d for 15-d. Control period values are an average of samples taken at -40 and 0 min. Values for Steps 1 and 2 of the experimental period are an average of the 3 samples taken during the last h of each step at 30 min intervals. * $P < 0.05$ vs. Saline @ $P < 0.05$ vs. Lipid

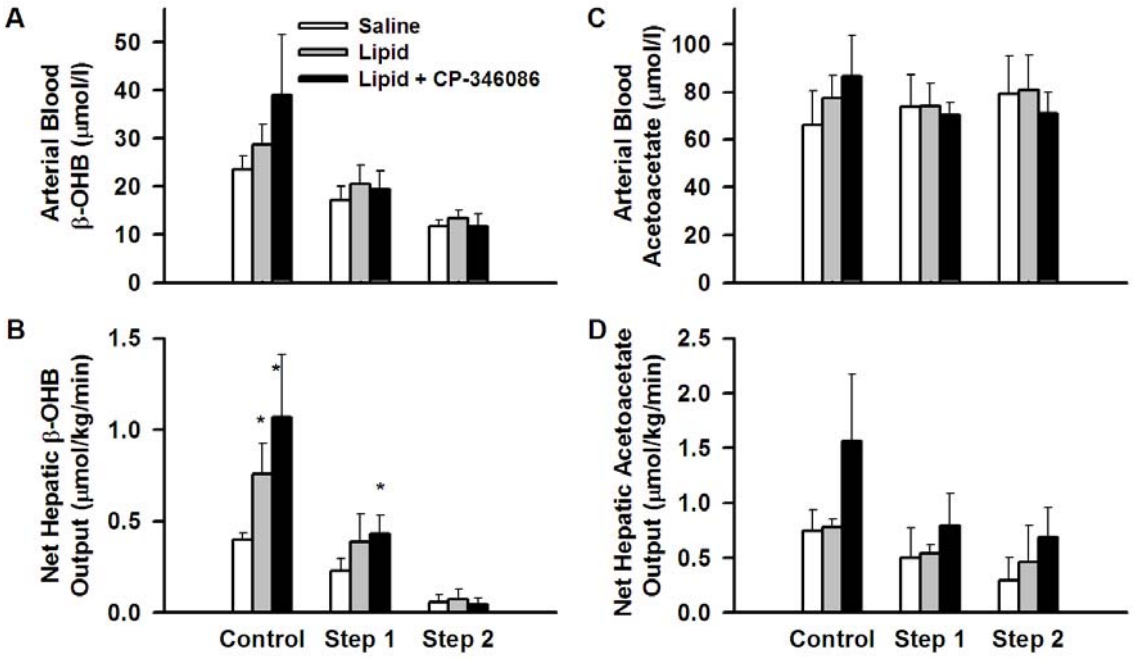

Figure 5.8. Arterial blood levels and net hepatic outputs of β-OHB and acetoacetate. Arterial blood levels (A) and net hepatic balance (B) of β-OHB and arterial blood levels (C) and net hepatic output (D) of acetoacetate during a 2-step hyperinsulinemic-euglycemic clamp in conscious 18 h fasted dogs. Insulin was infused intraportally at 600 μU/kg/min in Step 1 and 2000 μU/kg/min in Step 2. The clamp was performed following treatment with saline, Intralipid/heparin (Lipid), or Intralipid/heparin in the presence of a microsomal triglyceride transfer protein inhibitor, CP-346086 for 3 h/d for 15 d. Values are means ± SE. * $P < 0.05$ vs. Saline. @ $P < 0.05$ vs. Lipid.

TABLE 5.1

Arterial blood levels, net hepatic balances, and fractional extraction of individual and total gluconeogenic amino acids during a 2 step hyperinsulinemic-euglycemic clamp in conscious 18 h fasted dogs. Insulin was infused intraportally at 600 mU/kg/min in Step 1 and 2000 mU/kg/min in Step 2. The clamp was performed following treatment with saline, Intralipid/heparin (Lipid), or Intralipid/heparin in the presence of a MTP inhibitor, CP-346086 for 3h/d for 15d.

	Arterial Blood Level µmol/l			Net Hepatic Balance µmol/kg/min			Fractional Extraction †		
	Control period	Experimental period (min)		Control period	Experimental period		Control period	Experimental period	
		Step 1	Step 2		Step 1	Step 2		Step 1	Step 2
	-40 - 0	(60 - 120)	(180 - 240)	-40 - 0	(60 - 120)	(180 - 240)	-40 - 0	(60 - 120)	(180 - 240)
Alanine									
Saline	373 ± 33	300 ± 25	188 ± 13	-2.1 ± 0.2	-2.5 ± 0.2	-2.6 ± 0.2	0.20 ± 0.02	0.30 ± 0.02	0.44 ± 0.02
Lipid	276 ± 15*	238 ± 22*	174 ± 18	-2.1 ± 0.5	-2.5 ± 0.5	-3.7 ± 1.6	0.24 ± 0.03	0.34 ± 0.03	0.43 ± 0.02
Lipid + CP-346086	274 ± 4*	213 ± 20*	200 ± 22	-1.8 ± 0.2	-2.5 ± 0.4	-2.6 ± 0.2	0.24 ± 0.06	0.32 ± 0.06	0.35 ± 0.03*@
Glutamine									
Saline	860 ± 61	775 ± 66	606 ± 61	1.41 ± 0.4	0.81 ± 0.4	-0.21 ± 0.4	0.07 ± 0.02	-0.05 ± 0.03	0.00 ± 0.02
Lipid	802 ± 42	735 ± 42	589 ± 33	1.00 ± 0.5	0.96 ± 0.3	0.52 ± 0.5	-0.05 ± 0.04	-0.06 ± 0.02	-0.03 ± 0.03
Lipid + CP-346086	746 ± 38	696 ± 44	506 ± 115	1.26 ± 0.3	2.07 ± 0.8	0.94 ± 0.7	-0.07 ± 0.02	- 0.12 ± 0.05	-0.07 ± 0.05
Glutamate									
Saline	68 ± 8	63 ± 7	58 ± 8	-0.03 ± 0.1	-0.02 ± 0.1	-0.13 ± 0.1	0.00 ± 0.03	0.02 ± 0.06	0.05 ± 0.04
Lipid	98 ± 20	86 ± 20	74 ± 12	-0.10 ± 0.1	0.02 ± 0.1	-0.16 ± 0.1	0.03 ± 0.03	-0.01 ± 0.06	0.05 ± 0.04
Lipid + CP-346086	94 ± 9*	82 ± 9*	65 ± 8	-0.02 ± 0.1	0.06 ± 0.1	0.04 ± 0.2	0.00 ± 0.04	-0.28 ± 0.33	-0.11 ± 0.17
Glycine									
Saline	211 ± 26	150 ± 21	110 ± 12	-0.28 ± 0.5	-0.70 ± 0.3	-0.54 ± 1.0	0.01 ± 0.07	0.14 ± 0.06	0.13 ± 0.17
Lipid	212 ± 47	199 ± 45	117 ± 25	0.05 ± 0.4	0.11 ± 0.2*	-0.98 ± 0.4	0.01 ± 0.04	-0.02 ± 0.05*	0.33 ± 0.07
Lipid + CP-346086	216 ± 18	162 ± 17	133 ± 18	-0.14 ± 0.3	-0.57 ± 0.3	-0.27 ± 0.1	0.03 ± 0.08	0.24 ± 0.22	0.08 ± 0.03@
Serine									
Saline	131 ± 24	84 ± 20	65 ± 12	-0.64 ± 0.3	-0.58 ± 0.3	-0.84 ± 0.6	0.12 ± 0.05	0.15 ± 0.07	0.32 ± 0.16
Lipid	76 ± 8*	71 ± 6	60 ± 8	-0.43 ± 0.1	-0.44 ± 0.1	-0.60 ± 0.1	0.16 ± 0.03	0.28 ± 0.06	0.39 ± 0.01
Lipid + CP-346086	125 ± 17@	82 ± 17	73 ± 16	-0.05 ± 0.2	-0.81 ± 0.1	-0.81 ± 0.2	0.14 ± 0.06	0.31 ± 0.08	0.3 ± 0.03
Threonine									
Saline	144 ± 9	119 ± 14	94 ± 8	-0.40 ± 0.3	-0.68 ± 0.3	-0.69 ± 0.4	0.16 ± 0.03	0.28 ± 0.06	0.39 ± 0.05
Lipid	140 ± 21	149 ± 25	112 ± 19	-0.73 ± 0.3	-0.60 ±0.5	-0.74 ± 0.2	0.13 ± 0.06	0.13 ± 0.10	-0.19 ± 0.06
Lipid + CP-346086	148 ± 21	107 ± 19	97 ± 15	-0.13 ± 0.3	-0.39 ± 0.2	-0.31 ± 0.2	0.07 ± 0.08	0.15 ± 0.07	0.11 ± 0.07
Total Gluconeogenic IAA									
Saline	947 ± 71	717 ± 75	516 ± 41	-3.57 ± 1.0	-4.48 ± 0.7	-4.83 ± 1.9	0.12 ± 0.03	0.20 ± 0.02	0.27 ± 0.09
Lipid	801± 74	743 ± 58	536 ± 42	-3.42 ± 0.7	-4.32 ± 0.6	-5.28 ± 0.7	0.14 ± 0.03	0.20 ± 0.02	0.26 ± 0.02
Lipid + CP-346086	858 ± 31	648 ± 37	568 ± 25	-2.54 ± 0.6	-4.26 ± 0.6	-3.86 ± 0.30@	0.16 ± 0.04	0.27± 0.02*@	0.29 ± 0.04

Values are means ± SE. Basal period values are an average of samples taken at -40 and 0 min. Values for Steps 1 and 2 of the experimental period are an average of the 3 samples taken during the last h of each step at 30 min intervals. Values for all Total IAA data exclude glutamine. Negative and positive values of net hepatic balance represent net hepatic uptake and output, respectively. * $P < 0.05$ vs. Saline. @ $P < 0.05$ vs. Lipid. † calculated as net hepatic balance per load in.

CHAPTER VI

SUMMARY AND CONCLUSIONS

Although diabetes mellitus was long considered a disease of minor significance to world health, it is now the most common disease in the world. In fact, over the past two decades an explosive increase has been observed in the number of people diagnosed with diabetes worldwide. The epidemic is chiefly of type 2 diabetes and is largely due to the escalating rates of obesity. Analyses by the International Obesity Task force indicate that approximately 58% of diabetes mellitus globally can be attributed to weight gain. More specifically, in western countries, around 90% of type 2 diabetes cases are attributable to weight gain.

Weight gain leads to insulin resistance and consequently hyperglycemia due to increase hepatic glucose production and decreased peripheral glucose uptake. Insulin resistance places a greater demand on the pancreatic capacity to produce insulin. Although the primary cause of the disease is unknown, the major causative link between type 2 diabetes and obesity is an elevation of circulating (free fatty acids, FFA) and intracellular lipids. To optimize therapy with insulin sensitizing agents, it would be useful to understand how increased lipids contribute to insulin resistance. Therefore, the goal of this dissertation was to gain a better understanding of how changes in lipid metabolism alter glucose homeostasis.

Glucose homeostasis reflects a delicate balance between glucose production and glucose uptake. This balance is best demonstrated during periods following food consumption and fasting when plasma glucose levels remain in a narrow range.

Following an overnight fast (post absorptive state), the liver is the major contributor of endogenous hepatic glucose production and is thus the principal organ which delivers glucose to both the non-insulin-sensitive (nervous, red blood cells, skin, smooth muscle) and the insulin sensitive (muscle and fat) tissues. Following a meal (postprandial state) minimization of postprandial hyperglycemia results from the suppression of endogenous glucose production and stimulation of glucose uptake (110). Thus, the factors that regulate balance between glucose production and glucose uptake are extremely important to glucoregulation.

Glucoregulatory hormones tightly control glucose production and uptake by their direct actions on glucose metabolism and indirect actions on both lipid and protein metabolism. Three main glucoregulatory hormones are insulin, epinephrine, and glucagon. Insulin, secreted by the β-cells of the pancreas, rises in response to hyperglycemia, rapidly suppressing hepatic glucose production, and stimulating glucose uptake in peripheral tissues. On the other hand, epinephrine and glucagon, secreted from the adrenal medulla and pancreatic α-cells, respectively, rise in response hypoglycemia acting on the liver to stimulate hepatic glucose production. Additionally, the metabolic effects of insulin and epinephrine on lipid and protein metabolism in peripheral tissues indirectly mediate their glucoregulatory action.

In fact, our laboratory (255) and others (2, 109, 225) have shown that the main substrate responsible for the reduction in insulin's indirect effect on HGP is FFA. Insulin inhibits lipolysis and thus decreases the plasma FFA levels. Cellular uptake of FFA subsequently increases FA oxidation and alters enzymatic activity of glucose metabolic pathways by increasing $P1,6P_2$ase and decreasing PFK-1 activities, thereby

simultaneously stimulating GNG and hindering glycolysis. Thus, the antilipolytic effects of insulin mediate its ability to suppress HGP by reducing GNG.

Likewise, the lipolytic action of epinephrine influences its ability to stimulate HGP. The direct action of epinephrine on the liver results in the stimulation of GLY, however, Chu et al. (53) have shown that in the presence of elevated FFA epinephrine's glycolytic effect is limited but its gluconeogenic action is augmented. Thus, epinephrine's ability to release FFA from adipose tissue mediates its action on the liver by stimulating hepatic GNG. The simultaneous inhibition of glycolysis causes an increase in intracellular G6P and could possibly result in the inhibition of GLY.

Although glucagon receptors are located on adipocytes and glucagon has been shown to be capable of stimulating lipolysis *in vitro*, the hormone has little to no effect on adipose tissue *in vivo*. Since the direct actions of both epinephrine and glucagon on HGP are mediated by cAMP, it could be hypothesized that elevations in FFA would alter hepatic glucagon action in a similar manner to that seen with epinephrine. In overt type 2 diabetes, lower plasma insulin levels during the postprandial period results in a decreased insulin effect at both the pancreatic α-cell and adipocyte, contributing to the elevation of glucagon and FFA levels (75, 243). As an insufficient decrease in HGP is thought to be a main contributor of the postprandial hyperglycemia observed in type 2 diabetes, it is possible that elevated levels of glucagon and FFA could be responsible for the increase in glucose production by the liver in these patients. Therefore the goal of *Specific Aim I* was to determine how elevations in glucagon and FFA interact to acutely regulate HGP. Our findings indicate that elevated FFA inhibit the glycogenolytic effects of glucagon, as they do the glycogenolytic effect of epinephrine. However, this effect is

short-lived compared to epinephrine. In contrast to the results with the combination of elevated FFA and epinephrine, an increase in FFA does not augment glucagon-stimulated hepatic gluconeogenesis. One possible explanation for this could be that the potency of glucagon to stimulate glycogenolysis and thus force carbon down the glycolytic pathway is greater than that of epinephrine. This would override FFA's ability to inhibit glycolysis or fuel gluconeogenesis. Therefore, the question arises as to whether epinephrine levels of equal biological effectiveness to the glucagon dosage used in this study would prevent FFA-stimulated gluconeogenesis.

Although postprandial levels of glucagon and FFA are elevated in individuals with type 2 diabetes, our results suggest that their interaction alone does not potentiate HGP nor do FFA alter the mechanisms by which glucagon stimulates HGP. Therefore, it is likely that lower levels of insulin as well as elevated levels of glucagon and FFA are responsible for the increases in HGP observed during the postprandial period of patients with type 2 diabetes.

Even though elevated postprandial FFA may not alter glucagon action in type 2 diabetes, there is strong evidence for elevated fasting and postprandial FFA levels in type 2 diabetes and those at risk for the disease. Both acute (20, 26, 229, 257) and chronic (20, 237) elevations of FFA have been shown to induce insulin resistance. Actually, it has been estimated that elevated plasma FFA account for the entire insulin resistance in non-diabetic obese patients and ~50% of the insulin resistance in obese patients with type 2 diabetes (19). The mechanism(s) by which elevations in FFA impair insulin action is unclear however it has been hypothesized that insulin resistance occurs via oxidative and/or non-oxidative mechanisms. As alluded to above, FFA compete with glucose for

substrate oxidation which consequently leads to the inhibition of glycolysis and could therefore reduce peripheral glucose uptake and/or stimulate hepatic gluconeogenesis. An alternative hypothesis, as proposed by Shulman (252) and Boden (19), is that elevations of intracellular FA metabolites (diacylglycerol, fatty acyl CoA, and ceramides) following increased FFA delivery activate PKC. PKC then leads to decreased activity of the insulin receptor and IRS-1 and consequently results in decreased PI3K activity and reduced insulin-stimulated muscle glucose transport. Although this mechanism has primarily been established in muscle, studies have indicated that a similar mechanism may also occur in liver (28, 156) and adipose tissue (104).

More recently, it has been suggested that FFA-induced hepatic (28, 36) and peripheral (194, 208) insulin resistance is associated not only with elevations of intracellular FFA metabolites but also activation of proinflammatory signaling pathways (JNK and IkB/NFκB) and increased expression of proinflammatory cytokines such as TNF-α and IL-6. Activation of an inflammatory state is thought to play an important role in insulin resistance and is thus an important link to the pathogenesis of type 2 diabetes. Additionally, acute infusion of Intralipid has been shown to activate the NFκB pathway in mouse (36, 150) and human (150, 302), and the associated insulin resistance has been shown to be ameliorated by salicylate.

Accumulation of intracellular lipids, specifically, triglycerides in liver and skeletal muscle has also been strongly implicated in the development of insulin resistance. Interestingly, an increase in triglycerides in skeletal muscle shows a stronger correlation with insulin resistance than elevated levels of plasma FFA (152, 195, 202). Accummulation of hepatic triglycerides, or hepatic steatosis, has a very robust

association with hepatic insulin sensitivity; in fact, studies have indicated that insulin resistance is more closely related to changes in hepatocellular than intramyocellular triglyceride content (11, 173, 242). It is proposed that the triglycerides themselves do not alter insulin action but rather provide a reservoir of FFA and/or FA metabolites that arise during lipid synthesis or hydrolysis and thus impair insulin signaling via activation of PKC, JNK, and/or IKK-β. Although there is a strong correlation with increased triglyceride content in non-adipose tissues (152, 195, 202) and type 2 diabetes it unclear whether the accumulation of intracellular lipid is a cause of or result of the decreased insulin response. The putative role of triglyceride accumulation in non-adipose tissues is based solely upon correlative results. Therefore, one remains unconvinced regarding the importance of triglyceride accumulation as a direct cause of insulin resistance and a contributor to the pathogenesis of diabetes. Since our laboratory uses the conscious dog as an experimental model due to its good reflection of glucose metabolism in humans and allowance for invasive experimental design, the goal of *Specific Aim II* was to create a canine model of hepatic steatosis. In attempt to do so, lipid metabolism was altered by 3 different treatments: 1) a 10% fructose diet, 2) elevating hepatic FFA flux, or 3) elevating hepatic FFA flux while simultaneously inhibiting triglyceride export from the liver using the microsomal triglyceride transfer protein inhibitor, CP-346086. A 10% fructose diet given over a four month period and repeated elevations of FFA (3-h/d for 15-d) were not successful in elevating hepatic triglycerides. However, as triglyceride levels were elevated 2-fold following the combined lipid and CP-346086 treatment we were thus successful in creating a canine model of hepatic steatosis.

Although it is well established that both acute and chronic increases of FFA cause insulin resistance, it remains unclear if recurring elevations of plasma FFA levels, such as might occur during the postprandial period in type 2 diabetes, can alter insulin sensitivity. For that reason, even though repeated elevations of FFA did not result in a rise in hepatic triglycerides, it was of interest to evaluate insulin sensitivity following the treatment regimen. Therefore the goal of *Specific Aim III* was to examine whole body insulin sensitivity following treatment regimens to induce hepatic steatosis.

Interestingly, repeated brief elevations of FFA also altered the mechanisms by glucose is produced by the liverin the basal state in both of the lipid treated groups. In a normal 18-h fasted dog, glucose is produced primarily via hepatic glycogenolysis and a state of net hepatic glycolysis is present (117). However, following the 15-d of lipid treatment, HGP resulted from both glycogenolysis and gluconeogenesis as NHGNG flux had shifted from a net glycolysis to net gluconeogenesis. A possible explanation for this difference in basal NHGNG flux is suggested by the higher rates of hepatic production of ketone bodies observed in both Lipid groups compared to the Saline treatment. As mentioned above, increased fatty acid oxidation subsequently raises intracellular citrate levels, leading to decreased PFK-1 and increased $P1,6P_2$ase activities, and thus suppression of glycolysis and/or stimulation of gluconeogenesis. Thus, as increased basal hepatic ketone production positively correlated with changes in basal NHGNG flux in both of the lipid groups, it is likely a new steady state had been achieved, whereby the daily elevated hepatic FFA load was compensated for by an increase in the removal of hepatic lipids via mitochondrial β-oxidation and ketogenesis, which in turn inhibited glycolysis and/or stimulated gluconeogenesis.

Furthermore, our results show for the first time that repeated daily elevations of FFA induce chronic insulin resistance in liver, skeletal muscle, and adipose tissue. This finding suggests that recurring elevations of FFA, such as might occur during the postprandial period in type 2 diabetes, could progressively lead to chronic insulin resistance. In addition, we show that accumulation of hepatic triglycerides does not worsen the effects of repeated elevations of FFA. We speculate that it is rather the compensatory mechanism(s) of the liver to remove excess lipids that results in hepatic insulin resistance. Therefore, it is possible that hepatic triglyceride hydrolysis and subsequent increases in intracellular FFA and/or FA metabolites and impaired insulin signaling via activation of PKC, JNK, and/or IKK-β contribute to the insulin resistance associated with steatosis.

Taken together, this dissertation clearly demonstrates that elevations of circulating and intracellular lipids alter glucoregulatory hormone action. We have shown that acute elevations of FFA affect hormone (insulin, epinephrine and glucagon) regulated hepatic glucose production by altering the mechanisms by which glucose is produced by the liver. Our findings also suggest that compensatory increases in triglyceride hydrolysis by the liver also alter mechanisms of basal hepatic glucose production and reduce insulin's ability to suppress glycogenolysis. And lastly, this work suggests that repeated brief elevations, such as might occur during the postprandial period in type 2 diabetes, could progressively lead to chronic insulin resistance. Although several mechanism(s) have been proposed by which elevated circulating and intracellular lipids alter glucoregulatory hormone action (particularly for that of insulin), the means by which changes in lipid metabolism alter glucose homeostasis still remains unclear. Elucidating the biochemical

and molecular mechanisms by which a dysregulation of lipid metabolism could interact with glucoregulatory hormones and cause harmful metabolic effects is of particular interest in order to optimize insulin sensitizing agents and thus ultimately better the lives of those affected with type 2 diabetes.

REFERENCES

1. **Abumrad NN, Cherrington AD, Williams PE, Lacy WW, and Rabin D.** Absorption and disposition of a glucose load in the conscious dog. *Am J Physiol* 242: E398-406, 1982.
2. **Ader M and Bergman RN.** Peripheral effects of insulin dominate suppression of fasting hepatic glucose production. *Am J Physiol* 258: E1020-1032, 1990.
3. **Agati JM, Yeagley D, and Quinn PG.** Assessment of the roles of mitogen-activated protein kinase, phosphatidylinositol 3-kinase, protein kinase B, and protein kinase C in insulin inhibition of cAMP-induced phosphoenolpyruvate carboxykinase gene transcription. *J Biol Chem* 273: 18751-18759, 1998.
4. **Aguirre V, Uchida T, Yenush L, Davis R, and White MF.** The c-Jun NH(2)-terminal kinase promotes insulin resistance during association with insulin receptor substrate-1 and phosphorylation of Ser(307). *J Biol Chem* 275: 9047-9054, 2000.
5. **Ally A and Park G.** Rapid determination of creatine, phosphocreatine, purine bases and nucleotides (ATP, ADP, AMP, GTP, GDP) in heart biopsies by gradient ion-pair reversed-phase liquid chromatography. *J Chromatogr* 575: 19-27, 1992.
6. **Altszuler N, De Bodo RC, Steele R, and Wall JS.** Measurement of size and turnover rate of body glucose pool by the isotope dilution method. *Am J Physiol* 187: 15-24, 1956.
7. **Anton AH and Sayre DF.** A study of the factors affecting the aluminum oxide-trihydroxyindole procedure for the analysis of catecholamines. *J Pharmacol Exp Ther* 138: 360-375, 1962.
8. **Antonetti DA, Algenstaedt P, and Kahn CR.** Insulin receptor substrate 1 binds two novel splice variants of the regulatory subunit of phosphatidylinositol 3-kinase in muscle and brain. *Mol Cell Biol* 16: 2195-2203, 1996.
9. **Araki E, Lipes MA, Patti ME, Bruning JC, Haag B, 3rd, Johnson RS, and Kahn CR.** Alternative pathway of insulin signalling in mice with targeted disruption of the IRS-1 gene. *Nature* 372: 186-190, 1994.
10. **Asano T, Kanda A, Katagiri H, Nawano M, Ogihara T, Inukai K, Anai M, Fukushima Y, Yazaki Y, Kikuchi M, Hooshmand-Rad R, Heldin CH, Oka Y, and Funaki M.** p110beta is up-regulated during differentiation of 3T3-L1 cells and contributes to the highly insulin-responsive glucose transport activity. *J Biol Chem* 275: 17671-17676, 2000.
11. **Bajaj M, Suraamornkul S, Pratipanawatr T, Hardies LJ, Pratipanawatr W, Glass L, Cersosimo E, Miyazaki Y, and DeFronzo RA.** Pioglitazone reduces hepatic fat content and augments splanchnic glucose uptake in patients with type 2 diabetes. *Diabetes* 52: 1364-1370, 2003.
12. **Baldeweg SE, Golay A, Natali A, Balkau B, Del Prato S, and Coppack SW.** Insulin resistance, lipid and fatty acid concentrations in 867 healthy Europeans. European Group for the Study of Insulin Resistance (EGIR). *Eur J Clin Invest* 30: 45-52, 2000.
13. **Baron AD.** Hemodynamic actions of insulin. *Am J Physiol* 267: E187-202, 1994.
14. **Bergman RN.** New concepts in extracellular signaling for insulin action: the single gateway hypothesis. *Recent Prog Horm Res* 52: 359-385; discussion 385-357, 1997.

15. **Bergman RN and Ader M.** Free fatty acids and pathogenesis of type 2 diabetes mellitus. *Trends Endocrinol Metab* 11: 351-356, 2000.
16. **Bergman RN, Bradley DC, and Ader M.** On insulin action in vivo: the single gateway hypothesis. *Adv Exp Med Biol* 334: 181-198, 1993.
17. **Bernt E and Bergamini E.** L-Glutamate, U-V assay with glutamate hydrogenase and NAD. *Academic Press*, 1963.
18. **Best JD, Ward WK, Pfeifer MA, and Halter JB.** Lack of a direct alpha-adrenergic effect of epinephrine on glucose production in human subjects. *Am J Physiol* 246: E271-276, 1984.
19. **Boden G and Carnell LH.** Nutritional effects of fat on carbohydrate metabolism. *Best Pract Res Clin Endocrinol Metab* 17: 399-410, 2003.
20. **Boden G and Chen X.** Effects of fat on glucose uptake and utilization in patients with non-insulin-dependent diabetes. *J Clin Invest* 96: 1261-1268, 1995.
21. **Boden G, Chen X, Capulong E, and Mozzoli M.** Effects of free fatty acids on gluconeogenesis and autoregulation of glucose production in type 2 diabetes. *Diabetes* 50: 810-816, 2001.
22. **Boden G, Chen X, and Iqbal N.** Acute lowering of plasma fatty acids lowers basal insulin secretion in diabetic and nondiabetic subjects. *Diabetes* 47: 1609-1612, 1998.
23. **Boden G, Chen X, Rosner J, and Barton M.** Effects of a 48-h fat infusion on insulin secretion and glucose utilization. *Diabetes* 44: 1239-1242, 1995.
24. **Boden G, Chen X, Ruiz J, White JV, and Rossetti L.** Mechanisms of fatty acid-induced inhibition of glucose uptake. *J Clin Invest* 93: 2438-2446, 1994.
25. **Boden G, Cheung P, Stein TP, Kresge K, and Mozzoli M.** FFA cause hepatic insulin resistance by inhibiting insulin suppression of glycogenolysis. *Am J Physiol Endocrinol Metab* 283: E12-19, 2002.
26. **Boden G, Jadali F, White J, Liang Y, Mozzoli M, Chen X, Coleman E, and Smith C.** Effects of fat on insulin-stimulated carbohydrate metabolism in normal men. *J Clin Invest* 88: 960-966, 1991.
27. **Boden G, Lebed B, Schatz M, Homko C, and Lemieux S.** Effects of acute changes of plasma free fatty acids on intramyocellular fat content and insulin resistance in healthy subjects. *Diabetes* 50: 1612-1617, 2001.
28. **Boden G, She P, Mozzoli M, Cheung P, Gumireddy K, Reddy P, Xiang X, Luo Z, and Ruderman N.** Free fatty acids produce insulin resistance and activate the proinflammatory nuclear factor-kappaB pathway in rat liver. *Diabetes* 54: 3458-3465, 2005.
29. **Boss O, Bachman E, Vidal-Puig A, Zhang CY, Peroni O, and Lowell BB.** Role of the beta(3)-adrenergic receptor and/or a putative beta(4)-adrenergic receptor on the expression of uncoupling proteins and peroxisome proliferator-activated receptor-gamma coactivator-1. *Biochem Biophys Res Commun* 261: 870-876, 1999.
30. **Bouscarel B, Gettys TW, Fromm H, and Dubner H.** Ursodeoxycholic acid inhibits glucagon-induced cAMP formation in hamster hepatocytes: a role for PKC. *Am J Physiol* 268: G300-310, 1995.
31. **Bouzakri K, Roques M, Gual P, Espinosa S, Guebre-Egziabher F, Riou JP, Laville M, Le Marchand-Brustel Y, Tanti JF, and Vidal H.** Reduced activation of phosphatidylinositol-3 kinase and increased serine 636 phosphorylation of insulin

receptor substrate-1 in primary culture of skeletal muscle cells from patients with type 2 diabetes. *Diabetes* 52: 1319-1325, 2003.
32. **Bray GA, Nielsen SJ, and Popkin BM.** Consumption of high-fructose corn syrup in beverages may play a role in the epidemic of obesity. *Am J Clin Nutr* 79: 537-543, 2004.
33. **Brissova M, Fowler MJ, Nicholson WE, Chu A, Hirshberg B, Harlan DM, and Powers AC.** Assessment of human pancreatic islet architecture and composition by laser scanning confocal microscopy. *J Histochem Cytochem* 53: 1087-1097, 2005.
34. **Bruning JC, Michael MD, Winnay JN, Hayashi T, Horsch D, Accili D, Goodyear LJ, and Kahn CR.** A muscle-specific insulin receptor knockout exhibits features of the metabolic syndrome of NIDDM without altering glucose tolerance. *Mol Cell* 2: 559-569, 1998.
35. **Cai D, Dhe-Paganon S, Melendez PA, Lee J, and Shoelson SE.** Two new substrates in insulin signaling, IRS5/DOK4 and IRS6/DOK5. *J Biol Chem* 278: 25323-25330, 2003.
36. **Cai D, Yuan M, Frantz DF, Melendez PA, Hansen L, Lee J, and Shoelson SE.** Local and systemic insulin resistance resulting from hepatic activation of IKK-beta and NF-kappaB. *Nat Med* 11: 183-190, 2005.
37. **Calera MR, Martinez C, Liu H, Jack AK, Birnbaum MJ, and Pilch PF.** Insulin increases the association of Akt-2 with Glut4-containing vesicles. *J Biol Chem* 273: 7201-7204, 1998.
38. **Canas X, Fernandez-Lopez JA, Ardevol A, Adan C, Esteve M, Rafecas I, Remesar X, and Alemany M.** Rat insulin turnover in vivo. *Endocrinology* 136: 3871-3876, 1995.
39. **Carpentier JL.** Insulin receptor internalization: molecular mechanisms and physiopathological implications. *Diabetologia* 37 Suppl 2: S117-124, 1994.
40. **Castillo MJ, Scheen AJ, Letiexhe MR, and Lefebvre PJ.** How to measure insulin clearance. *Diabetes Metab Rev* 10: 119-150, 1994.
41. **Cersosimo E, Judd RL, and Miles JM.** Insulin regulation of renal glucose metabolism in conscious dogs. *J Clin Invest* 93: 2584-2589, 1994.
42. **Chalkley SM, Hettiarachchi M, Chisholm DJ, and Kraegen EW.** Five-hour fatty acid elevation increases muscle lipids and impairs glycogen synthesis in the rat. *Metabolism* 47: 1121-1126, 1998.
43. **Charlton M, Sreekumar R, Rasmussen D, Lindor K, and Nair KS.** Apolipoprotein synthesis in nonalcoholic steatohepatitis. *Hepatology* 35: 898-904, 2002.
44. **Chen X, Iqbal N, and Boden G.** The effects of free fatty acids on gluconeogenesis and glycogenolysis in normal subjects. *J Clin Invest* 103: 365-372, 1999.
45. **Cherrington AD, Chiasson JL, Liljenquist JE, Lacy WW, and Park CR.** Control of hepatic glucose output by glucagon and insulin in the intact dog. *Biochem Soc Symp*: 31-45, 1978.
46. **Cherrington AD, Fuchs H, Stevenson RW, Williams PE, Alberti KG, and Steiner KE.** Effect of epinephrine on glycogenolysis and gluconeogenesis in conscious overnight-fasted dogs. *Am J Physiol* 247: E137-144, 1984.

47. **Cherrington AD, Sindelar D, Edgerton D, Steiner K, and McGuinness OP.** Physiological consequences of phasic insulin release in the normal animal. *Diabetes* 51 Suppl 1: S103-108, 2002.
48. **Cherrington AD, Williams PE, Shulman GI, and Lacy WW.** Differential time course of glucagon's effect on glycogenolysis and gluconeogenesis in the conscious dog. *Diabetes* 30: 180-187, 1981.
49. **Chhibber VL, Soriano C, and Tayek JA.** Effects of low-dose and high-dose glucagon on glucose production and gluconeogenesis in humans. *Metabolism* 49: 39-46, 2000.
50. **Cho H, Mu J, Kim JK, Thorvaldsen JL, Chu Q, Crenshaw EB, 3rd, Kaestner KH, Bartolomei MS, Shulman GI, and Birnbaum MJ.** Insulin resistance and a diabetes mellitus-like syndrome in mice lacking the protein kinase Akt2 (PKB beta). *Science* 292: 1728-1731, 2001.
51. **Cho H, Thorvaldsen JL, Chu Q, Feng F, and Birnbaum MJ.** Akt1/PKBalpha is required for normal growth but dispensable for maintenance of glucose homeostasis in mice. *J Biol Chem* 276: 38349-38352, 2001.
52. **Choi CS, Lee FN, and Youn JH.** Free fatty acids induce peripheral insulin resistance without increasing muscle hexosamine pathway product levels in rats. *Diabetes* 50: 418-424, 2001.
53. **Chu CA, Galassetti P, Igawa K, Sindelar DK, Neal DW, Burish M, and Cherrington AD.** Interaction of free fatty acids and epinephrine in regulating hepatic glucose production in conscious dogs. *Am J Physiol Endocrinol Metab* 284: E291-301, 2003.
54. **Chu CA, Sherck SM, Igawa K, Sindelar DK, Neal DW, Emshwiller M, and Cherrington AD.** Effects of free fatty acids on hepatic glycogenolysis and gluconeogenesis in conscious dogs. *Am J Physiol Endocrinol Metab* 282: E402-411, 2002.
55. **Chu CA, Sindelar DK, Igawa K, Sherck S, Neal DW, Emshwiller M, and Cherrington AD.** The direct effects of catecholamines on hepatic glucose production occur via alpha(1)- and beta(2)-receptors in the dog. *Am J Physiol Endocrinol Metab* 279: E463-473, 2000.
56. **Chu CA, Sindelar DK, Neal DW, Allen EJ, Donahue EP, and Cherrington AD.** Comparison of the direct and indirect effects of epinephrine on hepatic glucose production. *J Clin Invest* 99: 1044-1056, 1997.
57. **Chu CA, Sindelar DK, Neal DW, and Cherrington AD.** Direct effects of catecholamines on hepatic glucose production in conscious dog are due to glycogenolysis. *Am J Physiol* 271: E127-137, 1996.
58. **Chu CA, Sindelar DK, Neal DW, and Cherrington AD.** Portal adrenergic blockade does not inhibit the gluconeogenic effects of circulating catecholamines on the liver. *Metabolism* 46: 458-465, 1997.
59. **Clore JN, Glickman PS, Nestler JE, and Blackard WG.** In vivo evidence for hepatic autoregulation during FFA-stimulated gluconeogenesis in normal humans. *Am J Physiol* 261: E425-429, 1991.
60. **Clore JN, Stillman JS, Li J, O'Keefe SJ, and Levy JR.** Differential effect of saturated and polyunsaturated fatty acids on hepatic glucose metabolism in humans. *Am J Physiol Endocrinol Metab* 287: E358-365, 2004.

61. **Clutter WE, Bier DM, Shah SD, and Cryer PE.** Epinephrine plasma metabolic clearance rates and physiologic thresholds for metabolic and hemodynamic actions in man. *J Clin Invest* 66: 94-101, 1980.
62. **Cobelli C, Mari A, and Ferrannini E.** Non-steady state: error analysis of Steele's model and developments for glucose kinetics. *Am J Physiol* 252: E679-689, 1987.
63. **Coon PJ, Rogus EM, Drinkwater D, Muller DC, and Goldberg AP.** Role of body fat distribution in the decline in insulin sensitivity and glucose tolerance with age. *J Clin Endocrinol Metab* 75: 1125-1132, 1992.
64. **Cortez-Pinto H, Zhi Lin H, Qi Yang S, Odwin Da Costa S, and Diehl AM.** Lipids up-regulate uncoupling protein 2 expression in rat hepatocytes. *Gastroenterology* 116: 1184-1193, 1999.
65. **Cowan JS and Hetenyi G, Jr.** Glucoregulatory responses in normal and diabetic dogs recorded by a new tracer method. *Metabolism* 20: 360-372, 1971.
66. **Craik JD and Elliott KR.** Kinetics of 3-O-methyl-D-glucose transport in isolated rat hepatocytes. *Biochem J* 182: 503-508, 1979.
67. **Crespin SR, Greenough WB, 3rd, and Steinberg D.** Stimulation of insulin secretion by long-chain free fatty acids. A direct pancreatic effect. *J Clin Invest* 52: 1979-1984, 1973.
68. **Darville MI and Eizirik DL.** Regulation by cytokines of the inducible nitric oxide synthase promoter in insulin-producing cells. *Diabetologia* 41: 1101-1108, 1998.
69. **Davis MA, Williams PE, and Cherrington AD.** Effect of a mixed meal on hepatic lactate and gluconeogenic precursor metabolism in dogs. *Am J Physiol* 247: E362-369, 1984.
70. **Davis SN, Dunham B, Walmsley K, Shavers C, Neal D, Williams P, and Cherrington AD.** Brain of the conscious dog is sensitive to physiological changes in circulating insulin. *Am J Physiol* 272: E567-575, 1997.
71. **Debodo RC, Steele R, Altszuler N, Dunn A, and Bishop JS.** On the Hormonal Regulation of Carbohydrate Metabolism; Studies with C14 Glucose. *Recent Prog Horm Res* 19: 445-488, 1963.
72. **Deibert DC and DeFronzo RA.** Epinephrine-induced insulin resistance in man. *J Clin Invest* 65: 717-721, 1980.
73. **Dickens M, Svitek CA, Culbert AA, O'Brien RM, and Tavare JM.** Central role for phosphatidylinositide 3-kinase in the repression of glucose-6-phosphatase gene transcription by insulin. *J Biol Chem* 273: 20144-20149, 1998.
74. **DiGirolamo M, Newby FD, and Lovejoy J.** Lactate production in adipose tissue: a regulated function with extra-adipose implications. *Faseb J* 6: 2405-2412, 1992.
75. **Dinneen S, Alzaid A, Turk D, and Rizza R.** Failure of glucagon suppression contributes to postprandial hyperglycaemia in IDDM. *Diabetologia* 38: 337-343, 1995.
76. **Diraison F, Moulin P, and Beylot M.** Contribution of hepatic de novo lipogenesis and reesterification of plasma non esterified fatty acids to plasma triglyceride synthesis during non-alcoholic fatty liver disease. *Diabetes Metab* 29: 478-485, 2003.
77. **Dobbins RL, Davis SN, Neal D, Caumo A, Cobelli C, and Cherrington AD.** Rates of glucagon activation and deactivation of hepatic glucose production in conscious dogs. *Metabolism* 47: 135-142, 1998.

78. **Dobbins RL, Davis SN, Neal DW, Cobelli C, and Cherrington AD.** Pulsatility does not alter the response to a physiological increment in glucagon in the conscious dog. *Am J Physiol* 266: E467-478, 1994.
79. **Donnelly KL, Smith CI, Schwarzenberg SJ, Jessurun J, Boldt MD, and Parks EJ.** Sources of fatty acids stored in liver and secreted via lipoproteins in patients with nonalcoholic fatty liver disease. *J Clin Invest* 115: 1343-1351, 2005.
80. **Dresner A, Laurent D, Marcucci M, Griffin ME, Dufour S, Cline GW, Slezak LA, Andersen DK, Hundal RS, Rothman DL, Petersen KF, and Shulman GI.** Effects of free fatty acids on glucose transport and IRS-1-associated phosphatidylinositol 3-kinase activity. *J Clin Invest* 103: 253-259, 1999.
81. **Du K, Herzig S, Kulkarni RN, and Montminy M.** TRB3: a tribbles homolog that inhibits Akt/PKB activation by insulin in liver. *Science* 300: 1574-1577, 2003.
82. **Duckworth WC, Hamel FG, and Peavy DE.** Hepatic metabolism of insulin. *Am J Med* 85: 71-76, 1988.
83. **Edgerton DS, Cardin S, Emshwiller M, Neal D, Chandramouli V, Schumann WC, Landau BR, Rossetti L, and Cherrington AD.** Small increases in insulin inhibit hepatic glucose production solely caused by an effect on glycogen metabolism. *Diabetes* 50: 1872-1882, 2001.
84. **Edgerton DS, Cardin S, Neal D, Farmer B, Lautz M, Pan C, and Cherrington AD.** Effects of hyperglycemia on hepatic gluconeogenic flux during glycogen phosphorylase inhibition in the conscious dog. *Am J Physiol Endocrinol Metab* 286: E510-522, 2004.
85. **Edgerton DS, Cardin S, Pan C, Neal D, Farmer B, Converse M, and Cherrington AD.** Effects of insulin deficiency or excess on hepatic gluconeogenic flux during glycogenolytic inhibition in the conscious dog. *Diabetes* 51: 3151-3162, 2002.
86. **Edgerton DS, Lautz M, Scott M, Everett CA, Stettler KM, Neal DW, Chu CA, and Cherrington AD.** Insulin's direct effects on the liver dominate the control of hepatic glucose production. *J Clin Invest* 116: 521-527, 2006.
87. **Eitel K, Staiger H, Rieger J, Mischak H, Brandhorst H, Brendel MD, Bretzel RG, Haring HU, and Kellerer M.** Protein kinase C delta activation and translocation to the nucleus are required for fatty acid-induced apoptosis of insulin-secreting cells. *Diabetes* 52: 991-997, 2003.
88. **Ekberg K, Landau BR, Wajngot A, Chandramouli V, Efendic S, Brunengraber H, and Wahren J.** Contributions by kidney and liver to glucose production in the postabsorptive state and after 60 h of fasting. *Diabetes* 48: 292-298, 1999.
89. **Elchebly M, Payette P, Michaliszyn E, Cromlish W, Collins S, Loy AL, Normandin D, Cheng A, Himms-Hagen J, Chan CC, Ramachandran C, Gresser MJ, Tremblay ML, and Kennedy BP.** Increased insulin sensitivity and obesity resistance in mice lacking the protein tyrosine phosphatase-1B gene. *Science* 283: 1544-1548, 1999.
90. **Ensick JW.** Immunoassays for glucagon. In: *Handbook of Experimental Pharmacology*,, 1983, p. 203-221.
91. **Exton JH.** Mechanisms of hormonal regulation of hepatic glucose metabolism. *Diabetes Metab Rev* 3: 163-183, 1987.

92. **Exton JH, Corbin JG, and Park CR.** Control of gluconeogenesis in liver. IV. Differential effects of fatty acids and glucagon on ketogenesis and gluconeogenesis in the perfused rat liver. *J Biol Chem* 244: 4095-4102, 1969.
93. **Fantin VR, Sparling JD, Slot JW, Keller SR, Lienhard GE, and Lavan BE.** Characterization of insulin receptor substrate 4 in human embryonic kidney 293 cells. *J Biol Chem* 273: 10726-10732, 1998.
94. **Farese RV.** Function and dysfunction of aPKC isoforms for glucose transport in insulin-sensitive and insulin-resistant states. *Am J Physiol Endocrinol Metab* 283: E1-11, 2002.
95. **Farese RV, Sajan MP, and Standaert ML.** Atypical protein kinase C in insulin action and insulin resistance. *Biochem Soc Trans* 33: 350-353, 2005.
96. **Felber JP and Vannotti A.** Effects of Fat Infusion on Glucose Tolerance and Insulin Plasma Levels. *Med Exp Int J Exp Med* 10: 153-156, 1964.
97. **Feliu JE, Hue L, and Hers HG.** Hormonal control of pyruvate kinase activity and of gluconeogenesis in isolated hepatocytes. *Proc Natl Acad Sci U S A* 73: 2762-2766, 1976.
98. **Ferrannini E, Barrett EJ, Bevilacqua S, and DeFronzo RA.** Effect of fatty acids on glucose production and utilization in man. *J Clin Invest* 72: 1737-1747, 1983.
99. **Fisher SJ and Kahn CR.** Insulin signaling is required for insulin's direct and indirect action on hepatic glucose production. *J Clin Invest* 111: 463-468, 2003.
100. **Folch J, Lees M, and Sloane Stanley GH.** A simple method for the isolation and purification of total lipides from animal tissues. *J Biol Chem* 226: 497-509, 1957.
101. **Foster LB and Dunn RT.** Single-antibody technique for radioimmunoassay of cortisol in unextracted serum or plasma. *Clin Chem* 20: 365-368, 1974.
102. **Gao T, Furnari F, and Newton AC.** PHLPP: a phosphatase that directly dephosphorylates Akt, promotes apoptosis, and suppresses tumor growth. *Mol Cell* 18: 13-24, 2005.
103. **Gao Z, Hwang D, Bataille F, Lefevre M, York D, Quon MJ, and Ye J.** Serine phosphorylation of insulin receptor substrate 1 by inhibitor kappa B kinase complex. *J Biol Chem* 277: 48115-48121, 2002.
104. **Gao Z, Zhang X, Zuberi A, Hwang D, Quon MJ, Lefevre M, and Ye J.** Inhibition of insulin sensitivity by free fatty acids requires activation of multiple serine kinases in 3T3-L1 adipocytes. *Mol Endocrinol* 18: 2024-2034, 2004.
105. **Gastaldelli A, Miyazaki Y, Pettiti M, Matsuda M, Mahankali S, Santini E, DeFronzo RA, and Ferrannini E.** Metabolic effects of visceral fat accumulation in type 2 diabetes. *J Clin Endocrinol Metab* 87: 5098-5103, 2002.
106. **Gastaldelli A, Toschi E, Pettiti M, Frascerra S, Quinones-Galvan A, Sironi AM, Natali A, and Ferrannini E.** Effect of physiological hyperinsulinemia on gluconeogenesis in nondiabetic subjects and in type 2 diabetic patients. *Diabetes* 50: 1807-1812, 2001.
107. **Gerich JE.** Control of glycaemia. *Baillieres Clin Endocrinol Metab* 7: 551-586, 1993.
108. **Giacca A, Fisher SJ, McCall RH, Shi ZQ, and Vranic M.** Direct and indirect effects of insulin in suppressing glucose production in depancreatized dogs: role of glucagon. *Endocrinology* 138: 999-1007, 1997.

109. **Giacca A, Fisher SJ, Shi ZQ, Gupta R, Lickley HL, and Vranic M.** Importance of peripheral insulin levels for insulin-induced suppression of glucose production in depancreatized dogs. *J Clin Invest* 90: 1769-1777, 1992.
110. **Gin H and Rigalleau V.** Post-prandial hyperglycemia. post-prandial hyperglycemia and diabetes. *Diabetes Metab* 26: 265-272, 2000.
111. **Goberna R, Tamarit J, Jr., Osorio J, Fussganger R, Tamarit J, and Pfeiffer EF.** Action of B-hydroxy butyrate, acetoacetate and palmitate on the insulin release in the perfused isolated rat pancreas. *Horm Metab Res* 6: 256-260, 1974.
112. **Goldstein DS, Feuerstein G, Izzo JL, Jr., Kopin IJ, and Keiser HR.** Validity and reliability of liquid chromatography with electrochemical detection for measuring plasma levels of norepinephrine and epinephrine in man. *Life Sci* 28: 467-475, 1981.
113. **Goresky CA, Bach GG, and Nadeau BE.** Red cell carriage of label: its limiting effect on the exchange of materials in the liver. *Circ Res* 36: 328-351, 1975.
114. **Granner DK, Petersen DD, Koch SR, Sasaki K, and Beale EG.** Multihormonal control of phosphoenolpyruvate carboxykinase gene transcription: the dominant role of insulin. *Trans Assoc Am Physicians* 97: 33-40, 1984.
115. **Griffin ME, Marcucci MJ, Cline GW, Bell K, Barucci N, Lee D, Goodyear LJ, Kraegen EW, White MF, and Shulman GI.** Free fatty acid-induced insulin resistance is associated with activation of protein kinase C theta and alterations in the insulin signaling cascade. *Diabetes* 48: 1270-1274, 1999.
116. **Gustavson SM, Chu CA, Nishizawa M, Farmer B, Neal D, Yang Y, Donahue EP, Flakoll P, and Cherrington AD.** Interaction of glucagon and epinephrine in the control of hepatic glucose production in the conscious dog. *Am J Physiol Endocrinol Metab* 284: E695-707, 2003.
117. **Gustavson SM, Chu CA, Nishizawa M, Farmer B, Neal D, Yang Y, Vaughan S, Donahue EP, Flakoll P, and Cherrington AD.** Glucagon's actions are modified by the combination of epinephrine and gluconeogenic precursor infusion. *Am J Physiol Endocrinol Metab* 285: E534-544, 2003.
118. **Gustavson SM, Chu CA, Nishizawa M, Neal D, Farmer B, Yang Y, Donahue EP, Flakoll P, and Cherrington AD.** Effects of hyperglycemia, glucagon, and epinephrine on renal glucose release in the conscious dog. *Metabolism* 53: 933-941, 2004.
119. **Hallfrisch J.** Metabolic effects of dietary fructose. *Faseb J* 4: 2652-2660, 1990.
120. **Hamel FG, Upward JL, and Bennett RG.** In vitro inhibition of insulin-degrading enzyme by long-chain fatty acids and their coenzyme A thioesters. *Endocrinology* 144: 2404-2408, 2003.
121. **Hamilton KS, Gibbons FK, Bracy DP, Lacy DB, Cherrington AD, and Wasserman DH.** Effect of prior exercise on the partitioning of an intestinal glucose load between splanchnic bed and skeletal muscle. *J Clin Invest* 98: 125-135, 1996.
122. **Harrington LS, Findlay GM, Gray A, Tolkacheva T, Wigfield S, Rebholz H, Barnett J, Leslie NR, Cheng S, Shepherd PR, Gout I, Downes CP, and Lamb RF.** The TSC1-2 tumor suppressor controls insulin-PI3K signaling via regulation of IRS proteins. *J Cell Biol* 166: 213-223, 2004.
123. **Hawkins M, Barzilai N, Liu R, Hu M, Chen W, and Rossetti L.** Role of the glucosamine pathway in fat-induced insulin resistance. *J Clin Invest* 99: 2173-2182, 1997.

124. **He J, Watkins S, and Kelley DE.** Skeletal muscle lipid content and oxidative enzyme activity in relation to muscle fiber type in type 2 diabetes and obesity. *Diabetes* 50: 817-823, 2001.
125. **Hendrick GK.** *Dissertation*. Nashville: Vanderbilt University, 1986.
126. **Hernandez-Sotomayor SM, Macias-Silva M, Malbon CC, and Garcia-Sainz JA.** Modulation of Gs activity by phorbol myristate acetate in rat hepatocytes. *Am J Physiol* 260: C259-265, 1991.
127. **Hieble JP, Bondinell WE, and Ruffolo RR, Jr.** Alpha- and beta-adrenoceptors: from the gene to the clinic. 1. Molecular biology and adrenoceptor subclassification. *J Med Chem* 38: 3415-3444, 1995.
128. **Hirosumi J, Tuncman G, Chang L, Gorgun CZ, Uysal KT, Maeda K, Karin M, and Hotamisligil GS.** A central role for JNK in obesity and insulin resistance. *Nature* 420: 333-336, 2002.
129. **Hornbuckle LA, Everett CA, Martin CC, Gustavson SS, Svitek CA, Oeser JK, Neal DW, Cherrington AD, and O'Brien RM.** Selective stimulation of G-6-Pase catalytic subunit but not G-6-P transporter gene expression by glucagon in vivo and cAMP in situ. *Am J Physiol Endocrinol Metab* 286: E795-808, 2004.
130. **Horton JD, Shah NA, Warrington JA, Anderson NN, Park SW, Brown MS, and Goldstein JL.** Combined analysis of oligonucleotide microarray data from transgenic and knockout mice identifies direct SREBP target genes. *Proc Natl Acad Sci U S A* 100: 12027-12032, 2003.
131. **Hsieh PS, Moore MC, Neal DW, and Cherrington AD.** Hepatic glucose uptake rapidly decreases after removal of the portal signal in conscious dogs. *Am J Physiol* 275: E987-992., 1998.
132. **Hue L, Maisin L, and Rider MH.** Palmitate inhibits liver glycolysis. Involvement of fructose 2,6-bisphosphate in the glucose/fatty acid cycle. *Biochem J* 251: 541-545, 1988.
133. **Hung JH, Su IJ, Lei HY, Wang HC, Lin WC, Chang WT, Huang W, Chang WC, Chang YS, Chen CC, and Lai MD.** Endoplasmic reticulum stress stimulates the expression of cyclooxygenase-2 through activation of NF-kappaB and pp38 mitogen-activated protein kinase. *J Biol Chem* 279: 46384-46392, 2004.
134. **Imazu M, Strickland WG, Chrisman TD, and Exton JH.** Phosphorylation and inactivation of liver glycogen synthase by liver protein kinases. *J Biol Chem* 259: 1813-1821, 1984.
135. **Imazu M, Strickland WG, and Exton JH.** Multiple phosphorylation of rat-liver glycogen synthase by protein kinases. *Biochim Biophys Acta* 789: 285-293, 1984.
136. **Inoue G, Cheatham B, Emkey R, and Kahn CR.** Dynamics of insulin signaling in 3T3-L1 adipocytes. Differential compartmentalization and trafficking of insulin receptor substrate (IRS)-1 and IRS-2. *J Biol Chem* 273: 11548-11555, 1998.
137. **Itani SI, Ruderman NB, Schmieder F, and Boden G.** Lipid-induced insulin resistance in human muscle is associated with changes in diacylglycerol, protein kinase C, and IkappaB-alpha. *Diabetes* 51: 2005-2011, 2002.
138. **Jefferson LS, Exton JH, Butcher RW, Sutherland EW, and Park CR.** Role of adenosine 3',5'-monophosphate in the effects of insulin and anti-insulin serum on liver metabolism. *J Biol Chem* 243: 1031-1038, 1968.

139. **Jerusalem F, Engel AG, and Peterson HA.** Human muscle fiber fine structure: morphometric data on controls. *Neurology* 25: 127-134, 1975.
140. **Jiang G and Zhang BB.** Glucagon and regulation of glucose metabolism. *Am J Physiol Endocrinol Metab* 284: E671-678, 2003.
141. **Johnston P, Hollenbeck C, Sheu W, Chen YD, and Reaven GM.** Acute changes in plasma non-esterified fatty acid concentration do not change hepatic glucose production in people with type 2 diabetes. *Diabet Med* 7: 871-875, 1990.
142. **Jungermann K and Katz N.** Functional specialization of different hepatocyte populations. *Physiol Rev* 69: 708-764, 1989.
143. **Kaiyala KJ, Prigeon RL, Kahn SE, Woods SC, Porte D, Jr., and Schwartz MW.** Reduced beta-cell function contributes to impaired glucose tolerance in dogs made obese by high-fat feeding. *Am J Physiol* 277: E659-667, 1999.
144. **Kawai Y, Powell A, and Arinze IJ.** Adrenergic receptors in human liver plasma membranes: predominance of beta 2- and alpha 1-receptor subtypes. *J Clin Endocrinol Metab* 62: 827-832, 1986.
145. **Kelley DE, He J, Menshikova EV, and Ritov VB.** Dysfunction of mitochondria in human skeletal muscle in type 2 diabetes. *Diabetes* 51: 2944-2950, 2002.
146. **Kelley DE, Mokan M, Simoneau JA, and Mandarino LJ.** Interaction between glucose and free fatty acid metabolism in human skeletal muscle. *J Clin Invest* 92: 91-98, 1993.
147. **Kelpe CL, Johnson LM, and Poitout V.** Increasing triglyceride synthesis inhibits glucose-induced insulin secretion in isolated rat islets of langerhans: a study using adenoviral expression of diacylglycerol acyltransferase. *Endocrinology* 143: 3326-3332, 2002.
148. **Kharroubi I, Ladriere L, Cardozo AK, Dogusan Z, Cnop M, and Eizirik DL.** Free fatty acids and cytokines induce pancreatic beta-cell apoptosis by different mechanisms: role of nuclear factor-kappaB and endoplasmic reticulum stress. *Endocrinology* 145: 5087-5096, 2004.
149. **Kim JK, Fillmore JJ, Sunshine MJ, Albrecht B, Higashimori T, Kim DW, Liu ZX, Soos TJ, Cline GW, O'Brien WR, Littman DR, and Shulman GI.** PKC-theta knockout mice are protected from fat-induced insulin resistance. *J Clin Invest* 114: 823-827, 2004.
150. **Kim JK, Kim YJ, Fillmore JJ, Chen Y, Moore I, Lee J, Yuan M, Li ZW, Karin M, Perret P, Shoelson SE, and Shulman GI.** Prevention of fat-induced insulin resistance by salicylate. *J Clin Invest* 108: 437-446, 2001.
151. **Kok N, Roberfroid M, and Delzenne N.** Dietary oligofructose modifies the impact of fructose on hepatic triacylglycerol metabolism. *Metabolism* 45: 1547-1550, 1996.
152. **Koyama K, Chen G, Lee Y, and Unger RH.** Tissue triglycerides, insulin resistance, and insulin production: implications for hyperinsulinemia of obesity. *Am J Physiol* 273: E708-713, 1997.
153. **Kraus-Friedmann N.** Effects of glucagon and vasopressin on hepatic Ca2+ release. *Proc Natl Acad Sci U S A* 83: 8943-8946, 1986.
154. **Kraus-Friedmann N and Feng L.** The role of intracellular Ca2+ in the regulation of gluconeogenesis. *Metabolism* 45: 389-403, 1996.

155. **Kubota N, Terauchi Y, Tobe K, Yano W, Suzuki R, Ueki K, Takamoto I, Satoh H, Maki T, Kubota T, Moroi M, Okada-Iwabu M, Ezaki O, Nagai R, Ueta Y, Kadowaki T, and Noda T.** Insulin receptor substrate 2 plays a crucial role in beta cells and the hypothalamus. *J Clin Invest* 114: 917-927, 2004.
156. **Lam TK, Yoshii H, Haber CA, Bogdanovic E, Lam L, Fantus IG, and Giacca A.** Free fatty acid-induced hepatic insulin resistance: a potential role for protein kinase C-delta. *Am J Physiol Endocrinol Metab* 283: E682-691, 2002.
157. **Lavan BE, Lane WS, and Lienhard GE.** The 60-kDa phosphotyrosine protein in insulin-treated adipocytes is a new member of the insulin receptor substrate family. *J Biol Chem* 272: 11439-11443, 1997.
158. **Lee KU, Park JY, Kim CH, Hong SK, Suh KI, Park KS, and Park SW.** Effect of decreasing plasma free fatty acids by acipimox on hepatic glucose metabolism in normal rats. *Metabolism* 45: 1408-1414, 1996.
159. **Leevy CM, Mendenhall CL, Lesko W, and Howard MM.** Estimation of hepatic blood flow with indocyanine green. *J Clin Invest* 41: 1169-1179, 1962.
160. **Lefkowitz RJ.** Heterogeneity of adenylate cyclase-coupled beta-adrenergic receptors. *Biochem Pharmacol* 24: 583-590, 1975.
161. **Lewis GF, Vranic M, and Giacca A.** Glucagon enhances the direct suppressive effect of insulin on hepatic glucose production in humans. *Am J Physiol* 272: E371-378, 1997.
162. **Lewis GF, Zinman B, Groenewoud Y, Vranic M, and Giacca A.** Hepatic glucose production is regulated both by direct hepatic and extrahepatic effects of insulin in humans. *Diabetes* 45: 454-462, 1996.
163. **Lillioja S, Mott DM, Spraul M, Ferraro R, Foley JE, Ravussin E, Knowler WC, Bennett PH, and Bogardus C.** Insulin resistance and insulin secretory dysfunction as precursors of non-insulin-dependent diabetes mellitus. Prospective studies of Pima Indians. *N Engl J Med* 329: 1988-1992, 1993.
164. **Liu MS and Ghosh S.** Changes in beta-adrenergic receptors in dog livers during endotoxic shock. *Am J Physiol* 244: R718-723, 1983.
165. **Lloyd B, Burrin J, Smythe P, Alberti KG, and Fingerhut B.** Enzymic fluorometric continuous-flow assays for blood glucose, lactate, pyruvate, alanine, glycerol, and 3-hydroxybutyrate. *Clinical Chemistry* 24: 1724-1729, 1978.
166. **Lombardo YB, Hron WT, and Menahan LA.** Effect of insulin in vitro on the isolated, perfused alloxan-diabetic rat liver. *Diabetologia* 14: 47-51, 1978.
167. **Luo J, Field SJ, Lee JY, Engelman JA, and Cantley LC.** The p85 regulatory subunit of phosphoinositide 3-kinase down-regulates IRS-1 signaling via the formation of a sequestration complex. *J Cell Biol* 170: 455-464, 2005.
168. **Lupi R, Dotta F, Marselli L, Del Guerra S, Masini M, Santangelo C, Patane G, Boggi U, Piro S, Anello M, Bergamini E, Mosca F, Di Mario U, Del Prato S, and Marchetti P.** Prolonged exposure to free fatty acids has cytostatic and pro-apoptotic effects on human pancreatic islets: evidence that beta-cell death is caspase mediated, partially dependent on ceramide pathway, and Bcl-2 regulated. *Diabetes* 51: 1437-1442, 2002.
169. **Magnusson I, Rothman DL, Gerard DP, Katz LD, and Shulman GI.** Contribution of hepatic glycogenolysis to glucose production in humans in response to a physiological increase in plasma glucagon concentration. *Diabetes* 44: 185-189, 1995.

170. **Malmstrom R, Packard CJ, Caslake M, Bedford D, Stewart P, Shepherd J, and Taskinen MR.** Effect of heparin-stimulated plasma lipolytic activity on VLDL APO B subclass metabolism in normal subjects. *Atherosclerosis* 146: 381-390, 1999.
171. **Mari A.** Estimation of the rate of appearance in the non-steady state with a two-compartment model. *Am J Physiol* 263: E400-415, 1992.
172. **Matschinsky FM.** Banting Lecture 1995. A lesson in metabolic regulation inspired by the glucokinase glucose sensor paradigm. *Diabetes* 45: 223-241, 1996.
173. **Mayerson AB, Hundal RS, Dufour S, Lebon V, Befroy D, Cline GW, Enocksson S, Inzucchi SE, Shulman GI, and Petersen KF.** The effects of rosiglitazone on insulin sensitivity, lipolysis, and hepatic and skeletal muscle triglyceride content in patients with type 2 diabetes. *Diabetes* 51: 797-802, 2002.
174. **McGarry JD, Mannaerts GP, and Foster DW.** A possible role for malonyl-CoA in the regulation of hepatic fatty acid oxidation and ketogenesis. *J Clin Invest* 60: 265-270, 1977.
175. **McGuinness OP, Burgin K, Moran C, Bracy D, and Cherrington AD.** Role of glucagon in the metabolic response to stress hormone infusion in the conscious dog. *Am J Physiol* 266: E438-447, 1994.
176. **McGuinness OP, Fugiwara T, Murrell S, Bracy D, Neal D, O'Connor D, and Cherrington AD.** Impact of chronic stress hormone infusion on hepatic carbohydrate metabolism in the conscious dog. *Am J Physiol* 265: E314-322, 1993.
177. **Miles JM, Nissen SL, Gerich JE, and Haymond MW.** Effects of epinephrine infusion on leucine and alanine kinetics in humans. *Am J Physiol* 247: E166-172, 1984.
178. **Miller BS, Shankavaram UT, Horney MJ, Gore AC, Kurtz DT, and Rosenzweig SA.** Activation of cJun NH2-terminal kinase/stress-activated protein kinase by insulin. *Biochemistry* 35: 8769-8775, 1996.
179. **Mithieux G.** The new functions of the gut in the control of glucose homeostasis. *Curr Opin Clin Nutr Metab Care* 8: 445-449, 2005.
180. **Mithieux G, Bordeto JC, Minassian C, Ajzannay A, Mercier I, and Riou JP.** Characteristics and specificity of the inhibition of liver glucose-6-phosphatase by arachidonic acid. Lesser inhibitability of the enzyme of diabetic rats. *Eur J Biochem* 213: 461-466, 1993.
181. **Mithieux G and Zitoun C.** Mechanisms by which fatty-acyl-CoA esters inhibit or activate glucose-6-phosphatase in intact and detergent-treated rat liver microsomes. *Eur J Biochem* 235: 799-803, 1996.
182. **Moncany ML and Plas C.** Interaction of glucagon and epinephrine in the regulation of adenosine 3',5'-monophosphate-dependent glycogenolysis in the cultured fetal hepatocyte. *Endocrinology* 107: 1667-1675, 1980.
183. **Moore MC, Cherrington AD, and Wasserman DH.** Regulation of hepatic and peripheral glucose disposal. *Best Pract Res Clin Endocrinol Metab* 17: 343-364, 2003.
184. **Moore MC, Pagliassotti MJ, Swift LL, Asher J, Murrell J, Neal D, and Cherrington AD.** Disposition of a mixed meal by the conscious dog. *Am J Physiol* 266: E666-675, 1994.
185. **Moore MC, Satake S, Lautz M, Soleimanpour SA, Neal DW, Smith M, and Cherrington AD.** Nonesterified fatty acids and hepatic glucose metabolism in the conscious dog. *Diabetes* 53: 32-40, 2004.

186. **Morand C, Besson C, Demigne C, and Remesy C.** Importance of the modulation of glycolysis in the control of lactate metabolism by fatty acids in isolated hepatocytes from fed rats. *Arch Biochem Biophys* 309: 254-260, 1994.
187. **Morgan L.** Immunoassay of insulin: 2 antibody system. Plasma insulin of normal, subdiabetic, and diabetic rats. *Diabetes* 12: 115-126, 1963.
188. **Morrison WR and Smith LM.** Preparation of Fatty Acid Methyl Esters and Dimethylacetals from Lipids with Boron Fluoride--Methanol. *J Lipid Res* 5: 600-608, 1964.
189. **Myers SR, Diamond MP, Adkins-Marshall BA, Williams PE, Stinsen R, and Cherrington AD.** Effects of small changes in glucagon on glucose production during a euglycemic, hyperinsulinemic clamp. *Metabolism* 40: 66-71, 1991.
190. **Namikawa C, Shu-Ping Z, Vyselaar JR, Nozaki Y, Nemoto Y, Ono M, Akisawa N, Saibara T, Hiroi M, Enzan H, and Onishi S.** Polymorphisms of microsomal triglyceride transfer protein gene and manganese superoxide dismutase gene in non-alcoholic steatohepatitis. *J Hepatol* 40: 781-786, 2004.
191. **Narcisi TM, Shoulders CC, Chester SA, Read J, Brett DJ, Harrison GB, Grantham TT, Fox MF, Povey S, de Bruin TW, and et al.** Mutations of the microsomal triglyceride-transfer-protein gene in abetalipoproteinemia. *Am J Hum Genet* 57: 1298-1310, 1995.
192. **Nelson N.** A photometric adaptation of the Somogyi method for determination of glucose. *J Biol Chem* 153, 1944.
193. **Nemecz M, Preininger K, Englisch R, Furnsinn C, Schneider B, Waldhausl W, and Roden M.** Acute effect of leptin on hepatic glycogenolysis and gluconeogenesis in perfused rat liver. *Hepatology* 29: 166-172, 1999.
194. **Nguyen MT, Satoh H, Favelyukis S, Babendure JL, Imamura T, Sbodio JI, Zalevsky J, Dahiyat BI, Chi NW, and Olefsky JM.** JNK and tumor necrosis factor-alpha mediate free fatty acid-induced insulin resistance in 3T3-L1 adipocytes. *J Biol Chem* 280: 35361-35371, 2005.
195. **Oakes ND, Cooney GJ, Camilleri S, Chisholm DJ, and Kraegen EW.** Mechanisms of liver and muscle insulin resistance induced by chronic high-fat feeding. *Diabetes* 46: 1768-1774, 1997.
196. **Obici S, Feng Z, Karkanias G, Baskin DG, and Rossetti L.** Decreasing hypothalamic insulin receptors causes hyperphagia and insulin resistance in rats. *Nat Neurosci* 5: 566-572, 2002.
197. **Obici S, Zhang BB, Karkanias G, and Rossetti L.** Hypothalamic insulin signaling is required for inhibition of glucose production. *Nat Med* 8: 1376-1382, 2002.
198. **O'Doherty RM, Lehman DL, Telemaque-Potts S, and Newgard CB.** Metabolic impact of glucokinase overexpression in liver: lowering of blood glucose in fed rats is accompanied by hyperlipidemia. *Diabetes* 48: 2022-2027, 1999.
199. **Ogihara T, Shin BC, Anai M, Katagiri H, Inukai K, Funaki M, Fukushima Y, Ishihara H, Takata K, Kikuchi M, Yazaki Y, Oka Y, and Asano T.** Insulin receptor substrate (IRS)-2 is dephosphorylated more rapidly than IRS-1 via its association with phosphatidylinositol 3-kinase in skeletal muscle cells. *J Biol Chem* 272: 12868-12873, 1997.

200. **Ozcan U, Cao Q, Yilmaz E, Lee AH, Iwakoshi NN, Ozdelen E, Tuncman G, Gorgun C, Glimcher LH, and Hotamisligil GS.** Endoplasmic reticulum stress links obesity, insulin action, and type 2 diabetes. *Science* 306: 457-461, 2004.
201. **Pagliassotti MJ, Holste LC, Moore MC, Neal DW, and Cherrington AD.** Comparison of the time courses of insulin and the portal signal on hepatic glucose and glycogen metabolism in the conscious dog. *Journal of Clinical Investigation* 97: 81-91, 1996.
202. **Pan DA, Lillioja S, Kriketos AD, Milner MR, Baur LA, Bogardus C, Jenkins AB, and Storlien LH.** Skeletal muscle triglyceride levels are inversely related to insulin action. *Diabetes* 46: 983-988, 1997.
203. **Patti ME and Kahn CR.** The insulin receptor--a critical link in glucose homeostasis and insulin action. *J Basic Clin Physiol Pharmacol* 9: 89-109, 1998.
204. **Pelkonen R, Miettinen TA, Taskinen MR, and Nikkila EA.** Effect of acute elevation of plasma glycerol, triglyceride and FFA levels on glucose utilization and plasma insulin. *Diabetes* 17: 76-82, 1968.
205. **Perez-Carreras M, Del Hoyo P, Martin MA, Rubio JC, Martin A, Castellano G, Colina F, Arenas J, and Solis-Herruzo JA.** Defective hepatic mitochondrial respiratory chain in patients with nonalcoholic steatohepatitis. *Hepatology* 38: 999-1007, 2003.
206. **Pernalete N, Garcia JC, Betts CR, and Martin KJ.** Inhibitors of protein kinase-C modulate desensitization of the parathyroid hormone receptor-adenylate cyclase system in opossum kidney cells. *Endocrinology* 126: 407-413, 1990.
207. **Perseghin G, Ghosh S, Gerow K, and Shulman GI.** Metabolic defects in lean nondiabetic offspring of NIDDM parents: a cross-sectional study. *Diabetes* 46: 1001-1009, 1997.
208. **Perseghin G, Petersen K, and Shulman GI.** Cellular mechanism of insulin resistance: potential links with inflammation. *Int J Obes Relat Metab Disord* 27 Suppl 3: S6-11, 2003.
209. **Petersen KF, Befroy D, Dufour S, Dziura J, Ariyan C, Rothman DL, DiPietro L, Cline GW, and Shulman GI.** Mitochondrial dysfunction in the elderly: possible role in insulin resistance. *Science* 300: 1140-1142, 2003.
210. **Petersen KF, Dufour S, Befroy D, Garcia R, and Shulman GI.** Impaired mitochondrial activity in the insulin-resistant offspring of patients with type 2 diabetes. *N Engl J Med* 350: 664-671, 2004.
211. **Pilkis SJ, Claus TH, and el-Maghrabi MR.** The role of cyclic AMP in rapid and long-term regulation of gluconeogenesis and glycolysis. *Adv Second Messenger Phosphoprotein Res* 22: 175-191, 1988.
212. **Pilkis SJ and Granner DK.** Molecular physiology of the regulation of hepatic gluconeogenesis and glycolysis. *Annu Rev Physiol* 54: 885-909, 1992.
213. **Pocai A, Lam TK, Gutierrez-Juarez R, Obici S, Schwartz GJ, Bryan J, Aguilar-Bryan L, and Rossetti L.** Hypothalamic K(ATP) channels control hepatic glucose production. *Nature* 434: 1026-1031, 2005.
214. **Popkin BM.** The nutrition transition and its health implications in lower-income countries. *Public Health Nutr* 1: 5-21, 1998.
215. **Prager R, Wallace P, and Olefsky JM.** Direct and indirect effects of insulin to inhibit hepatic glucose output in obese subjects. *Diabetes* 36: 607-611, 1987.

216. **Price CP, Llyod B, and Alberti GM.** A kinetic spectrophotometric assay for rapid determination of acetoacetate in blood. *Clin Chem* 23: 1893-1897, 1977.
217. **Puhakainen I and Yki-Jarvinen H.** Inhibition of lipolysis decreases lipid oxidation and gluconeogenesis from lactate but not fasting hyperglycemia or total hepatic glucose production in NIDDM. *Diabetes* 42: 1694-1699, 1993.
218. **Raabe M, Veniant MM, Sullivan MA, Zlot CH, Bjorkegren J, Nielsen LB, Wong JS, Hamilton RL, and Young SG.** Analysis of the role of microsomal triglyceride transfer protein in the liver of tissue-specific knockout mice. *J Clin Invest* 103: 1287-1298, 1999.
219. **Radziuk J, Norwich KH, and Vranic M.** Experimental validation of measurements of glucose turnover in nonsteady state. *Am J Physiol* 234: E84-93, 1978.
220. **Radziuk J and Pye S.** Hepatic glucose uptake, gluconeogenesis and the regulation of glycogen synthesis. *Diabetes Metab Res Rev* 17: 250-272, 2001.
221. **Randle PJ.** Regulatory interactions between lipids and carbohydrates: the glucose fatty acid cycle after 35 years. *Diabetes Metab Rev* 14: 263-283, 1998.
222. **Ravichandran LV, Esposito DL, Chen J, and Quon MJ.** Protein kinase C-zeta phosphorylates insulin receptor substrate-1 and impairs its ability to activate phosphatidylinositol 3-kinase in response to insulin. *J Biol Chem* 276: 3543-3549, 2001.
223. **Reaven GM.** Compensatory hyperinsulinemia and the development of an atherogenic lipoprotein profile: the price paid to maintain glucose homeostasis in insulin-resistant individuals. *Endocrinol Metab Clin North Am* 34: 49-62, 2005.
224. **Reaven GM, Hollenbeck C, Jeng CY, Wu MS, and Chen YD.** Measurement of plasma glucose, free fatty acid, lactate, and insulin for 24 h in patients with NIDDM. *Diabetes* 37: 1020-1024, 1988.
225. **Rebrin K, Steil GM, Mittelman SD, and Bergman RN.** Causal linkage between insulin suppression of lipolysis and suppression of liver glucose output in dogs. *J Clin Invest* 98: 741-749, 1996.
226. **Rehberg EF, Samson-Bouma ME, Kienzle B, Blinderman L, Jamil H, Wetterau JR, Aggerbeck LP, and Gordon DA.** A novel abetalipoproteinemia genotype. Identification of a missense mutation in the 97-kDa subunit of the microsomal triglyceride transfer protein that prevents complex formation with protein disulfide isomerase. *J Biol Chem* 271: 29945-29952, 1996.
227. **Rizza RA, Cryer PE, Haymond MW, and Gerich JE.** Adrenergic mechanisms of catecholamine action on glucose homeostasis in man. *Metabolism* 29: 1155-1163, 1980.
228. **Roden M and Bernroider E.** Hepatic glucose metabolism in humans--its role in health and disease. *Best Pract Res Clin Endocrinol Metab* 17: 365-383, 2003.
229. **Roden M, Price TB, Perseghin G, Petersen KF, Rothman DL, Cline GW, and Shulman GI.** Mechanism of free fatty acid-induced insulin resistance in humans. *J Clin Invest* 97: 2859-2865, 1996.
230. **Roden M, Stingl H, Chandramouli V, Schumann WC, Hofer A, Landau BR, Nowotny P, Waldhausl W, and Shulman GI.** Effects of free fatty acid elevation on postabsorptive endogenous glucose production and gluconeogenesis in humans. *Diabetes* 49: 701-707, 2000.

231. **Rognstad R and Katz J.** Effects of hormones and of ethanol on the fructose 6-P-fructose 1,6-P2 futile cycle during gluconeogenesis in the liver. *Arch Biochem Biophys* 177: 337-345, 1976.
232. **Rohl M, Pasparakis M, Baudler S, Baumgartl J, Gautam D, Huth M, De Lorenzi R, Krone W, Rajewsky K, and Bruning JC.** Conditional disruption of IkappaB kinase 2 fails to prevent obesity-induced insulin resistance. *J Clin Invest* 113: 474-481, 2004.
233. **Rossetti L.** Perspective: Hexosamines and nutrient sensing. *Endocrinology* 141: 1922-1925, 2000.
234. **Sacca L, Vigorito C, Cicala M, Corso G, and Sherwin RS.** Role of gluconeogenesis in epinephrine-stimulated hepatic glucose production in humans. *Am J Physiol* 245: E294-302, 1983.
235. **Sako Y and Grill VE.** A 48-hour lipid infusion in the rat time-dependently inhibits glucose-induced insulin secretion and B cell oxidation through a process likely coupled to fatty acid oxidation. *Endocrinology* 127: 1580-1589, 1990.
236. **Saltiel AR and Kahn CR.** Insulin signalling and the regulation of glucose and lipid metabolism. *Nature* 414: 799-806, 2001.
237. **Santomauro AT, Boden G, Silva ME, Rocha DM, Santos RF, Ursich MJ, Strassmann PG, and Wajchenberg BL.** Overnight lowering of free fatty acids with Acipimox improves insulin resistance and glucose tolerance in obese diabetic and nondiabetic subjects. *Diabetes* 48: 1836-1841, 1999.
238. **Sanyal AJ, Campbell-Sargent C, Mirshahi F, Rizzo WB, Contos MJ, Sterling RK, Luketic VA, Shiffman ML, and Clore JN.** Nonalcoholic steatohepatitis: association of insulin resistance and mitochondrial abnormalities. *Gastroenterology* 120: 1183-1192, 2001.
239. **Sato H, Terasaki T, Mizuguchi H, Okumura K, and Tsuji A.** Receptor-recycling model of clearance and distribution of insulin in the perfused mouse liver. *Diabetologia* 34: 613-621, 1991.
240. **Sato R, Miyamoto W, Inoue J, Terada T, Imanaka T, and Maeda M.** Sterol regulatory element-binding protein negatively regulates microsomal triglyceride transfer protein gene transcription. *J Biol Chem* 274: 24714-24720, 1999.
241. **Schmitz-Peiffer C, Browne CL, Oakes ND, Watkinson A, Chisholm DJ, Kraegen EW, and Biden TJ.** Alterations in the expression and cellular localization of protein kinase C isozymes epsilon and theta are associated with insulin resistance in skeletal muscle of the high-fat-fed rat. *Diabetes* 46: 169-178, 1997.
242. **Schoonjans K and Auwerx J.** Thiazolidinediones: an update. *Lancet* 355: 1008-1010, 2000.
243. **Shah P, Vella A, Basu A, Basu R, Schwenk WF, and Rizza RA.** Lack of suppression of glucagon contributes to postprandial hyperglycemia in subjects with type 2 diabetes mellitus. *J Clin Endocrinol Metab* 85: 4053-4059, 2000.
244. **Sharp D, Blinderman L, Combs KA, Kienzle B, Ricci B, Wager-Smith K, Gil CM, Turck CW, Bouma ME, Rader DJ, and et al.** Cloning and gene defects in microsomal triglyceride transfer protein associated with abetalipoproteinaemia. *Nature* 365: 65-69, 1993.
245. **Shepherd PR, Withers DJ, and Siddle K.** Phosphoinositide 3-kinase: the key switch mechanism in insulin signalling. *Biochem J* 333 (Pt 3): 471-490, 1998.

246. **Shimabukuro M, Koyama K, Chen G, Wang MY, Trieu F, Lee Y, Newgard CB, and Unger RH.** Direct antidiabetic effect of leptin through triglyceride depletion of tissues. *Proc Natl Acad Sci U S A* 94: 4637-4641, 1997.
247. **Shimabukuro M, Ohneda M, Lee Y, and Unger RH.** Role of nitric oxide in obesity-induced beta cell disease. *J Clin Invest* 100: 290-295, 1997.
248. **Shimabukuro M, Zhou YT, Levi M, and Unger RH.** Fatty acid-induced beta cell apoptosis: a link between obesity and diabetes. *Proc Natl Acad Sci U S A* 95: 2498-2502, 1998.
249. **Shimomura I, Bashmakov Y, and Horton JD.** Increased levels of nuclear SREBP-1c associated with fatty livers in two mouse models of diabetes mellitus. *J Biol Chem* 274: 30028-30032, 1999.
250. **Shiota M, Galassetti P, Igawa K, Neal DW, and Cherrington AD.** Inclusion of low amounts of fructose with an intraportal glucose load increases net hepatic glucose uptake in the presence of relative insulin deficiency in dog. *Am J Physiol Endocrinol Metab* 288: E1160-1167, 2005.
251. **Shoelson SE, Lee J, and Goldfine AB.** Inflammation and insulin resistance. *J Clin Invest* 116: 1793-1801, 2006.
252. **Shulman GI.** Cellular mechanisms of insulin resistance. *J Clin Invest* 106: 171-176, 2000.
253. **Sindelar DK, Balcom JH, Chu CA, Neal DW, and Cherrington AD.** A comparison of the effects of selective increases in peripheral or portal insulin on hepatic glucose production in the conscious dog. *Diabetes* 45: 1594-1604, 1996.
254. **Sindelar DK, Chu CA, Neal DW, and Cherrington AD.** Interaction of equal increments in arterial and portal vein insulin on hepatic glucose production in the dog. *Am J Physiol* 273: E972-980, 1997.
255. **Sindelar DK, Chu CA, Rohlie M, Neal DW, Swift LL, and Cherrington AD.** The role of fatty acids in mediating the effects of peripheral insulin on hepatic glucose production in the conscious dog. *Diabetes* 46: 187-196, 1997.
256. **Sindelar DK, Chu CA, Venson P, Donahue EP, Neal DW, and Cherrington AD.** Basal hepatic glucose production is regulated by the portal vein insulin concentration. *Diabetes* 47: 523-529, 1998.
257. **Sivan E, Homko CJ, Whittaker PG, Reece EA, Chen X, and Boden G.** Free fatty acids and insulin resistance during pregnancy. *J Clin Endocrinol Metab* 83: 2338-2342, 1998.
258. **Sleeman MW, Wortley KE, Lai KM, Gowen LC, Kintner J, Kline WO, Garcia K, Stitt TN, Yancopoulos GD, Wiegand SJ, and Glass DJ.** Absence of the lipid phosphatase SHIP2 confers resistance to dietary obesity. *Nat Med* 11: 199-205, 2005.
259. **Smogyi M.** Notes on sugar determination. *J Biol Chem* 195: 19-23, 1952.
260. **Somogyi M.** Determination of blood sugar. *J Biol Chem* 160: 69-73, 1945.
261. **Sonne O.** The reversible receptor binding of insulin in isolated rat adipocytes measured at 37 degrees C. The binding is not rate limiting for cellular uptake. *Biochim Biophys Acta* 886: 302-309, 1986.
262. **Standaert ML, Bandyopadhyay G, Kanoh Y, Sajan MP, and Farese RV.** Insulin and PIP3 activate PKC-zeta by mechanisms that are both dependent and

independent of phosphorylation of activation loop (T410) and autophosphorylation (T560) sites. *Biochemistry* 40: 249-255, 2001.
263. **Steinberg HO, Paradisi G, Hook G, Crowder K, Cronin J, and Baron AD.** Free fatty acid elevation impairs insulin-mediated vasodilation and nitric oxide production. *Diabetes* 49: 1231-1238, 2000.
264. **Steinberg HO, Tarshoby M, Monestel R, Hook G, Cronin J, Johnson A, Bayazeed B, and Baron AD.** Elevated circulating free fatty acid levels impair endothelium-dependent vasodilation. *J Clin Invest* 100: 1230-1239, 1997.
265. **Stevenson RW, Steiner KE, Connolly CC, Fuchs H, Alberti KG, Williams PE, and Cherrington AD.** Dose-related effects of epinephrine on glucose production in conscious dogs. *Am J Physiol* 260: E363-370, 1991.
266. **Stevenson RW, Steiner KE, Davis MA, Hendrick GK, Williams PE, Lacy WW, Brown L, Donahue P, Lacy DB, and Cherrington AD.** Similar dose responsiveness of hepatic glycogenolysis and gluconeogenesis to glucagon in vivo. *Diabetes* 36: 382-389, 1987.
267. **Straczkowski M, Kowalska I, Nikolajuk A, Dzienis-Straczkowska S, Kinalska I, Baranowski M, Zendzian-Piotrowska M, Brzezinska Z, and Gorski J.** Relationship between insulin sensitivity and sphingomyelin signaling pathway in human skeletal muscle. *Diabetes* 53: 1215-1221, 2004.
268. **Studer RK, Snowdowne KW, and Borle AB.** Regulation of hepatic glycogenolysis by glucagon in male and female rats. Role of cAMP and Ca2+ and interactions between epinephrine and glucagon. *J Biol Chem* 259: 3596-3604, 1984.
269. **Stumvoll M, Chintalapudi U, Perriello G, Welle S, Gutierrez O, and Gerich J.** Uptake and release of glucose by the human kidney. Postabsorptive rates and responses to epinephrine. *J Clin Invest* 96: 2528-2533, 1995.
270. **Stumvoll M and Jacob S.** Multiple sites of insulin resistance: muscle, liver and adipose tissue. *Exp Clin Endocrinol Diabetes* 107: 107-110, 1999.
271. **Summers RJ and McMartin LR.** Adrenoceptors and their second messenger systems. *J Neurochem* 60: 10-23, 1993.
272. **Summers SA.** Ceramides in insulin resistance and lipotoxicity. *Prog Lipid Res* 45: 42-72, 2006.
273. **Sun XJ, Rothenberg P, Kahn CR, Backer JM, Araki E, Wilden PA, Cahill DA, Goldstein BJ, and White MF.** Structure of the insulin receptor substrate IRS-1 defines a unique signal transduction protein. *Nature* 352: 73-77, 1991.
274. **Sun XJ, Wang LM, Zhang Y, Yenush L, Myers MG, Jr., Glasheen E, Lane WS, Pierce JH, and White MF.** Role of IRS-2 in insulin and cytokine signalling. *Nature* 377: 173-177, 1995.
275. **Taha C and Klip A.** The insulin signaling pathway. *J Membr Biol* 169: 1-12, 1999.
276. **Taniguchi CM, Emanuelli B, and Kahn CR.** Critical nodes in signalling pathways: insights into insulin action. *Nat Rev Mol Cell Biol* 7: 85-96, 2006.
277. **Taniguchi CM, Ueki K, and Kahn R.** Complementary roles of IRS-1 and IRS-2 in the hepatic regulation of metabolism. *J Clin Invest* 115: 718-727, 2005.
278. **Thiebaud D, DeFronzo RA, Jacot E, Golay A, Acheson K, Maeder E, Jequier E, and Felber JP.** Effect of long chain triglyceride infusion on glucose metabolism in man. *Metabolism* 31: 1128-1136, 1982.

279. **Tietge UJ, Bakillah A, Maugeais C, Tsukamoto K, Hussain M, and Rader DJ.** Hepatic overexpression of microsomal triglyceride transfer protein (MTP) results in increased in vivo secretion of VLDL triglycerides and apolipoprotein B. *J Lipid Res* 40: 2134-2139, 1999.
280. **Tripathy D, Mohanty P, Dhindsa S, Syed T, Ghanim H, Aljada A, and Dandona P.** Elevation of free fatty acids induces inflammation and impairs vascular reactivity in healthy subjects. *Diabetes* 52: 2882-2887, 2003.
281. **Tschopp O, Yang ZZ, Brodbeck D, Dummler BA, Hemmings-Mieszczak M, Watanabe T, Michaelis T, Frahm J, and Hemmings BA.** Essential role of protein kinase B gamma (PKB gamma/Akt3) in postnatal brain development but not in glucose homeostasis. *Development* 132: 2943-2954, 2005.
282. **Tsuruzoe K, Emkey R, Kriauciunas KM, Ueki K, and Kahn CR.** Insulin receptor substrate 3 (IRS-3) and IRS-4 impair IRS-1- and IRS-2-mediated signaling. *Mol Cell Biol* 21: 26-38, 2001.
283. **Unger RH, Zhou YT, and Orci L.** Regulation of fatty acid homeostasis in cells: novel role of leptin. *Proc Natl Acad Sci U S A* 96: 2327-2332, 1999.
284. **Valera Mora ME, Scarfone A, Calvani M, Greco AV, and Mingrone G.** Insulin clearance in obesity. *J Am Coll Nutr* 22: 487-493, 2003.
285. **Venkatakrishnan A, Abel MJ, Campbell RA, Donahue EP, Uselton TC, and Flakoll PJ.** Whole blood analysis of gluconeogenic amino acids for estimation of de novo gluconeogenesis using pre-column o-phthalaldehyde derivatization and high-performance liquid chromatography. *J Chromatogr B Biomed Appl* 676: 1-6, 1996.
286. **Wall JS, Steele R, De Bodo RC, and Altszuler N.** Effect of insulin on utilization and production of circulating glucose. *Am J Physiol* 189: 43-50, 1957.
287. **Wang MY, Koyama K, Shimabukuro M, Newgard CB, and Unger RH.** OB-Rb gene transfer to leptin-resistant islets reverses diabetogenic phenotype. *Proc Natl Acad Sci U S A* 95: 714-718, 1998.
288. **Weigert C, Klopfer K, Kausch C, Brodbeck K, Stumvoll M, Haring HU, and Schleicher ED.** Palmitate-induced activation of the hexosamine pathway in human myotubes: increased expression of glutamine:fructose-6-phosphate aminotransferase. *Diabetes* 52: 650-656, 2003.
289. **Weisberg SP, McCann D, Desai M, Rosenbaum M, Leibel RL, and Ferrante AW, Jr.** Obesity is associated with macrophage accumulation in adipose tissue. *J Clin Invest* 112: 1796-1808, 2003.
290. **Wetterau JR, Aggerbeck LP, Bouma ME, Eisenberg C, Munck A, Hermier M, Schmitz J, Gay G, Rader DJ, and Gregg RE.** Absence of microsomal triglyceride transfer protein in individuals with abetalipoproteinemia. *Science* 258: 999-1001, 1992.
291. **Wide L, Porath, J.** Radioimmunoassay of proteins with the use of Sephadex-coupled antibodies. *Biochim Biphys Acta* 130: 257-260, 1966.
292. **Wijesekara N, Konrad D, Eweida M, Jefferies C, Liadis N, Giacca A, Crackower M, Suzuki A, Mak TW, Kahn CR, Klip A, and Woo M.** Muscle-specific Pten deletion protects against insulin resistance and diabetes. *Mol Cell Biol* 25: 1135-1145, 2005.
293. **Wolfe RR.** Radioactive and Stable Isotope Tracers in Biomedicine. *Wiley-Liss*, 1992.

294. **Wrede CE, Dickson LM, Lingohr MK, Briaud I, and Rhodes CJ.** Protein kinase B/Akt prevents fatty acid-induced apoptosis in pancreatic beta-cells (INS-1). *J Biol Chem* 277: 49676-49684, 2002.
295. **Xiao J, Gregersen S, Kruhoffer M, Pedersen SB, Orntoft TF, and Hermansen K.** The effect of chronic exposure to fatty acids on gene expression in clonal insulin-producing cells: studies using high density oligonucleotide microarray. *Endocrinology* 142: 4777-4784, 2001.
296. **Yin MJ, Yamamoto Y, and Gaynor RB.** The anti-inflammatory agents aspirin and salicylate inhibit the activity of I(kappa)B kinase-beta. *Nature* 396: 77-80, 1998.
297. **Yki-Jarvinen H, Puhakainen I, and Koivisto VA.** Effect of free fatty acids on glucose uptake and nonoxidative glycolysis across human forearm tissues in the basal state and during insulin stimulation. *J Clin Endocrinol Metab* 72: 1268-1277, 1991.
298. **Yoon JC, Puigserver P, Chen G, Donovan J, Wu Z, Rhee J, Adelmant G, Stafford J, Kahn CR, Granner DK, Newgard CB, and Spiegelman BM.** Control of hepatic gluconeogenesis through the transcriptional coactivator PGC-1. *Nature* 413: 131-138, 2001.
299. **Yoshii H, Lam TK, Gupta N, Goh T, Haber CA, Uchino H, Kim TT, Chong VZ, Shah K, Fantus IG, Mari A, Kawamori R, and Giacca A.** Effects of portal free fatty acid elevation on insulin clearance and hepatic glucose flux. *Am J Physiol Endocrinol Metab* 290: E1089-1097, 2006.
300. **Yu C, Chen Y, Cline GW, Zhang D, Zong H, Wang Y, Bergeron R, Kim JK, Cushman SW, Cooney GJ, Atcheson B, White MF, Kraegen EW, and Shulman GI.** Mechanism by which fatty acids inhibit insulin activation of insulin receptor substrate-1 (IRS-1)-associated phosphatidylinositol 3-kinase activity in muscle. *J Biol Chem* 277: 50230-50236, 2002.
301. **Yu J, Wjasow C, and Backer JM.** Regulation of the p85/p110alpha phosphatidylinositol 3'-kinase. Distinct roles for the n-terminal and c-terminal SH2 domains. *J Biol Chem* 273: 30199-30203, 1998.
302. **Yuan M, Konstantopoulos N, Lee J, Hansen L, Li ZW, Karin M, and Shoelson SE.** Reversal of obesity- and diet-induced insulin resistance with salicylates or targeted disruption of Ikkbeta. *Science* 293: 1673-1677, 2001.
303. **Zhou YP and Grill VE.** Long-term exposure of rat pancreatic islets to fatty acids inhibits glucose-induced insulin secretion and biosynthesis through a glucose fatty acid cycle. *J Clin Invest* 93: 870-876, 1994.